

UNIVERSITY OF ZIMBABWE

**MATHEMATICAL MODELLING OF RESPIRATORY DISEASES WITH
WEAK AND STRONG INFECTION**

BY

WILSON ZHUWAKI

R206362K

zhuwakiwilson1@gmail.com

**PROJECT SUBMITTED IN FULFILMENT OF
BACHELOR OF SCIENCE HONOURS DEGREE IN MATHEMATICS
AND COMPUTATIONAL SCIENCE
IN THE DEPARTMENT OF
MATHEMATICS AND COMPUTATIONAL SCIENCE**

**FACULTY OF SCIENCE
AT
UNIVERSITY OF ZIMBABWE**

JUNE 2024

**SUPERVISOR
PROFESSOR S.MUSHAYABASA**

Declaration

I, Wilson Zhuwaki, confirm that this project report faithfully encapsulates the outcomes of my self-directed research carried out during my final year at the University of Zimbabwe. This document holds significant value in fulfilling the criteria for obtaining the Bachelor of Science Honours Degree in Mathematics and Computational Science. It reflects solely my original contributions, with appropriate acknowledgment given to any external resources consulted during its preparation.

Student's Signature: _____ Date: _____

Dedication

This project is a culmination of dedication, perseverance, and the unwavering support of my dear family, Mr. and Mrs. Zhuwaki, whose love and guidance have been my guiding light. Additionally, it embodies the encouragement and camaraderie of my brother, Munyaradzi Zhuwaki, whose belief in my abilities has fueled my determination. Furthermore, it reflects the invaluable friendships and support of my cherished friends, whose laughter and encouragement have made this journey memorable. This project stands as a testament to the collective effort and belief in my potential, and it is with profound gratitude that I dedicate its success to my loved ones.

Acknowledgements

I humbly acknowledge the indispensable guidance and unwavering support of Professor S. Mushayabasa, whose expertise has profoundly influenced the fruition of this project. My deepest gratitude extends to my dear friend Walter for his unwavering encouragement and steadfast belief in my capabilities, which have been a source of strength throughout this journey. I also want to express my heartfelt appreciation to all those who have supported and inspired me, including my family, mentors, and peers, whose faith in me has been instrumental in overcoming obstacles. Finally, I offer my sincerest thanks to the Almighty for His countless blessings and divine guidance, without which this achievement would not have been possible.

Abstract

In this thesis, a deterministic system of coupled differential equations is proposed to examine the transmission dynamics of respiratory diseases, encompassing both weak and strong infections such as Tuberculosis, COVID-19, and Influenza. The research establishes the existence and uniqueness of classical solutions for the respiratory disease model, along with verifying the model's positivity. Additionally, the model is non-dimensionalized, and an invariant region is identified. Equilibrium points are thoroughly analyzed, and basic reproduction numbers are derived. Both local and global asymptotic stability analyses are conducted to understand the system's behavior. Bifurcation analysis is performed using the Center Manifold method, and sensitivity analysis is carried out for the two reproduction numbers. Numerical simulations are employed to approximate solutions, revealing insights into the dynamics of infection spread. Results demonstrate that increased immunity loss heightens the incidence of weak infections, possibly due to heightened susceptibility to reinfection, while concurrently reducing the prevalence of strong infections, likely attributed to recovery, partial immunity gain, or a transition to milder infection states. Moreover, enhanced cross-immunity decelerates the decline of strongly infected cases, indicative of a protective effect against severe disease outcomes.

Keywords: COVID-19, Tuberculosis, and Influenza, Local stability, Global stability, Basic reproduction number, Numerical simulation, Bifurcation analysis, Center Manifold method

Nomenclature

$N(t)$: Total population size at time t .

$f(x)$: General function used in modeling.

$\frac{d}{dt}$: Derivative with respect to time.

∂_t : Partial derivative with respect to time.

∂_x : Partial derivative with respect to spatial coordinate x .

∂_{xx} : Second partial derivative with respect to spatial coordinate x .

∂_{tt} : Second partial derivative with respect to time.

∂_{xx} : Second partial derivative with respect to x .

∂_{xy} : Second partial derivative with respect to spatial coordinates x and y .

\int : Integral symbol.

\int_a^b : Definite integral from a to b .

\int_0^t : Integral from 0 to t .

\sum : Summation symbol.

\lim : Limit symbol.

\rightarrow : Arrow indicating a limit or convergence.

$S(0)$: Initial number of susceptible individuals.

$I_2(0)$: Initial number of strongly infectious individuals.

$I_1(0)$: Initial number of weakly infected individuals.

R_0 : Basic reproduction number.

Contents

Dedication	III
Acknowledgements	IV
Abstract	V
Nomenclature	VI
1 Introduction	1
1.1 COVID 19	1
1.1.1 Immunopathology of COVID 19 Disease	2
1.1.2 Influenza	3
1.1.3 Tuberculosis	4
1.2 Statement of the Problem	5
1.3 Research Aim and Objectives	6
1.3.1 Aim	6
1.3.2 Objectives	6
1.4 Research Questions	6
1.5 Justification of Study	6
1.6 Roadmap	7
1.7 Definitions of Used Terms	8
1.8 Chapter Summary	9
2 Literature Review	10
2.1 Introduction	10
2.2 Empirical Literature Review	10
2.2.1 Covid-19	10
2.2.2 Tuberculosis	13
2.2.3 Influenza	15
2.3 Chapter Summary	18
3 Model Formulation and Analysis	19
3.1 Introduction	19

3.2	Model Formulation	19
3.3	Deterministic Model Formulation	20
3.3.1	Detailed Definition of Variables	20
3.3.2	Model Assumptions	21
3.3.3	Parameter Definitions	22
3.4	Model Equations	22
3.5	Model Non Dimensionalization	24
3.6	Qualitative Analysis of the Model	26
3.6.1	Positivity and Boundedness of a solutions	26
3.6.2	Boundedness of the solution	29
3.6.3	Existence and Uniqueness Theorem	31
3.6.4	Analysis of Equilibria	33
3.6.5	Disease Free Equilibrium Point (E_0)	33
3.6.6	Reproduction Number(R_0)	34
3.6.7	Other Equilibrium Points(E_1, E_2)	36
3.6.8	Local Stability of Disease Free	38
3.6.9	Local Stability of Strain 1 Outcompetes Strain 2 (E_1)	39
3.6.10	Local Stability of Strain 2 Outcompetes Strain 1 (E_2)	42
3.6.11	Global Stability Analysis for (E_0)	44
3.6.12	Analysis of Bifurcation	47
3.6.13	Sensitivity Analysis of R_0	51
3.7	Chapter Overview	53
4	Numerical Simulations	54
4.1	Chapter Overview	64
5	Discussion and Conclusion	65
5.1	Introduction	65
5.2	Key Findings	65
5.3	Summary	70
5.4	Future Works	72
A	Python Codes	77

List of Figures

1.1	Dissertation Structure	8
3.1	Compartmentalised diagram showing the respiratory diseases model	23
4.1	Graphical presentation of the bifurcation for the model 3.3 for all values of $\phi > 1$. .	56
4.2	The population dynamics with initial conditions $S(0) = 0.85$, $I1_0 = 0.1$, and $I2_0 = 0.05$.When the basic reproduction numbers $(R_0^s)=1.916$ and $(R_0^r)=0.918$	57
4.3	The population variations with initial conditions $(S, I1, I2, R1, P1, P2, R1, R2) = (0.4, 0.1, 0.1, 0.15, 0.15, 0.05, 0.05)$.When $R_0 = (0.674, 0.751)$, comprising $R_0^s = 0.674$ and $R_0^r = 0.751$	59
4.4	The combined population variations with initial conditions $(S, I1, I2, R1, P1, P2, R1, R2) = (0.4, 0.1, 0.1, 0.15, 0.15, 0.05, 0.05)$.When $R_0 = (0.674, 0.751)$, comprising $R_0^s = 0.674$ and $R_0^r = 0.751$,	60
4.5	Effects of Reduction in Immunity On the Weakly Infected and Strongly Infected Group with $R_0^s = 2.432$ and $R_0^r = 1.854$	61
4.6	Effects of Cross Immunity On the Weakly Infected and Strongly Infected Class with $R_0^s = 2.432$ and $R_0^r = 1.854$	62
4.7	Effects of $R_0^s > 1$ and $R_0^r > 1$ on the Strongly Infected Class	63

List of Tables

3.1	Parameter Definitions	22
4.1	Parameter Definitions, Values, and Sources	55
5.1	Questions and Answers	71

1 Introduction

Respiratory diseases burden healthcare systems globally, causing illness, death, and straining infrastructure. To effectively combat these threats, we need to understand how they spread and what factors influence them. Mathematical modeling has become a powerful tool, providing insights into these complex dynamics and aiding in designing interventions. This dissertation explores mathematical modeling of respiratory diseases, focusing on how the strength of their infectiousness shapes transmission and control strategies. We will categorize diseases based on their infectiousness (e.g., weak like tuberculosis or strong like COVID-19 and influenza) to understand the mechanisms driving their spread and how these differences influence how we control them. Furthermore, this research delves into critical factors like population immunity, environmental conditions, and human behavior to create a more comprehensive picture of disease dynamics. By incorporating these elements, our models can provide valuable insights for public health officials, allowing them to tailor interventions to the specific characteristics of each respiratory disease. Ultimately, this research aspires to contribute to the development of more effective strategies to prevent and control these devastating illnesses.

1.1 COVID 19

The World Health Organization, also known as the WHO, classified COVID-19 to be a pandemic on March 11, 2020. SARS-CoV-2, as the virus is now known to be, has killed over 6 million people since the initial case of infection was recorded in China in December 2019. In total, there have been over 600 million reported instances of the virus[42]. Since the coronavirus's first epidemic, it has spread to nearly every nation on Earth. Coronaviruses are a large family of viruses that can cause everything from a common cold to more serious infections like Middle East Respiratory Syndrome (MERS) and severe acute respiratory syndrome (SARS). [1] When an infector and the infected individual come into close, harmful contact, dust particles and fomites transmit COVID-19. It is possible that aerosol-generating procedures could be used in medical institutions, however there has been no empirical proof of airborne spread of COVID-19. Nevertheless, it is not known to be a substantial mode of transmission. A tiny percentage of clinical trials have reported the presence of the active virus, and faecal dissemina-

tion has been observed in certain individuals. Additionally, it appears that the faecal-oral route is not a COVID-19 transmission media; hence, its purpose and significance for COVID-19 must be determined. As of the third week of April 2020, there were approximately 18,738,580 laboratory-confirmed cases on record. Of those cases, the largest percentage (77.8%) belonged to the age range of 30 to 69. Of the instances that have been documented, 21.6% are employed or farmers by trade, 51.1% are men, and 77.0% are from Hubei.

COVID-19 initially surfaced in 2019, however it wasn't until the 20th of March in 2020 that it made its way to Zimbabwe. The Zimbabwean government has been working harder through the Ministry of Health and Child Care to quickly contain and manage any outbreaks that occur there. The National Emergency Operations Center was established by the multi-sector Coronavirus Preparedness Group, under the direction of the Zimbabwe COVID 19 Inter-Ministerial Task Force, in order to address this case and implement stringent control measures. Late in March 2020, Zimbabwe went into lockdown for the first time. Crowd areas and even places of worship were limited before the shutdown. Later, as it was hard to stop the spread, several lock-downs happened. Gradually, limitations and an all-out lockdown were announced. Palliatives were handed to the government and then distributed among the states of Zimbabwe as the economy remained sluggish. Even though there were a lot of palliatives available, many news sources stated that many people were only getting little[15].

There were certain establishments that were closed during lockdown. People are only allowed to leave their houses at specific hours in other states, including Harare, if they are wearing protective gear, like face guards & nasal masks. Despite the strict measures implemented, the virus continued to spread and had a substantial negative impact on families, individuals, and businesses. In March 2021, COVID-19 vaccinations were made available in Zimbabwe. The nation's top authorities received vaccinations to kick off the vaccination campaign. Even with the officials' example, the majority of Zimbabweans were highly reluctant to take the shots. Since a vaccination certificate is needed to access some facilities and other benefits, it has been seen that a large number of people have received both the first and second doses of the immunization in recent years. Even after the federal government lifted the restriction, some locations—especially in the banking sector—retain the "no mask, no entry" regulation. One of the most important documents that everyone needs to have is the immunization certificate, which is now required[33].

1.1.1 Immunopathology of COVID 19 Disease

Although the etiology of COVID-19 is unknown, studies from numerous nations suggest that the virus invades or enters host cells using a similar method to SARS-COV. Although the exact origin of SARS-CoV-2 is unknown, it is known that bats are the source of similar viruses and that human-to-human transmission is a key factor in the disease's pathogenesis. Viral RNA

is encapsulated & polyadenylated after it enters target cells as a result of Spike protein binding with its receptor. This process codes for a variety of structural & non-structural polypeptide genes. These polyproteins are broken down by proteases that function similarly to chymotrypsin. Despite being the primary protease linked to CoV activation and transmembrane serine protease 2 (TMPRSS2), recent single-cell RNA-sequencing (scRNA-seq) analysis data indicates that both ACE2 and TMPRSS2 are not expressed in the same cell, pointing to the potential involvement of other proteases, including cathepsin B and L, in this process[38].

Pattern recognition receptors (PRRs) are generally capable of identifying viruses and other invasive diseases. A number of crucial host immune responses are triggered by viruses, including an increase in the release of inflammatory factors, the activation and maturation of the dendritic cells (DCs), and an increase in the manufacture of type I interferons (IFNs), which are crucial in preventing the spread of viruses. SARS-CoV-2 stimulates both the innate & acquired immune systems. Immunoglobulin (Ig)G and IgM, two virus-specific antibodies, are produced by B cells under the stimulation of CD4 + T cells, while CD8 + T cells directly destroy virus-infected cells. To support the other immune cells, T helper cells release mediators and pro-inflammatory cytokines. Through the suppression of T cell activities, such as apoptosis, SARS-CoV-2 can impede the host immune response [32].

1.1.2 Influenza

The influenza virus, also referred to as the flu, is the cause of influenza, a respiratory infectious disease. The influenza virus comes in three varieties, A, B, and C. Every year, there is an outbreak of influenza viruses, particularly during the winter months, although the viruses from the previous year are not the source of this outbreak. It is easily contagious between people when someone coughs or sneezes, or when hands come into contact with their mouth, nose, or eyes. Influenza symptoms include a high temperature, headache, sore throat, runny nose, coughing, and weakness. The virus often manifests as a cough after two days and lasts for no more than a week, though it sometimes lasts longer. Children under five, adults over 65, pregnant women, those with chronic conditions such as diabetes, heart disease, renal disease, or asthma, and those with weakened immune systems are among the groups most at risk for influenza. According to Carrat et al. (2008), influenza A is a transient infection that requires about two days to incubate. The virus begins to shed in respiratory secretions around one day before to the beginning of symptoms. Rapid exponential growth characterizes the normal pattern of virus kinetics, reaching a peak in viral load up to 1-3 days after infection and then declining over the next 3-5 days [21].

One of the most researched viral infections, co-infections, and interactions for respiratory viruses in general is influenza. People can contract it more than once in their lifetime, and

it results in annual chronic epidemic outbreaks [6]. According to Kamal et al. (2017), they can be identified by variations in the two main viral surface proteins, HA and NA. Nine different types of NA and sixteen different types of HA are present. As a result, influenza A viruses may have 144 different subtypes. Because virus A can recombine its genes with the ones from strains circulating in populations of animals (birds, swine, and horses), it is epidemiologically essential for humans. Typha infection can affect humans, pigs, whales, birds, and particularly wild animals. It is one of the most severe categories out there. The virus is further separated by the presence of neuraminidase (NA) and hemagglutinin (HA) proteins on its surface [31]. There are sixteen variations of hemagglutinin (H1–H16) and nine varieties of neuraminidase (N1–N9). The nomenclature of an influenza virus subtype is derived from the combination of HA and NA. As an example, the influenza A virus known as H1N1 carries both the HA1 & NA1 proteins. There are just three of these combinations that are more common in humans: H1N1, H1N2, and H3N2. Type B can infect both humans and birds, and it can also propagate epidemics. The last variety (C) only affects humans and is hard to differentiate from the common cold because it does not spread like an epidemic [37].

Additionally, strains of the influenza A and the influenza B virus can be distinguished. [40], A novel influenza strain can emerge primarily through two mechanisms: antigenic drift & antigenic shift. Antigenic drift is the result of the virus gradually changing over time. When new strains emerge, the host antibodies may not recognize them at first. Conversely, antigenic shift refers to an abrupt alteration in influenza a virus that gives rise to a novel strain that is unidentified. While influenza B exclusively experiences antigenic drift, influenza A experiences both modifications.

There are many antiviral medicines available in the market for influenza. By the use of antiviral medicines, influenza can be prevented. During the infected period of influenza, people should drink plenty of fluid and sufficient rest. Antiviral medicines cannot remove the symptoms of influenza but it can reduce the appearance and duration of symptoms of the disease. Every person need not go for active antiviral treatment for influenza but should take action based on several factors. If the person is very ill and suffering other disease also, then there is a risk factor and the person need antiviral medicines. If a person is suffering influenza for more than 48 hours with all symptoms of influenza, then it is advisable to consult a doctor for treatment.

1.1.3 Tuberculosis

Mycobacterium tuberculosis (MTB) is the pathogen that causes tuberculosis (TB), a bacterial infectious illness that affects both people and animals. The formation of tubercles in the lungs and other bodily tissues, which frequently occur decades after the initial infection, is the disease's defining feature. It is one of the most prevalent infectious diseases and is spread by the air. Among the earliest known diseases in humans and animals is tuberculosis. It before

the emergence of the species of human in animals.[8] ,there is centuries' worth of evidence to establish both the existence of human cases of tuberculosis and its connection to mortality. When someone is infected, it is not always obvious, which facilitates the disease's spread. The transmission of tuberculosis (TB) occurs through contact with infected people, mainly through sharing a closed space. Once a person is infected, the infection may remain latent for the rest of their life and last for many years.

Clinical examination of this illness indicates that the patient has a latent fever that starts in the evening and goes away in the morning. There is a strong cough that produces thin, purulent sputum. The patient exhibits heated cheeks, labored breathing, and a raspy voice when speaking. The whole body would get pale. Wheezes are frequently audible in the chest region, and as the illness progresses, upper chest perspiration is visible. The patient experiences hunger sensations or lacks appetite [35]. A common trait of them is extreme thirst. The fingernails curl strangely, and the tips of the fingers bulge. Because of how terrible this infectious disease is, it has inspired researchers to build the disciplines of bacteriology and contemporary epidemiology. Yang Y and others. Every year, tuberculosis kills over 2 million people worldwide and results in 8 million new instances of the illness[20].

1.2 Statement of the Problem

Existing models of respiratory disease transmission predominantly focus on single forms of infection, overlooking the detailed dynamics arising from coexistence of multiple infection types within populations. Moreover, these models often neglect the crucial aspect of environmental dispersion, failing to account for the simultaneous release of pathogens from infected individuals into the environment. Consequently, there is a pressing need to develop a comprehensive mathematical model that integrates both weak and strong forms of respiratory infection and incorporates their simultaneous dissemination into the environment.

This study aims to address this gap by formulating a new mathematical framework capable of simulating the transmission dynamics of respiratory diseases characterized by varying degrees of infection severity. Specifically, the model will account for the concurrent presence of weak and strong infections, reflecting the diverse manifestations of respiratory pathogens within populations. Additionally, the model will incorporate mechanisms for environmental dispersion, capturing the release of infectious particles into the surrounding air or surfaces by infected individuals.

1.3 Research Aim and Objectives

1.3.1 Aim

To model the dynamics of respiratory diseases with weak and strong infection.

1.3.2 Objectives

The objectives of the study are:

- ① Construct a mathematical model to simulate the transmission dynamics of respiratory diseases considering both weak and strong infections.
- ② Determine the disease-free equilibrium point.
- ③ Compute the basic reproduction number R_0 to quantify the average number of secondary infections caused by a single infected individual in a completely susceptible population.
- ④ Assess the local stability of disease-free and endemic equilibrium points through linear stability analysis.
- ⑤ Implement numerical simulations to visualize the dynamics of disease transmission over time.

1.4 Research Questions

The researcher will address the following research questions:

- ② How does reduction in immunity affect population susceptibility to respiratory diseases over time?
- ② How does cross-immunity influence disease dynamics?
- ② What are the bifurcation directions in disease models?
- ② How does different values of basic reproduction number (R_0) influence the infected populations

1.5 Justification of Study

Understanding the transmission dynamics of respiratory diseases is essential for effective public health interventions and preparedness efforts. By developing an innovative mathematical model that integrates both weak and strong forms of infection while considering environmental

dispersion, our study aims to provide a comprehensive understanding of disease spread. This approach addresses the complexity of real-world transmission scenarios, allowing for the evaluation of intervention strategies such as vaccination campaigns and social distancing measures. By optimizing these strategies, we can mitigate the burden of respiratory diseases on healthcare systems and improve public health outcomes. Additionally, our interdisciplinary collaboration encourages synergies between epidemiology, mathematics, biology, and public health, facilitating a well-rounded approach to tackling these complex public health challenges and enhancing preparedness for future outbreaks.

1.6 Roadmap

The remaining chapters of this dissertation are organised as follows:

Chapter 2: Literature Review, this chapter reviews existing respiratory disease transmission models, emphasizing gaps in addressing multiple infection types and environmental dispersion. It also covers relevant mathematical preliminaries for model formulation and stability analysis.

Chapter 3: Methodology here, the study's approach is detailed, focusing on model formulation, stability analysis, and nondimensionalization. The mathematical framework for the transmission model is described, including equations for susceptible, infected, and recovered individuals. Techniques for stability analysis and nondimensionalization are explained, alongside numerical methods for model analysis and simulation.

Chapter 4: Numerical Simulations, this chapter presents the results of numerical simulations conducted with the transmission model. It discusses the effects of parameters and intervention strategies on disease spread dynamics, and compares simulation outcomes with real-world data where available.

Chapter 5: Discussion and Conclusions, the final chapter synthesizes the study's findings and discusses their implications. It evaluates the model's strengths and limitations, suggests future research directions, and emphasizes the importance of the study's contribution to public health interventions. The conclusions summarize key findings, offer recommendations, and underscore the study's significance in advancing understanding of respiratory disease transmission.

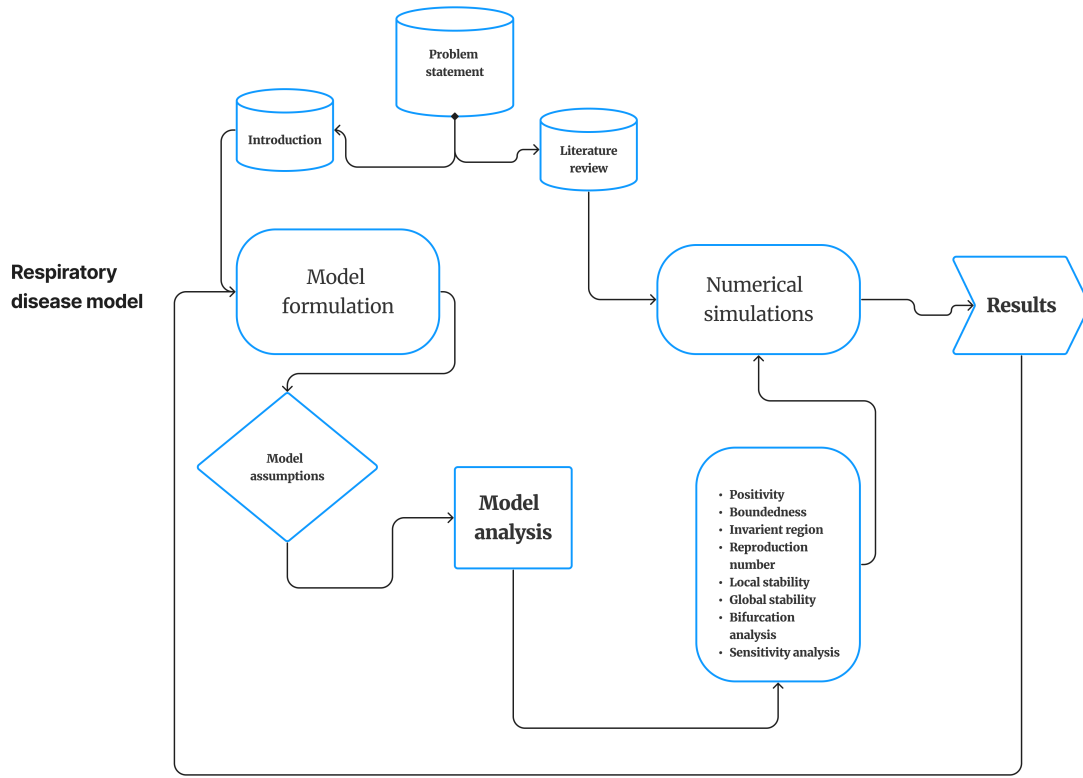


Figure 1.1: Dissertation Structure

1.7 Definitions of Used Terms

In this study, important terms and concepts are defined. Many of these definitions are based on those found in [11]

Mathematical Model: A mathematical model describes a system or process using mathematical concepts and language.

Autonomous System: An ordinary differential equation is called autonomous if it is in the form:

$$\dot{x} = f(x), \quad x \in \mathbb{R}^n, \quad (n \in \mathbb{N})$$

where \dot{x} denotes the derivative with respect to a smooth function x .

Equilibrium Point: A point $x = x_0 \in \mathbb{R}^n$ is an equilibrium point of the system if $f(x_0) = 0$.

Stable Equilibrium Point: An equilibrium point $x_0 \in \mathbb{R}^n$ is stable if, for any $\epsilon > 0$, there exists $\delta = \delta(\epsilon) > 0$ such that any solution $y(t) \in C^1(t_0, \infty)$ of the system satisfies $|x_0 - y(t)| < \epsilon$ whenever $|x_0 - y(t_0)| < \delta$, for $t > t_0 \in \mathbb{R}$.

Asymptotically Stable: The equilibrium x_0 is asymptotically stable if there exists a constant $c > 0$ such that, for any solution $y(t) \in C^1(t_0, \infty)$ of the system satisfying $|x_0 - y(t_0)| < c$, then $\lim_{t \rightarrow \infty} |x_0 - y(t)| = 0$.

Unstable: An equilibrium point x_0 that is not stable is considered unstable.

Jacobian Matrix: The Jacobian matrix $J(x)$ of the function $f : \mathbb{R}^n \rightarrow \mathbb{R}^n$ is defined as:

$$J(x) = \begin{bmatrix} \frac{\partial f_1}{\partial x_1}(x) & \dots & \frac{\partial f_1}{\partial x_n}(x) \\ \vdots & \ddots & \vdots \\ \frac{\partial f_n}{\partial x_1}(x) & \dots & \frac{\partial f_n}{\partial x_n}(x) \end{bmatrix}$$

Disease-Free Equilibrium: The disease-free equilibrium (DFE) is the equilibrium point where there is an absence of disease in the population.

Susceptible Individuals: These individuals are members of a population who are at risk of becoming infected by a disease.

Infectious Individuals: These individuals have acquired the disease and can infect others.

Recovered: These individuals have been infected and have either recovered from the disease.

1.8 Chapter Summary

This chapter introduces the dissertation's focus on modeling respiratory diseases. It outlines the aims, objectives, and significance of the research. The chapter provides an overview of current trends in respiratory diseases, highlighting their impact on global health. Different respiratory illnesses are identified and discussed, setting the stage for the subsequent chapters' exploration of mathematical modeling techniques to better understand disease transmission dynamics and inform effective control strategies.

2 Literature Review

2.1 Introduction

In this section, we'll give you a quick rundown of the various mathematical models that scientists have used to study respiratory diseases such as TB, COVID-19, and influenza. Some models take a big-picture view, looking at how entire populations interact and how diseases spread among them. Others dive deep into individual behaviors, aiming to understand how people's actions impact disease transmission

2.2 Empirical Literature Review

2.2.1 Covid-19

The coronavirus happens to be one of among the most violent human viruses harming modern society. This virus continues to be a global threat because it targets the respiratory tract of humans. The World Health Organization (WHO) initially referred to the infection as "novel coronavirus 2019" (2019-nCoV) on January 12, 2020. The international a group of the Coronavirus Study Group (CSG) officially named the infection "severe acute respiratory syndrome coronavirus-2" (SARS-CoV-2). The WHO refers to the disease as "coronavirus disease 2019" (COVID-19). One such virus that might produce COVID-19 is SARS-CoV-2. China's Wuhan was the source of the first epidemic in December 2019. After that, COVID-19 spread over the world, becoming the fifth pandemic to be officially recorded since the 1918 epidemic of influenza. SARS-CoV-2 is a spherical, encapsulated particle that is a member of the order Nidovirales, family Coronaviridae, and subfamily Coronavirinae. Its genome is a positive-sense single-stranded RNA. Prior research has demonstrated that all human coronaviruses, including HCoV-229E, the SARS-CoV, HCoV-NL63, and MERS-CoV, have animal origins. One of the most significant natural reservoirs of both beta- and alpha-coronaviruses is the bat[26].

In order to comprehend the mechanisms of transmission and the management of newly and

reemerging infectious illnesses, mathematical models are crucial. Estimating the COVID-19 pandemic's intensity and recommending suitable public health response strategies are two of humanity's most urgent problems at the moment. Recently, several mathematical models have been proposed to study the patterns of transmission of the COVID-19 pandemic. In order to examine the impact of non-pharmaceutical control strategies on the population dynamics associated with the novel-coronavirus disease 2019,[12]. created a mathematical model. Forecasts for the total number of cases reported and active cases were given in their analysis for varying degrees of the control strategies incorporated into their model. They were successful in reaching their basic reproduction number, & their numerical simulations show that if at least 55% of the general population continues to practice social distancing and wearing face masks in public, the disease will finally disappear from the population. The authors recommended rigorously enforcing the use of face masks and social distancing measures, as well as vigorously screening and testing members of the public any new cases of COVID-19 infection, either symptomatic or asymptomatic. [4] used mathematical modeling during the initial outbreaks in Kano, Nigeria, to estimate the basic reproduction number R_0 and the total number of COVID 19 under ascertained cases (η). Their results show an exponential growth pattern similar to the COVID-19 epidemic curve in Kano. They found that the total number of COVID-19 cases, which happened during the 4th week of April 2020, is underreported. They recommended that in order to stop COVID-19 from proliferating in Kano, Nigeria, epidemiological research and mitigation measures be given top priority as soon as possible. Additionally, their results demonstrate the possibility for large-scale epidemics caused by the fundamental rate of reproduction R_0 , which has the value 2.74(95% CI : 2.53–2.96). Their predictions are essential for preparing for upcoming epidemics. [26] created a mathematical framework to study the dynamics and control of COVID-19 transmission in Nigeria. Data by the Nigeria-Centre for Disease' Control (NCDC) was used in a number of Nigerian jurisdictions to evaluate the effects of different control and mitigation strategies on the population as a whole. According to their research, COVID-19 can be successfully controlled in Nigeria if mitigation and control strategies can reach the threshold quantity of $R_c < 1$. Furthermore, if strict rules of social distancing are put in place (and kept up for a long time), COVID-19 won't be able to cause significant outbreaks in Nigeria.

A mathematical model was presented by [25] to forecast the dynamics of COVID-19 transmission in Ethiopia. They discovered that the equilibrium points of $R_0 < 1$ & $R_0 > 1$, accordingly, are asymptotically stable both locally and globally, indicating that they are disease-free and endemic. $R_0 = 1.5085$, the basic reproduction number, is more than 1. However, reducing the rate of transmission from gradually infected to suspected infection α is necessary to minimize the R_0 . This can be achieved, for example, by lowering the parameter α to 0.47, which will decrease the coronavirus from Egypt. The optimal combination of personal preventive measures, hospitalized or isolated case treatment, and public health education would significantly reduce the COVID-19 pandemic in Egyptian, according to the results of the optimum analysis and

simulation. Lastly, the Ethiopian government and other nations can use the research findings as a basis for policy. In order to guarantee that the subsequent preventative measures are regularly used during the pandemic, government officials must take the necessary actions.

A deterministic model that depicts the dynamics of COVID-19 in Nigeria was developed by [29]. The disease-equilibrium solution of the model was evaluated for stability using the computed basic reproduction number. The Nigeria-Centre for Disease-Control (NCDC) provided data that was used to estimate the key parameters of the model. Using Pontryagin's maximum principle, the authors looked into low-cost options for time-independent restrictions that would inhibit virus propagation within a specified time range. Their findings imply that population testing for COVID-19, strict adherence to WHO guidelines, and effective contact tracing may all be completed quickly to stop the disease's spread.

A mathematical model was presented by Deressa et al. to forecast the dynamics of COVID-19 transmission in Ethiopia. Their results showed that the equilibrium points for $R_0 > 1$ and $R_0 < 1$, respectively, are asymptotically stable both locally and globally, indicating that they are endemic and disease-free [9]. There is more than one basic reproduction number $R_0 = 1.5085$. Nevertheless, reducing the rate of transmission from asymptotically infected to suspected individuals (α) is necessary to minimize the R_0 . This can be achieved by lowering the parameter α to 0.47, which will decrease the coronavirus in Ethiopia. The optimal combination of personal preventive measures, hospitalized or isolated case treatment, and public health education would significantly reduce the COVID-19 pandemic in Ethiopia, according to the results of the optimal analysis and simulation. Lastly, the Ethiopian government along with other nations can use the research findings as a basis for policy. To guarantee that the following preventative measures are applied consistently throughout the pandemic, the government must take the necessary actions. A deterministic model that depicts the dynamics of COVID-19 in Nigeria was developed by Adewole et al. The disease-equilibrium solution of the model was evaluated for stability using the computed basic reproduction number. The Nigeria Centre for Disease Control (NCDC) provided data that was used to estimate the key parameters of the model. Using Pontryagin's maximum principle, the authors looked into low-cost options for time-independent restrictions that would inhibit virus propagation within a specified time range. Their findings imply that population testing for COVID-19, strict adherence to WHO guidelines, and effective contact tracing may all be completed quickly to stop the disease's spread. The influence of ignoring asymptomatic patients on COVID-19 transmission in Africa was theoretically investigated by [41]. They measured the number of basic reproductions and looked for bifurcation in the opposite direction. Furthermore, the asymptotic stabilities at the local and global levels were determined. Their results suggest that minimizing and decreasing the impact of COVID-19 in

Africa will be greatly aided by boosting case detection to identify infected individuals who are asymptomatic. Since it is unknown if a recovered person can contract the virus again, enforcing arrangements for living where recovered individuals are not allowed to interact with vulnerable or exposed individuals will also help to stop the spread of COVID-19.

The influence of ignoring asymptomatic patients on COVID-19 transmission in Africa was theoretically investigated by [2]. They measured the number of basic reproductions and looked for bifurcation in the opposite direction. The Global and Local asymptotic Stabilities were also proved. Their results suggest that minimizing and decreasing the impact of COVID-19 in Africa will be greatly aided by boosting case detection to identify infected individuals who are asymptomatic. Since it is unknown if a recovered person can contract the virus again, imposing living arrangements where those who have recovered are not allowed to interact with susceptible or exposed persons will also help to stop the spread of COVID-19.

2.2.2 Tuberculosis

Numerous pathogen strains can cause the flu, dengue fever, TB, and many other transferable illnesses. Numerous scientists investigated the outbreaks brought on by various kinds of illnesses. The basic reproduction ratio is crucial in this situation since it has been demonstrated that the strain(s) with the highest basic- reproduction ratio will perform better than the other strain(s). The majority of these mechanisms—which enable the coexistence of strains—involve the host population’s exponential expansion, co-infection, super-infection, vaccination, and mutation [5].

McCluskey and van den Driessche look into an SEI TB model with immigration that incorporates people who are infected (both infectious and latent). A constant percentage of students were expected to enroll in each class, according to the model. McCluskey and van den Driessche have demonstrated that the disease will converge to a distinct endemic level with specific limitations on the parameters (such as treatment rates, disease transmission-rates, and TB-induced death rates). Because of the inflow of sick people, the disease never fully vanishes and the typical threshold condition that is present in many epidemic-models is meaningless[34]. In his work, [34] examined two tuberculosis models, one of which included treating infected and latent cases. The stability study was conducted because the first model assumes continuous recruitment, with a set fraction of new participants entering each class. As a result, TB never becomes extinct. The focus of their second model was on a broad recruitment function that assigns all recruits to the susceptible group. They came to the conclusion that the initial model is relevant because it takes into account the immigration of infectious agents at a steady pace, indicating that tuberculosis will persist in its endemic state even with treatment. Furthermore,

they claimed that when the population size is zero overall, there is a singularity at the origin of the differential-equation system for a second model with general recruitment.

A two-group model for one strain and two strain tuberculosis (TB) was developed by [18]. The purpose of this model was to identify potential processes that could aid in the survival and dissemination of both naturally resistant and antibiotic-generated tuberculosis strains. According to their claims, their model's study will show that, although co-existence of naturally resistant strains and strains resulting from TB-infected patients' noncompliance with antibiotic treatment is almost always the case, it is rare for non-antibiotic co-existence to occur. Such an individual could potentially become infected with active tuberculosis as a result of external reinfection.

For the dynamics of tuberculosis (TB) disease transmission, [22] modeled the qualitative behavior of a system of ordinary differential equations and a system of differential-integral equations. They demonstrated how a reproduction number governs the changing dynamics of both models. They took into consideration the case when $R_0 > 1$, meaning that there is a single positive (endemic) equilibrium and the disease free equilibrium is unstable. Additionally, the positive balance remains steady. The outcomes demonstrated that the qualitative characteristics provided by the Tuberculosis model with an exponentially dispersed time of latency are comparable to those anticipated by the model with an arbitrarily distributed latent stage. They support the earlier conclusions and address the chance that an endogenous infection could cause an individual who is afflicted with TB to become actively infected.

Zhong-Wei Jia and colleagues introduce two novel theoretical models to examine how immigration affects the dynamics of TB transmission [30]. Their suggested model's behavior was demonstrated by numerical simulations along with analyses of the existence & stability of equilibria. They then applied the model to data on tuberculosis that were reported from Canada, and they found a good match between the model's prediction and the data. Additionally, they conducted analysis on the extended model, which incorporates the latent and infectious immigrant populations into the primary model. They discovered that there is a distinct equilibrium for every value of the parameters and that the typical threshold condition is not applicable. They suggested that immigrants have a significant impact on the overall transmission patterns behavior of tuberculosis and that the disease does not go away and becomes epidemic in the host location.

In order to examine the effects of this demographic difference on the short term incidence and long term transmission dynamics, [10] present a deterministic epidemiology model of TB transmission in two distinct demographical populations. Particular attention is paid to the effect of immigration latent TB cases on the general TB incidence rate in the population. In order to

generate short-term predictions, they talked about the qualitative study they conducted utilizing statistical data from Canada to estimate the parameters of their model.

A deterministic model was used by [7] to investigate the possible implications of the combined impact of TB case identification in the context of therapy. After examining the characteristics of its equilibria, they concluded that, in cases when the reproduction number is lower than one, the disease-free equilibrium might not be globally asymptotically stable. They found it simpler to evaluate the effects of an active TB case regardless of treatment thanks to the disease threshold number. Additionally, they demonstrated the phenomena of backward bifurcation using the center manifold theory, and they concluded that the likelihood of backward bifurcation decreasing with an increase in TB case detection occurs when the reproduction number is smaller than one.

[36], developed mathematical models to simulate the changing patterns of tuberculosis in a community where the disease must be reduced and ultimately eradicated. The impact of variations in the area size & recruitment rates was examined using both quantitative and qualitative analysis. A disease free-equilibrium point can be found, according to analysis, as long as the characteristic area is larger than the likelihood of surviving from the latent stage to the infectious stage and the total number of latent infections a typical infectious individuals produces during the course of his or her mean infectious period. To reduce tuberculosis occurrence, the study suggests that each individual's typical area should be greater than 0.25 square kilometers. According to this research, a characteristic location may also be considered an environmental stressor that raises the risk of developing tuberculosis. The tuberculosis model used in this investigation was derived from the authors' model. Nevertheless, the goal of this study is to demonstrate the disease's rapid progression, which the authors did not examine.

2.2.3 Influenza

The development of a pre-coalition model between the H1N1-p & H5N1 influenza viruses in Indonesia was reported by Hariyanto et al. (2013). The influenza viruses H1N1-p, which may adapt without hemagglutinin or amino acids, and H5N1, which has 170 mutations and three distinct types with significantly varying spreads, are frequently utilized in research in Indonesia. They thought of modeling the pre-coalition between one of the H5N1 strains that infect humans and poultry and the influenza virus H1N1-p. Through an analysis of the coexistence of both virus transmissions, the model is reduced based on the transition in and genetic changes on an individual population. In their work, they describe the construction of a mathematical model of the virus's multi-strain, multi-species propagation, based solely on susceptible as well as exposed populations of chicken and human hosts [36]. Based on each population's unique experiences with transition and change, the model is reduced. The method used places more of an

emphasis on the epidemiological than the mathematical aspects. The resulting model building is therefore more realistic. They came to the following conclusions based on their analysis of the virus's influence on the system: (1) In an unstable condition where $R_0 > 1$, the H1N1-p influenza virus does not affect system change if the density magnitude of susceptible population is greater than the density of infected population as well as the coefficient of minimum global diffusion; (2) In a stable condition where $R_0 < 1$, the H5N1 influenza virus still affects system change, albeit with a smaller influence, if the density magnitude of susceptible population is equal to the density of infected population; and (3) The coexistence from coinfection on H1N1-p as well as H5N1 virus can occur nearly simultaneously with the occurrence of each virus's spread [3].

In a boarding school in Maharashtra, India, in June and July of 2009, a unique influenza A/H1N1 (2009) outbreak was investigated by [17] for its transmission characteristics. For this, a susceptible-exposed-infectious-asymptomatic-recovered mathematical model was used. Epidemiological data analyses showed that close clustering within the population led to strong transmissibility, with a transmission rate (β) of 0.001566 and a basic reproduction number $R_0 = 2.61$. The model assisted in determining the epidemiological parameters for asymptomatic cases, the efficacy of the control measures, and the dynamics of transmission in a boarding school setting. Their method offers a paradigm for researching influenza outbreaks with comparable population clusters. According to them, these models can be used to evaluate the efficacy of control measures as well as forecast the pattern of illness spread in the event that the virus is introduced in comparable educational environments. The transmission dynamics study estimated a number of epidemic parameters, including the partial infectiousness and length of the outbreak in the asymptomatic individuals, but came to the conclusion that it was challenging to ascertain these parameters by clinical observations [3].

A mathematical model of avian influenza with half-saturated incidence" was given by [16]. They created a mathematical model of avian influenza that took into account populations of both birds and people. Investigations are conducted into how the disease's transmission dynamics are affected by half-saturated incidence. The levels at which avian influenza infects humans and birds are determined by the half-saturation constants. The corresponding half-saturation constants, in particular the half-saturation constant H_m for humans infected with the mutant strain, need to be raised in order to stop the spread of avian influenza. The fundamental reproduction number of this model is largely dependent on the value H_m . Moreover, an outbreak can be contained more successfully by lowering the rate b_m at which human-to-human mutant influenza is acquired. They suggest both non-pharmaceutical (personal protection & isolation) and pharmaceutical (vaccination) control measures to battle the outbreak and lessen the spread of avian influenza. Personal protection and vaccination will reduce b_m , but isolation will

raise H_m . All suggested control strategies, as shown by numerical simulations, will eventually eradicate the disease; however, if vaccination is the only strategy used, the disease will take a little longer to eradicate than if non-pharmaceutical along with a combination of pharmaceutical and non-pharmaceutical control methods is used exclusively. In conclusion, combating an outbreak of avian influenza necessitates the use of a variety of control strategies [36].

Modeling influenza epidemics & pandemics::insights into the future of swine flu (H1N1)” was given by [19]. After reviewing the body of research on influenza modeling, they talked about how the models can shed light on the future of the unique strain of influenza A (H1N1) that is now circulating and was originally known as swine flu. They talk about how the Basic Reproduction Number (R_0) has a vital role in determining whether an outbreak can be contained. They noted that the latest estimate of the R_0 for new influenza A (H1N1) was in the range of 1.4 to 1.6. The value was similar to R_0 values calculated for seasonal influenza strains (mean $R_0 = 1.3$: range 0.9 to 2.1) and below values of R_0 estimated for the 1918–1919 pandemic strain (mean $R_0 = 2$: range 1.4 to 2.8). Based on a study of earlier modeling research, they come to the conclusion that there is a chance that an H1N1 pandemic may be limited. Even in nations with abundant resources, it might not be possible to get the required vaccine and treatment rates for control. Controlling a pandemic will require an international coordinated effort, as demonstrated by a new modeling research. According to this plan, nations with abundant resources must provide vaccines and antivirals to those with scarce resources. They address the need for creating new, biologically complicated models as they wrap up their review. They recommended that the models monitor the dynamics of influenza strain transmission in pig, human, and avian populations concurrently. Planning for pandemic preparedness and finding novel, successful remedies may depend heavily on these models. Lastly, they demonstrate that it might be able to forecast the establishment of influenza pandemic strains by simulating cross-species transmission. They also suggest creating models with greater biological complexity[27].

Haghdoost et al. reported on the modeling of the H1N1 pandemic in Iran (2009). They saw that the novel H1N1 flu strain was spreading quickly over the world and posed a severe threat. Urgent preparation is required in order to lessen the pandemic’s effects as much as possible. Using this information, they created a simulated H1N1 outbreak in two Iranian cities (Kerman, which is medium in size, and Tehran, which is a metropolis). To estimate the anticipated number of individuals who would experience severe (S), very severe (VS), or fatal (D) disease, they created a compartmental model. They predicted that in Kerman and Tehran, respectively, the Basic Reproductive Number (R_{0w}) would drop to 1.6 and 1.8 in the winter. In Kerman, the corresponding statistics ranged from 1.2 (R_{0sMin}) to 1.4 (R_{0sMax}), while in Tehran, they varied from 1.3 to 1.5. Additionally, based on projections, they examined the impact of the initial number of imported infected cases during the outbreak. The findings show that there was at least a six-month gap between the virus’s introduction in June 2009 and the start of the

outbreak in December 2009. The number of infected cases and the R_0 both had an impact on the lag; a lower R_0 delayed the peak. In Kerman, there were 2,728, 546, & 468 S, VS, and D, respectively, with a R_{0sMax} of 1.4. In Tehran, corresponding numbers with R_{0sMax} of 1.5 were 16,673, 14,291, and 83,363. They concluded by saying that, unless additional precautions are made beforehand, the health care system most likely would not be able to deliver appropriate services due to the high number of S and VS cases that would be crammed during a short period of time. The peak of the outbreak could be delayed till the end of 2010 by lowering R_0 and the quantity of newly introduced infectious cases. This would present an excellent chance to immunize a significant section of the populace [28].

2.3 Chapter Summary

This chapter conducts an extensive review of literature concerning the modeling of various respiratory diseases. It explores a range of respiratory illnesses including influenza, tuberculosis, COVID-19, and others, examining the diverse modeling approaches utilized to understand their transmission dynamics. The review encompasses studies that have investigated the epidemiology, transmission patterns, and control strategies for each disease, highlighting the methodologies and findings in the field of respiratory disease modeling. Additionally, the chapter discusses the strengths and limitations of existing models, identifies gaps in knowledge, and outlines areas for further research. Through this thorough examination, it provides a foundation for the subsequent chapters' contributions to advancing the understanding and control of respiratory diseases through mathematical modeling.

3 Model Formulation and Analysis

3.1 Introduction

In this section, we introduce a comprehensive mathematical model designed to study the dynamics of respiratory diseases, specifically focusing on tuberculosis (TB), COVID-19, and influenza. We will outline the model's structure, including its assumptions, compartments, and governing equations. Following this, we will conduct a series of analyses to understand the model's behavior. Stability analysis will help determine the conditions for stable disease-free and endemic states. Bifurcation analysis will explore how changes in key parameters can lead to significant shifts in disease dynamics. Sensitivity analysis will identify which parameters most influence the model's outcomes, highlighting critical factors for disease control.

3.2 Model Formulation

We here introduce a compartmental model of respiratory diseases in a population. The size of the population, at a given time t , is denoted by $N(t)$. The model divides the entire population into 5 groups or classes according to their epidemiological status: S (Susceptible), representing individuals who are susceptible to the disease and have not yet been infected; I_1 (Affected by Weak Infection), comprising individuals infected by the disease with a weaker strain or experiencing milder symptoms; I_2 (Affected by Strong Infection), including individuals infected by the disease with a stronger strain or experiencing more severe symptoms; R_1 (Recovery from Weak Infection), consisting of individuals who have recovered from the weaker strain of the disease; and R_2 (Recovery from Strong Infection), encompassing individuals who have recovered from the stronger strain of the disease. The dynamics of the population can be described by the following equation, where $N(t)$ represents the total population size at time t :

$$N(t) = S(t) + I_1(t) + I_2(t) + R_1(t) + R_2(t). \quad (3.1)$$

This equation represents the sum of individuals in all five groups at any given time t . As individuals move between these compartments due to infection, recovery, or death, the total population size $N(t)$ changes dynamically over time.

3.3 Deterministic Model Formulation

We formulate a deterministic compartmental model to study the dynamics of respiratory diseases within a population. The model divides the population into distinct compartments based on their epidemiological status: Susceptible (S), Weakly Infected (I_1), Strongly Infected (I_2), Recovered from Weak Infection (R_1), and Recovered from Strong Infection (R_2). The dynamics of the population can be described by the following equation, where $N(t)$ represents the total population size at time t :

$$N(t) = S(t) + I_1(t) + I_2(t) + R_1(t) + R_2(t). \quad (3.2)$$

In addition to these compartments, the model incorporates environmental compartments P_1 and P_2 , representing the spread of the disease from individuals in I_1 and I_2 into the environment, respectively. Environmental transmission from P_1 and P_2 contributes to the overall transmission dynamics by influencing the likelihood of individuals becoming infected. These environmental compartments play a crucial role in the transmission dynamics of respiratory diseases, particularly in settings where environmental contamination is a significant factor in disease spread.

3.3.1 Detailed Definition of Variables

We present a deterministic compartmental model to analyze the dynamics of respiratory diseases within a population. The model categorizes individuals into distinct compartments based on their epidemiological status:

- **S (Susceptible):** Individuals who have not contracted the disease and are susceptible to infection. They remain at risk of contracting the disease if exposed to infectious individuals, leading to potential transmission.
- **I_1 (Weak Infection):** Individuals infected with a weaker strain of the disease or experiencing milder symptoms. They are infectious and can spread the disease to susceptible individuals, albeit with less severity compared to those infected with the stronger strain.
- **I_2 (Strong Infection):** Individuals infected with a stronger strain of the disease or experiencing more severe symptoms. They are infectious and have a higher likelihood of experiencing severe symptoms compared to those infected with the weaker strain.

- R_1 (**Recovery from Weak Infection**): Individuals who have recovered from the weaker strain of the disease. They are no longer infectious and contribute to overall immunity within the population.
- R_2 (**Recovery from Strong Infection**): Individuals who have recovered from the stronger strain of the disease. Similar to R_1 , they are no longer infectious and contribute to overall immunity within the population.
- P_1 (**Environmental Spread from Weak Infection**): Represents the environmental transmission of the disease from individuals infected with the weaker strain. Infected individuals in I_1 shed the pathogen into the environment, potentially leading to new infections.
- P_2 (**Environmental Spread from Strong Infection**): Represents the environmental transmission of the disease from individuals infected with the stronger strain. Infected individuals in I_2 shed the pathogen into the environment, potentially leading to new infections.

3.3.2 Model Assumptions

We make several assumptions to simplify the modeling process and provide a basis for analysis:

- ① The population is assumed to mix uniformly, meaning that every individual has an equal chance of encountering and interacting with every other individual in the population.
- ② There is no movement of individuals into or out of the population during the simulation period.
- ③ Environmental transmission compartments, such as P_1 and P_2 , are assumed to be well-mixed.
- ④ Individuals who recover from the infection develop complete immunity against future infections.
- ⑤ Disease transmission occurs instantaneously upon contact between an infectious individual and a susceptible individual.
- ⑥ All parameters used in this model, including transmission rates, recovery rates, and death rates, are assumed to be positive values.
- ⑦ Individuals infected with the disease may experience disease-related mortality.

3.3.3 Parameter Definitions

Table 3.1: Parameter Definitions

Symbol	Definition
μ	Natural death rate
β_1	Transmission rate of weak infection i_1
β_2	Transmission rate of strong infection i_2
κ_1	Weak infection into environment p_1
κ_2	Strong infection into environment p_2
α_1	Parameter for weak infection
α_2	Parameter for strong infection
d_1	Death rate from weak infection i_1
d_2	Death rate from strong infection i_2
δ_1	Immunity from the recovered group r_1 that suffered weak infection
δ_2	Immunity from the recovered group r_2 that suffered strong infection
γ_1	Recovery rate from weak infection i_1
γ_2	Recovery rate from strong infection i_2
ϕ	Cross-immunity parameter
ϵ	Reduction factor for cross-immunity

3.4 Model Equations

Taking into account the definitions, assumptions, and interconnections among the variables and parameters, the fundamental dynamics of transmitting respiratory diseases are described by the subsequent set of ordinary differential equations:

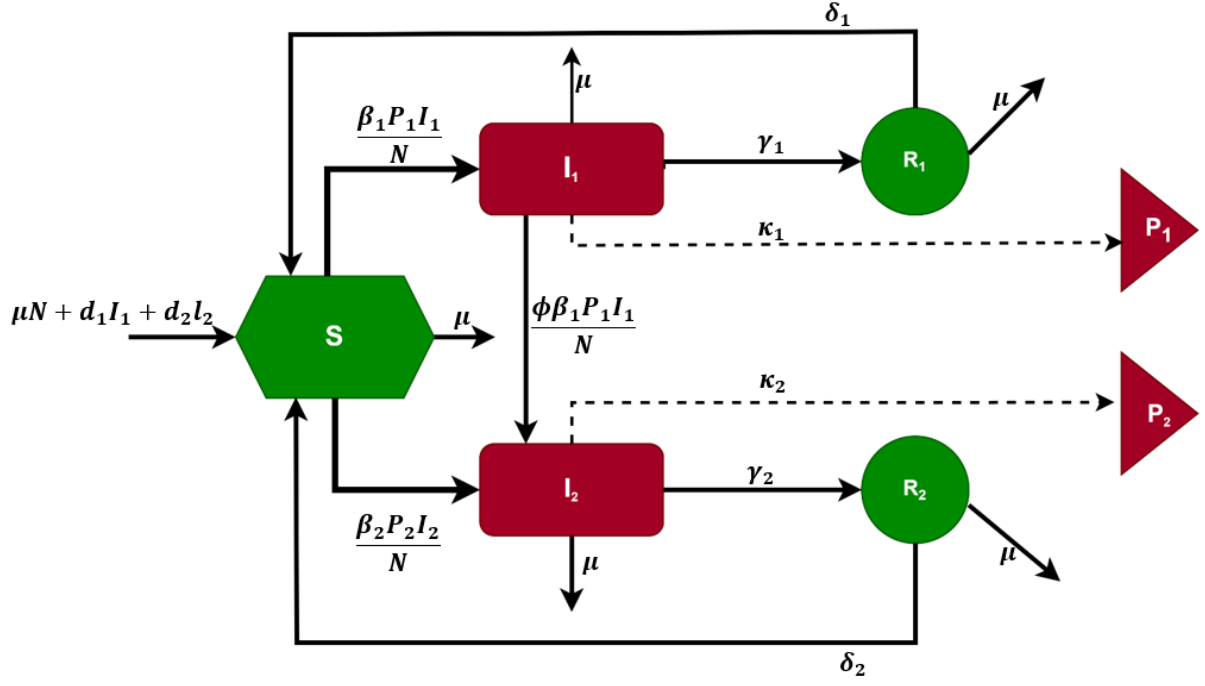


Figure 3.1: Compartmentalised diagram showing the respiratory diseases model

$$\left. \begin{aligned}
 \frac{dS}{dt} &= \mu N - \frac{\beta_1 P_1 S}{N} - \frac{\beta_2 P_2 S}{N} - \mu S + d_1 I_1 + d_2 I_2 + \delta_1 R_1 + \delta_2 R_2 \\
 \frac{dI_1}{dt} &= \frac{\beta_1 P_1 S}{N} - (\mu + \gamma_1 + d_1) I_1 - \frac{\phi \beta_2 P_2 I_1}{N} \\
 \frac{dI_2}{dt} &= \frac{\beta_2 P_2 S}{N} - (\mu + \gamma_2 + d_2) I_2 + \frac{\phi \beta_2 P_2 I_1}{N} + (1 - \varepsilon) \frac{\beta_2 P_2 R_1}{N} \\
 \frac{dP_1}{dt} &= \kappa_1 I_1 - \alpha_1 P_1 \\
 \frac{dP_2}{dt} &= \kappa_2 I_2 - \alpha_2 P_2 \\
 \frac{dR_1}{dt} &= \gamma_1 I_1 - \mu R_1 - (1 - \varepsilon) \frac{\beta_2 P_2 R_2}{N} - \delta_1 R_1 \\
 \frac{dR_2}{dt} &= \gamma_2 I_2 - \mu R_2 - \delta_2 R_2
 \end{aligned} \right\}. \quad (3.3)$$

The initial conditions for the differential equations (3.3):

$$\left. \begin{aligned}
 S(0) &= S_0 \geq 0 \\
 I_1(0) &= I_{1_0} \geq 0 \\
 I_2(0) &= I_{2_0} \geq 0 \\
 P_1(0) &= P_{1_0} \geq 0 \\
 P_2(0) &= P_{2_0} \geq 0 \\
 R_1(0) &= R_{1_0} \geq 0 \\
 R_2(0) &= R_{2_0} \geq 0
 \end{aligned} \right\} \quad (3.4)$$

Now, the rate of change of the total population ($\frac{dN}{dt}$) represents the flow of individuals into and out of the population over time. Mathematically, it can be expressed as the sum of the rates of change of each compartment:

$$\left. \begin{aligned} \frac{dN}{dt} &= \frac{dS}{dt} + \frac{dI_1}{dt} + \frac{dI_2}{dt} + \frac{dR_1}{dt} + \frac{dR_2}{dt} \\ &= \left(\mu N - \frac{\beta_1 P_1 S}{N} + \frac{\beta_2 P_2 S}{N} + d_1 I + d_2 I + \delta_1 R_1 + \delta_2 R_2 - \mu S \right) \\ &\quad + \left(\frac{\beta_1 P_1}{N} - (\mu + \gamma_1 + d_1) I_1 + \frac{\phi \beta_2 P_2}{N} \right) \\ &\quad + \left(\frac{\beta_2 P_2 S}{N} - (\mu + \gamma_2 + d_2) I_2 + \frac{\phi \beta_2 P_2}{N} + (1 - \varepsilon) \frac{\beta_2 P_2 R_1}{N} \right) \\ &\quad + \left(\gamma_1 I_1 - \mu R_1 - (1 - \varepsilon) \frac{\beta_2 P_2 R_1}{N} - \delta_1 R_1 \right) \\ &\quad + (\gamma_2 I_2 - \mu R_2 + \delta_2 R_2) \end{aligned} \right\} \quad (3.5)$$

$$\frac{dN}{dt} = \mu N - \mu(S + I_1 + I_2 + R_1 + R_2)$$

The equation (3.5) simplifies to $\frac{dN}{dt} = \mu N - \mu(S + I_1 + I_2 + R_1 + R_2) = 0$. This implies that the rate of change of the total population with respect to time is zero, indicating that the total population remains constant over time. Therefore, the solution to this differential equation is $N(t) = N_0$, where N_0 represents the initial total population size.

3.5 Model Non Dimensionalization

From equation (3.5), $\frac{dN}{dt} = 0$, hence without loss of generality, we can use a dimensionless system to explore the dynamics of respiratory diseases. To normalize the populations, let $s(t) = \frac{S(t)}{N(t)}$, $i_1(t) = \frac{I_1(t)}{N(t)}$, $i_2(t) = \frac{I_2(t)}{N(t)}$, $p_1(t) = \frac{\alpha_1 P_1(t)}{\kappa_1 N(t)}$, $p_2(t) = \frac{\alpha_2 P_2(t)}{\kappa_2 N(t)}$, $r_1(t) = \frac{R_1(t)}{N(t)}$, and $r_2(t) = \frac{R_2(t)}{N(t)}$.

To non-dimensionalize the system of differential equations in (3.1), we can employ the chain rule. This methodology enables us to express the rates of change with respect to time using non-dimensional variables. By applying the chain rule to the derivatives with respect to time, we derive expressions that relate to non-dimensionalized quantities.

Let's consider the initial equation from the system of differential equations (3.3)

$$\frac{ds}{dt} = \frac{1}{N} \cdot \frac{dS}{dt} = \frac{1}{N} \left[\mu N - \frac{\beta_1 P_1 S}{N} + \frac{\beta_2 P_2 S}{N} + d_1 I + d_2 I + \delta_1 R_1 + \delta_2 R_2 - \mu S \right] \quad (3.6)$$

Simplifying equation (3.6) we have:

$$\frac{ds}{dt} = \mu(1-s) - \frac{\beta_1 \kappa_1 p_1 s}{\alpha_1} - \frac{\beta_2 \kappa_2 p_2 s}{\alpha_2} + d_1 i_1 + d_2 i_2 + \delta_1 r_1 + \delta_2 r_2 \quad (3.7)$$

From the second equation from the system of differential equations (3.3)

$$\frac{di_1}{dt} = \frac{1}{N} \cdot \frac{dI_1}{dt} = \frac{1}{N} \left[\frac{\beta_1 P_1}{N} - (\mu + \gamma_1 + d_1)I_1 + \frac{\phi \beta_2 P_2 i_1}{N} \right] \quad (3.8)$$

Simplifying equation (3.8) it becomes:

$$\frac{di_1}{dt} = \frac{\beta_1 \kappa_1 p_1 s}{\alpha_1} - (\mu + \gamma_1 + d_1)i_1 - \frac{\phi \beta_2 \kappa_2 p_2 i_1}{\alpha_2} \quad (3.9)$$

Similarly ,from the third equation from the system of differential equations in (3.3)

$$\frac{di_2}{dt} = \frac{1}{N} \cdot \frac{dI_2}{dt} = \frac{1}{N} \left[\frac{\beta_2 P_2 S}{N} - (\mu + \gamma_2 + d_2)I_2 + \frac{\phi \beta_2 P_2}{N} + (1-\varepsilon) \frac{\beta_2 P_2 R_1}{N} \right] \quad (3.10)$$

The above equation simplifies to:

$$\frac{di_2}{dt} = \frac{\beta_2 \kappa_2 p_2 s}{\alpha_2} - (\mu + \gamma_2 + d_2)i_2 + \frac{\phi \beta_2 \kappa_2 p_2 i_1}{\alpha_2} + (1-\varepsilon) \frac{\beta_2 \kappa_2 p_2 r_1}{\alpha_2} \quad (3.11)$$

Also we took the fourth equation from (3.3)

$$\frac{dp_1}{dt} = \frac{1}{N} \cdot \frac{dP_1}{dt} = \frac{1}{N} [\kappa_1 I_1 - \alpha_1 P_1] \quad (3.12)$$

Thus, the above equation becomes:

$$\frac{dp_1}{dt} = \kappa_1 i_1 - \kappa_1 p_1 \quad (3.13)$$

From the fifth equation from the system of differential equations (3.3) we have

$$\frac{dp_2}{dt} = \frac{1}{N} \cdot \frac{dP_2}{dt} = \frac{1}{N} [\kappa_2 I_2 - \alpha_2 P_2] \quad (3.14)$$

Which simplifies to:

$$\frac{dp_2}{dt} = \kappa_2 i_2 - \kappa_2 p_2 \quad (3.15)$$

From the sixth equation from the system of differential equations (3.3) ,we have

$$\frac{dr_1}{dt} = \frac{1}{N} \cdot \frac{dR_1}{dt} = \frac{1}{N} \left[\gamma_1 I_1 - \mu R_1 - (1-\varepsilon) \frac{\beta_2 P_2 R_1}{N} - \delta_1 R_1 \right] \quad (3.16)$$

This above equation simplifies to:

$$\frac{dr_1}{dt} = \gamma_1 i_1 - \mu r_1 - (1 - \varepsilon) \frac{\beta_2 \kappa_2 p_2 r_1}{\alpha_2} - \delta_1 r_1 \quad (3.17)$$

Lastly we took the seventh equation from (3.3)

$$\frac{dr_2}{dt} = \frac{1}{N} \cdot \frac{dR_2}{dt} = \frac{1}{N} [\gamma_2 I_2 - \mu R_2 + \delta_2 R_2] \quad (3.18)$$

Which will simplify to:

$$\frac{dr_2}{dt} = \gamma_2 i_2 - \mu r_2 - \delta_2 r_2 \quad (3.19)$$

Combining the all the above equation we have:

$$\left. \begin{aligned} \frac{ds}{dt} &= \mu(1 - s) - \frac{\beta_1 \kappa_1 p_1 s}{\alpha_1} - \frac{\beta_2 \kappa_2 p_2 s}{\alpha_2} + d_1 i_1 + d_2 i_2 + \delta_1 r_1 + \delta_2 r_2 \\ \frac{di_1}{dt} &= \frac{\beta_1 \kappa_1 p_1 s}{\alpha_1} - (\mu + \gamma_1 + d_1) i_1 - \frac{\phi \beta_2 \kappa_2 p_2 i_1}{\alpha_2} \\ \frac{di_2}{dt} &= \frac{\beta_2 \kappa_2 p_2 s}{\alpha_2} - (\mu + \gamma_2 + d_2) i_2 + \frac{\phi \beta_2 \kappa_2 p_2 i_1}{\alpha_2} + (1 - \varepsilon) \frac{\beta_2 \kappa_2 p_2 r_1}{\alpha_2} \\ \frac{dp_1}{dt} &= \kappa_1 i_1 - \kappa_1 p_1 \\ \frac{dp_2}{dt} &= \kappa_2 i_2 - \kappa_2 p_2 \\ \frac{dr_1}{dt} &= \gamma_1 i_1 - \mu r_1 - (1 - \varepsilon) \frac{\beta_2 \kappa_2 p_2 r_1}{\alpha_2} - \delta_1 r_1 \\ \frac{dr_2}{dt} &= \gamma_2 i_2 - \mu r_2 - \delta_2 r_2 \end{aligned} \right\} \quad (3.20)$$

3.6 Qualitative Analysis of the Model

3.6.1 Positivity and Boundedness of a solutions

To investigate the dynamics of any disease, it is important to understand the behavior of the solution over time t . For human disease modeling, it is important to show that the solutions will be positive and bounded over a long time. Let $t_0 > 0$, then for all $t \in [0, t_0]$, the values of the parameters can be chosen so that the solution $(s(t), i_1(t), i_2(t), p_1(t), p_2(t), r_1(t))$, and $r_2(t)$ to ODE (3.20) with the positive initial conditions as defined.

Theorem 1. Let $\Omega = \{(s, i_1, i_2, r_1, r_2, p_1, p_2) \in \mathbb{R}_+^7 : s_0 > 0, i_1^O, i_2^O > 0, r_1^O > 0, r_2^O > 0, p_1^O > 0, p_2^O > 0\}$. Then the solutions of $\{s, i_1, i_2, r_1, r_2, p_1, p_2\}$ are positive for $t \geq 0$.

Lemma 2. Grownwall Inequality: Let y and g be non-negative integrable functions and c a non-

negative constant. If

$$\begin{aligned} y(t) &\leq c + \int_0^t g(x)y(x) ds, & \text{for } t \geq 0, \\ y(t) &\leq c \exp \left(\int_0^t g(x) dx \right), & \text{for } t \geq 0, \end{aligned}$$

then

$$y(t) \leq c \exp \left(\int_0^t g(x) dx \right), \quad \text{for } t \geq 0.$$

Proof. Considering the system of differential equations (3.20), let's examine the first equation by using the Grownwell Inequality

$$\frac{ds}{dt} = \mu(1-s) - \frac{\beta_1 \kappa_1 p_1 s}{\alpha_1} - \frac{\beta_2 \kappa_2 p_2 s}{\alpha_2} + d_1 i_1 + d_2 i_2 + \delta_1 r_1 + \delta_2 r_2. \quad (3.21)$$

Now, observe that $\frac{ds}{dt} \geq -\frac{\beta_1 \kappa_1 p_1(x)s(x)}{\alpha_1} - \frac{\beta_2 \kappa_2 p_2(x)s(x)}{\alpha_2} \Rightarrow$

$$\int \frac{ds}{s} \geq \int \left(-\mu - \frac{\beta_1 \kappa_1 p_1(x)}{\alpha_1} - \frac{\beta_2 \kappa_2 p_2(x)}{\alpha_2} \right) dt. \quad (3.22)$$

Upon employing separation of variables and incorporating the initial condition, the solution is obtained as follows:

$$s(t) \geq s_0 e^{\int_0^t \left(-\mu - \frac{\beta_1 \kappa_1 p_1(x)}{\alpha_1} - \frac{\beta_2 \kappa_2 p_2(x)}{\alpha_2} \right) dt} \geq 0. \quad (3.23)$$

Similarly, we considered the second equation from (3.20), which is:

$$\frac{di_1}{dt} = \frac{\beta_1 \kappa_1 p_1 s}{\alpha_1} - (\mu + \gamma_1 + d_1)i_1 - \frac{\phi \beta_2 \kappa_2 p_2}{\alpha_2}, \quad (3.24)$$

it is true that:

$$\frac{di_1}{dt} \geq -(\mu + \gamma_1 + d_1)i_1 - \frac{\phi \beta_2 \kappa_2 p_2(x)i_1(x)}{\alpha_2}. \quad (3.25)$$

Upon employing separation of variables and incorporating the initial condition, the solution is obtained as follows:

$$\int \frac{di_1}{i_1} \geq \int -(\mu + \gamma_1 + d_1) - \frac{\phi \beta_2 \kappa_2 p_2(x)}{\alpha_2} dt \Rightarrow \quad (3.26)$$

$$i_1(t) \geq i_1^o e^{\int_0^t \left(-\mu + \gamma_1 + d_1 - \frac{\phi \beta_2 \kappa_2 p_2(x)}{\alpha_2} \right) dt} \geq 0. \quad (3.27)$$

Now, we consider the third equation from (3.20), which is:

$$\frac{di_2}{dt} = \frac{\beta_2 \kappa_2 p_2 s}{\alpha_2} - (\mu + \gamma_2 + d_2)i_2 + \frac{\phi \beta_2 \kappa_2 p_2 i_1}{\alpha_2} + (1 - \varepsilon) \frac{\beta_2 \kappa_2 p_2 r_2}{\alpha_2}. \quad (3.28)$$

It is true that:

$$\frac{di_2}{dt} \geq -(\mu + \gamma_2 + d_2)i_2(x) \Rightarrow \quad (3.29)$$

$$\int \frac{di_2}{i_2} \geq \int -(\mu + \gamma_2 + d_2)dt. \quad (3.30)$$

Now, employing separation of variables and incorporating the initial condition, the solution is obtained as follows:

$$i_2(t) \geq i_2^o e^{-\int_0^t (\mu + \gamma_2 + d_2)dt} \geq 0, \quad (3.31)$$

$$i_2(t) \geq i_2^o e^{-(\mu + \gamma_2 + d_2)t} \geq 0. \quad (3.32)$$

We select the fourth equation from (3.20), which is

$$\frac{dp_1}{dt} = \kappa_1 i_1 - \kappa_1 p_1. \quad (3.33)$$

It is also true that,

$$\frac{dp_1}{dt} \geq -\kappa_1 p_1 \Rightarrow \quad (3.34)$$

$$\frac{dp_1}{p_1} \geq -\kappa_1 dt. \quad (3.35)$$

Now, employing separation of variables and incorporating the initial condition, the solution is obtained as follows:

$$p_1(t) \geq p_1^o e^{\kappa_1 t} \geq 0. \quad (3.36)$$

We select the fifth equation from (3.20), which is

$$\frac{dp_2}{dt} = \kappa_2 i_2 - \kappa_2 p_2. \quad (3.37)$$

It is also true that,

$$\frac{dp_2}{dt} \geq -\kappa_2 p_2 \Rightarrow \quad (3.38)$$

$$\frac{dp_2}{p_2} \geq -\kappa_2 dt. \quad (3.39)$$

Now, employing separation of variables and incorporating the initial condition, the solution is

obtained as follows:

$$p_2(t) \geq p_2^o e^{\kappa_2 t} \geq 0. \quad (3.40)$$

Now we select the sixth equation from (3.20), which is

$$\frac{dr_1}{dt} = \gamma_1 i_1 - \mu r_1 - (1 - \varepsilon) \frac{\beta_2 \kappa_2 p_2 r_2}{\alpha_2} - \delta_1 r_1. \quad (3.41)$$

It is also true that,

$$\frac{dr_1}{dt} \geq -(\mu r_1 + \delta_1 r_1) \Rightarrow \quad (3.42)$$

$$\int \frac{dr_1}{r_1} \geq \int -(\mu + \delta_1) dt. \quad (3.43)$$

Similarly, employing separation of variables and incorporating the initial condition, the solution is obtained as follows:

$$r_1(t) \geq r_1^o e^{-(\mu + \delta_1)t} \geq 0. \quad (3.44)$$

Lastly, from the seventh equation of (3.20)

$$\frac{dr_2}{dt} = \gamma_2 i_2 - \mu r_2 - \delta_2 r_2. \quad (3.45)$$

It is also true that,

$$\frac{dr_2}{dt} \geq -\mu r_2 - \delta_2 r_2 \Rightarrow \quad (3.46)$$

$$\int \frac{dr_2}{r_2} \geq \int -(\mu + \delta_2) dt. \quad (3.47)$$

Lastly, employing separation of variables and incorporating the initial condition, the solution is obtained as follows:

$$r_2(t) \geq r_2^o e^{-(\mu + \delta_2)t} \geq 0. \quad (3.48)$$

This concludes the proof of the theorem. Consequently, the solution of the model is non-negative \square

3.6.2 Boundedness of the solution

Lemma 3. *Boundedness: Positive constants $s^c, i_1^c, i_2^c, p_1^c, p_2^c, r_1^c$, and r_2^c exist for the solutions $(s(t), i_1(t), i_2(t), p_1(t), p_2(t), r_1(t), r_2(t))$ of the model equation (3.20) such that*

$$\begin{aligned}
 \limsup_{t \rightarrow \infty} s(t) &\leq s^c, & \limsup_{t \rightarrow \infty} i_1(t) &\leq i_1^c, \\
 \limsup_{t \rightarrow \infty} i_2(t) &\leq i_2^c, & \limsup_{t \rightarrow \infty} p_1(t) &\leq p_1^c, \\
 \limsup_{t \rightarrow \infty} p_2(t) &\leq p_2^c, & \limsup_{t \rightarrow \infty} r_1(t) &\leq r_1^c, \\
 \text{and } \limsup_{t \rightarrow \infty} r_2(t) &\leq r_2^c.
 \end{aligned}$$

for all $t \in [0, t_0]$, where $t_0 > 0$ and the solution vector is positive.

Proof. To show boundedness, we add all the equations in (3.20) and we obtain Let the total population be

$$n(t) = s(t) + i_1(t) + i_2(t) + p_1(t) + p_2(t) + r_1(t) + r_2(t), \quad (3.49)$$

then:

$$\begin{aligned}
 \frac{dn}{dt} &= \frac{ds}{dt} + \frac{di_1}{dt} + \frac{di_2}{dt} + \frac{dp_1}{dt} + \frac{dp_2}{dt} + \frac{dr_1}{dt} + \frac{dr_2}{dt}, \\
 &= \mu - \mu(s + i_1 + i_2 + p_1 + p_2 + r_1 + r_2), \\
 &= \mu(1 - n).
 \end{aligned} \quad (3.50)$$

It follows

$$\frac{dn}{dt} = \mu - \mu n. \quad (3.51)$$

Integration both sides of (3.51) yields

$$\begin{aligned}
 \int_0^n \frac{dn}{\mu - \mu n} &= \int_0^t dt, \\
 -\frac{1}{\mu} \ln(1 - n) \Big|_{t_0}^t &= t.
 \end{aligned} \quad (3.52)$$

Further simplification of (3.52) result in

$$n_t = 1 - [1 - n_0] e^{-\mu t}. \quad (3.53)$$

By taking $t \rightarrow \infty$, then we obtain $n_t \leq 1$. This implies that the model in equation (3.20) can be studied in the feasible region.

$$\Gamma = \{(s, i_1, i_2, p_1, p_2, r_1, r_2) \in \mathbb{R}^7 \mid 0 \leq n_t \leq 1\}, \quad (3.54)$$

$$D = \{(s, i_1, i_2, p_1, p_2, r_1, r_2) \in \mathbb{R}_+^7 : s(t) + i_1(t) + i_2(t) + p_1(t) + p_2(t) + r_1(t) \leq 1\}.$$

3.6.3 Existence and Uniqueness Theorem

Equation (3.20) is an autonomous system with f defined in equation below. Thus, we have,

$$\left. \begin{aligned} f_1(s, i_1, i_2, p_1, p_2, r_1, r_2) &= \mu(1 - s) - \frac{\beta_1 \kappa_1 p_1 s}{\alpha_1} - \frac{\beta_2 \kappa_2 p_2 s}{\alpha_2} + d_1 i_1 + d_2 i_2 + \delta_1 r_1 + \delta_2 r_2 \\ f_2(s, i_1, i_2, p_1, p_2, r_1, r_2) &= \frac{\beta_1 \kappa_1 p_1 s}{\alpha_1} - (\mu + \gamma_1 + d_1) i_1 - \frac{\phi \beta_2 \kappa_2 p_2 i_1}{\alpha_2} \\ f_3(s, i_1, i_2, p_1, p_2, r_1, r_2) &= \frac{\beta_2 \kappa_2 p_2 s}{\alpha_2} - (\mu + \gamma_2 + d_2) i_2 + \frac{\phi \beta_2 \kappa_2 p_2 i_1}{\alpha_2} + (1 - \varepsilon) \frac{\beta_2 \kappa_2 p_2 r_1}{\alpha_2} \\ f_4(s, i_1, i_2, p_1, p_2, r_1, r_2) &= \kappa_1 i_1 - \kappa_1 p_1 \\ f_5(s, i_1, i_2, p_1, p_2, r_1, r_2) &= \kappa_2 i_2 - \kappa_2 p_2 \\ f_6(s, i_1, i_2, p_1, p_2, r_1, r_2) &= \gamma_1 i_1 - \mu r_1 - (1 - \varepsilon) \frac{\beta_2 \kappa_2 p_2 r_1}{\alpha_2} - \delta_1 r_1 \\ f_7(s, i_1, i_2, p_1, p_2, r_1, r_2) &= \gamma_2 i_2 - \mu r_2 - \delta_2 r_2 \end{aligned} \right\} \quad (3.55)$$

We use the following theorem to establish the existence and uniqueness of solution for the model (3.20). To prove this, we need the following standard results.

Lemma 4. *Existence and Uniqueness Theorem: Define the domain D such that $D = \{|t - t_0| \leq a, \|X - X_0\| \leq b\} \subset C^1$ where $X = (s, i_1, i_2, p_1, p_2, r_1, r_2)^T$ and $X_0 = (s^0, i_1^0, i_2^0, p_1^0, p_2^0, r_1^0, r_2^0)^T$.*

Then, the problem (3.55) written in matrix form $\dot{X} = f(X)$ has a unique solution in D if f is continuous in D and there exist constants $K_1, K_2, K_3, K_4, K_5, K_6, K_7$ such that

$$\left| \frac{\partial f}{\partial s} \right| < K_1, \quad \left| \frac{\partial f}{\partial i_1} \right| < K_2, \quad \left| \frac{\partial f}{\partial i_2} \right| < K_3, \quad \left| \frac{\partial f}{\partial p_1} \right| < K_4, \quad \left| \frac{\partial f}{\partial p_2} \right| < K_5, \quad \left| \frac{\partial f}{\partial r_1} \right| < K_6, \quad \left| \frac{\partial f}{\partial r_2} \right| < K_7,$$

Proof. We aim to demonstrate the existence and uniqueness of the solution to the system (3.55).

Existence Theorem: It is evident that the functions f_1, \dots, f_7 as defined in (3.55) are continuous and bounded in D . Therefore, there exists a solution in D

Uniqueness Theorem. It is left to prove the uniqueness of the solution. To show that there is a unique solution to the system of equations (3.55), we shall show that $\frac{\partial f_i}{\partial x_j}, i, j = 1, 2, \dots, 6$ are continuous and bounded. We explore the following partial derivatives for all the model equations (3.55). Starting from the first equation in the functions (3.55), we have:

$$\begin{aligned}
 \frac{\partial f_1}{\partial S} &= -\mu - \frac{\beta_1 \kappa_1 p_1}{\alpha_1} - \frac{\beta_2 \kappa_2 p_2}{\alpha_2}, & \left| \frac{\partial f_1}{\partial S} \right| &\leq K < \infty, & \frac{\partial f_1}{\partial i_1} &= d_1, & \left| \frac{\partial f_1}{\partial i_1} \right| &\leq K < \infty \\
 \frac{\partial f_1}{\partial i_2} &= d_2, & \left| \frac{\partial f_1}{\partial i_2} \right| &\leq K < \infty, & \frac{\partial f_1}{\partial p_1} &= -\frac{\beta_1 \kappa_1 s}{\alpha_1}, & \left| \frac{\partial f_1}{\partial p_1} \right| &\leq K < \infty \\
 \frac{\partial f_1}{\partial p_2} &= -\frac{\beta_2 \kappa_2 s}{\alpha_2}, & \left| \frac{\partial f_1}{\partial p_2} \right| &\leq K < \infty, & \frac{\partial f_1}{\partial r_1} &= \delta_1, & \left| \frac{\partial f_1}{\partial r_1} \right| &\leq K < \infty \\
 \frac{\partial f_1}{\partial r_2} &= \delta_2, & \left| \frac{\partial f_1}{\partial r_2} \right| &\leq K < \infty
 \end{aligned}$$

Similarly, by differentiating the function f_2 in (3.55), we have:

$$\begin{aligned}
 \frac{\partial f_2}{\partial s} &= -\frac{\beta_1 \kappa_1 p_1}{\alpha_1}, & \left| \frac{\partial f_2}{\partial s} \right| &\leq K < \infty, & \frac{\partial f_2}{\partial i_1} &= -(\mu + \gamma_1 + d_1) - \frac{\phi \beta_2 \kappa_2 p_2}{\alpha_2}, & \left| \frac{\partial f_2}{\partial i_1} \right| &\leq K < \infty \\
 \frac{\partial f_2}{\partial i_2} &= 0, & \left| \frac{\partial f_2}{\partial i_2} \right| &< \infty, & \frac{\partial f_2}{\partial p_1} &= -\frac{\beta_1 \kappa_1 s}{\alpha_1}, & \left| \frac{\partial f_2}{\partial p_1} \right| &\leq K < \infty \\
 \frac{\partial f_2}{\partial p_2} &= -\frac{\phi \beta_2 \kappa_2 s}{\alpha_2}, & \left| \frac{\partial f_2}{\partial p_2} \right| &\leq K < \infty, & \frac{\partial f_2}{\partial r_1} &= 0, & \left| \frac{\partial f_2}{\partial r_1} \right| &< \infty \\
 \frac{\partial f_2}{\partial r_2} &= 0, & \left| \frac{\partial f_2}{\partial r_2} \right| &< \infty,
 \end{aligned}$$

Upon differentiating the third equation in (3.55), we obtain:

$$\begin{aligned}
 \frac{\partial f_3}{\partial s} &= \frac{\beta_2 \kappa_2 p_2}{\alpha_2}, & \left| \frac{\partial f_3}{\partial s} \right| &\leq K < \infty, & \frac{\partial f_3}{\partial i_1} &= \frac{\phi \beta_2 \kappa_2 p_2}{\alpha_2}, & \left| \frac{\partial f_3}{\partial i_1} \right| &\leq K < \infty \\
 \frac{\partial f_3}{\partial i_2} &= -(\mu + \gamma_1 + d_1), & \left| \frac{\partial f_3}{\partial i_2} \right| &\leq K < \infty, & \frac{\partial f_3}{\partial p_1} &= 0, & \left| \frac{\partial f_3}{\partial p_1} \right| &< \infty \\
 \frac{\partial f_3}{\partial p_2} &= \frac{\beta_2 \kappa_2 r_1}{\alpha_2} - (1 - \epsilon) \frac{\beta_2 \kappa_2 r_1}{\alpha_2}, & \left| \frac{\partial f_3}{\partial p_2} \right| &\leq K < \infty, & \frac{\partial f_3}{\partial r_1} &= -(1 - \epsilon) \frac{\beta_2 \kappa_2 p_2}{\alpha_2}, & \left| \frac{\partial f_3}{\partial r_1} \right| &\leq K < \infty \\
 \frac{\partial f_3}{\partial r_2} &= 0, & \left| \frac{\partial f_3}{\partial r_2} \right| &< \infty,
 \end{aligned}$$

Within the functions, focusing on the fourth equation in (3.55), differentiation yields:

$$\begin{aligned}
 \frac{\partial f_4}{\partial s} &= 0, & \left| \frac{\partial f_4}{\partial s} \right| &< \infty, & \frac{\partial f_4}{\partial i_1} &= \kappa_1, & \left| \frac{\partial f_4}{\partial i_1} \right| &\leq K < \infty \\
 \frac{\partial f_4}{\partial i_2} &= 0, & \left| \frac{\partial f_4}{\partial i_2} \right| &< \infty, & \frac{\partial f_4}{\partial p_1} &= -\kappa_1, & \left| \frac{\partial f_4}{\partial p_1} \right| &\leq K < \infty \\
 \frac{\partial f_4}{\partial p_2} &= 0, & \left| \frac{\partial f_4}{\partial p_2} \right| &< \infty, & \frac{\partial f_4}{\partial r_1} &= 0, & \left| \frac{\partial f_4}{\partial r_1} \right| &< \infty, & \frac{\partial f_4}{\partial r_2} &= 0, & \left| \frac{\partial f_4}{\partial r_2} \right| &< \infty,
 \end{aligned}$$

Starting with the fifth equation in (3.55), and upon differentiation, we get

$$\begin{aligned} \frac{\partial f_5}{\partial s} &= 0, & \left| \frac{\partial f_5}{\partial s} \right| &< \infty, & \frac{\partial f_5}{\partial i_1} &= 0, & \left| \frac{\partial f_5}{\partial i_1} \right| &< \infty \\ \frac{\partial f_5}{\partial i_2} &= \kappa, & \left| \frac{\partial f_5}{\partial i_2} \right| &\leq K < \infty, & \frac{\partial f_5}{\partial p_1} &= 0, & \left| \frac{\partial f_5}{\partial p_1} \right| &< \infty \\ \frac{\partial f_5}{\partial p_2} &= -\kappa, & \left| \frac{\partial f_5}{\partial p_2} \right| &\leq K < \infty, & \frac{\partial f_5}{\partial r_1} &= 0, & \left| \frac{\partial f_5}{\partial r_1} \right| &< \infty \\ & & & & \frac{\partial f_5}{\partial r_2} &= 0, & \left| \frac{\partial f_5}{\partial r_2} \right| &< \infty, \end{aligned}$$

Considering the sixth equation among the functions (3.55), upon differentiation, we obtain:

$$\begin{aligned} \frac{\partial f_6}{\partial s} &= 0, & \left| \frac{\partial f_6}{\partial s} \right| &< \infty, & \frac{\partial f_6}{\partial i_1} &= \gamma_1, & \left| \frac{\partial f_6}{\partial i_1} \right| &\leq K < \infty \\ \frac{\partial f_6}{\partial i_2} &= 0, & \left| \frac{\partial f_6}{\partial i_2} \right| &< \infty, & \frac{\partial f_6}{\partial p_1} &= 0, & \left| \frac{\partial f_6}{\partial p_1} \right| &< \infty \\ \frac{\partial f_6}{\partial p_2} &= -(1-\epsilon)\frac{\beta_2\kappa_2r_1}{\alpha_2}, & \left| \frac{\partial f_6}{\partial p_2} \right| &\leq K < \infty, & \frac{\partial f_6}{\partial r_1} &= -\mu - (1-\epsilon)\frac{\beta_2\kappa_2p_2r_1}{\alpha_2} - \delta_1, & \left| \frac{\partial f_6}{\partial r_1} \right| &\leq K < \infty \\ \frac{\partial f_6}{\partial r_2} &= 0, & \left| \frac{\partial f_6}{\partial r_2} \right| &< \infty, \end{aligned}$$

finally based on the seventh equation from (3.55) we have

$$\begin{aligned} \frac{\partial f_7}{\partial s} &= 0, & \left| \frac{\partial f_7}{\partial s} \right| &< \infty, & \frac{\partial f_7}{\partial i_1} &= 0, & \left| \frac{\partial f_7}{\partial i_1} \right| &< \infty \\ \frac{\partial f_7}{\partial i_2} &= \gamma, & \left| \frac{\partial f_7}{\partial i_2} \right| &\leq K < \infty, & \frac{\partial f_7}{\partial p_1} &= 0, & \left| \frac{\partial f_7}{\partial p_1} \right| &< \infty \\ \frac{\partial f_7}{\partial p_2} &= 0, & \left| \frac{\partial f_7}{\partial p_2} \right| &< \infty, & \frac{\partial f_7}{\partial r_1} &= 0, & \left| \frac{\partial f_7}{\partial r_1} \right| &< \infty \\ & & & & \frac{\partial f_7}{\partial r_2} &= -\mu - \delta_2, & \left| \frac{\partial f_7}{\partial r_2} \right| &< \infty, \end{aligned}$$

Therefore, we have convincingly demonstrated that all these partial derivatives remain within finite bounds and exhibit continuity. As a result, we can conclude that a sole solution exists for the model equation (3.55)

3.6.4 Analysis of Equilibria

The full system exhibits four biologically relevant steady states: a disease-free state E_0 , two states where either strain 1 outcompetes strain 2 E_1 or strain 2 outcompetes strain 1 E_2 , and a coexistence steady state E_2 . These steady states represent equilibrium conditions where the system's dynamics stabilize, resulting in distinct population distributions.

3.6.5 Disease Free Equilibrium Point (E_0)

The process of identifying the Disease-Free Equilibrium (DFE) involved setting the right-hand side of the model (3.20) equations to zero. This was done by assessing it when $i_1 = i_2 = r_1 =$

$r_2 = p_1 = p_2 = 0$ and solving for the non-infected and non-carrier state variables. Consequently, we arrived at the disease-free equilibrium denoted as $E_0 = (1, 0, 0, 0, 0, 0, 0)$.

3.6.6 Reproduction Number(R_0)

The concept of the basic reproductive number R_0 was explored in this section. Here, we derived the pivotal parameter governing disease spread, known as the basic reproduction number.[23], to calculate this parameter, we employed the next-generation matrix method, where it represents the spectral radius of the next-generation matrix. The model equations are reformulated, commencing with newly infected classes.

Lemma 5. *If x_0 represents a Disease-Free Equilibrium (DFE) of equation (3.20), and $F_i(x)$ satisfies the assumptions through, then the derivatives $DF(x_0)$ and $DV(x_0)$ can be partitioned as:*

$$DF(x_0) = \begin{pmatrix} F & 0 \\ 0 & 0 \end{pmatrix}, \quad \text{and} \quad DV(x_0) = \begin{pmatrix} V & 0 \\ J_3 & J_4 \end{pmatrix},$$

where F and V are $m \times m$ matrices defined by $F = \left[\frac{\partial F_i}{\partial x_j}(x_0) \right]$ and $V = \left[\frac{\partial V_i}{\partial x_j}(x_0) \right]$, where $1 \leq i, j \leq m$. Additionally, F is non-negative, V is a non-singular M-matrix, and all eigenvalues of J_4 have positive real parts. Consequently, the matrix V^{-1} is non-negative, as is FV^{-1} .

If an infected individual is introduced into compartment k of a disease-free population, then the (j, k) entry of V^{-1} can be interpreted as the average length of time an individual spends in compartment j during its lifetime. The (i, j) entry of F can be interpreted as the rate at which infected individuals in compartment j produce new infections in compartment i .

The matrix FV^{-1} is referred to as the next-generation matrix for the model. The (i, k) entry of the next-generation matrix represents the expected number of new infections in compartment i produced by the infected individual originally placed into compartment k . The basic reproduction number, R_0 , is calculated as:

$$R_0 = \rho(FV^{-1}),$$

where $\rho(FV^{-1})$ denotes the spectral radius of FV^{-1} . R_0 serves as a threshold parameter for the stability of the DFE.

Proof

$$\left. \begin{aligned} \frac{di_1}{dt} &= \frac{\beta_1 \kappa_1 p_1 s}{\alpha_1} - (\mu + \gamma_1 + d_1)i_1 - \frac{\phi \beta_2 \kappa_2 p_2 i_1}{\alpha_2} \\ \frac{dp_1}{dt} &= \kappa_1 i_1 - \kappa_1 p_1 \\ \frac{di_2}{dt} &= \frac{\beta_2 \kappa_2 p_2 s}{\alpha_2} - (\mu + \gamma_2 + d_2)i_2 + \frac{\phi \beta_2 \kappa_2 p_2 i_1}{\alpha_2} + (1 - \varepsilon) \frac{\beta_2 \kappa_2 p_2 r_1}{\alpha_2} \\ \frac{dp_2}{dt} &= \kappa_2 i_2 - \kappa_2 p_2 \end{aligned} \right\} \quad (3.56)$$

Now by the principle of the next-generation matrix, we obtained

$$f(s, i_1, i_2) = \begin{bmatrix} \frac{\beta_1 \kappa_1 p_1 s}{\alpha_1} - \frac{\phi \beta_2 \kappa_2 p_2 i_1}{\alpha_2} & 0 \\ \frac{\beta_2 \kappa_2 p_2 s}{\alpha_1} + \frac{\phi \beta_2 \kappa_2 p_2 i_1}{\alpha_2} + (1 - \varepsilon) \frac{\beta_2 \kappa_2 p_2 r_1}{\alpha} & 0 \end{bmatrix}, \quad (3.47)$$

$$v(s, i_1, i_2) = \begin{bmatrix} (\mu + \alpha_1 + d_1) i_1 \\ -\kappa_1 i_1 + \kappa_1 p_1 \\ (\mu + \alpha_2 + d_2) i_2 \\ -\kappa_2 i_2 + \kappa_2 p_2 \end{bmatrix}. \quad (3.48)$$

The matrices of f and v evaluated at diseases free are given by F and V , respectively, such that:

$$F = \begin{pmatrix} 0 & \frac{\beta_1 \kappa_1}{\alpha_1} & 0 & 0 \\ 0 & 0 & 0 & 0 \\ 0 & 0 & 0 & \frac{\beta_2 \kappa_2}{\alpha_2} \\ 0 & 0 & 0 & 0 \end{pmatrix}, \quad (3.49)$$

$$V = \begin{pmatrix} (\mu + \gamma_1 + d_1) & 0 & 0 & 0 \\ -\kappa_1 & \kappa_1 & 0 & 0 \\ 0 & 0 & (\mu + \gamma_2 + d_2) & 0 \\ 0 & 0 & -\kappa_2 & \kappa_2 \end{pmatrix}. \quad (3.50)$$

Now the inverse of V is given by:

$$V^{-1} = \begin{pmatrix} \frac{1}{(\mu + \gamma_1 + d_1)} & 0 & 0 & 0 \\ \frac{1}{(\mu + \gamma_1 + d_1)} & \frac{1}{\kappa_1} & 0 & 0 \\ 0 & 0 & \frac{1}{(\mu + \gamma_1 + d_1)} & 0 \\ 0 & 0 & \frac{1}{(\mu + \gamma_2 + d_2)} & \frac{1}{\kappa_2} \end{pmatrix}. \quad (3.51)$$

Now we multiply F and V^{-1}

$$FV^{-1} = \begin{pmatrix} \frac{\beta_1 \kappa_1}{(\mu + \gamma_1 + d_1)\alpha_1} & \frac{\beta_1 \kappa_1}{\alpha_1} & 0 & 0 \\ 0 & 0 & 0 & 0 \\ 0 & 0 & \frac{\beta_2 \kappa_2}{(\mu + \gamma_2 + d_2)\alpha_2} & \frac{\beta_2 \kappa_2}{\alpha_2} \\ 0 & 0 & 0 & 0 \end{pmatrix}. \quad (3.52)$$

The eigenvalues of FV^{-1}

$$\lambda_3 = \frac{\beta_1 \kappa_1}{(\mu + \gamma_1 + d_1)\alpha_1}, \lambda_4 = \frac{\beta_2 \kappa_2}{(\mu + \gamma_2 + d_2)\alpha_2},$$

The primary eigenvalues of FV^{-1} correspond to the fundamental reproduction rates of respiratory diseases for susceptible (sensitive strain) and resistant strains. These values indicate the typical number of new infections originating from each infected person, encompassing both susceptible and resistant strains. Therefore, the fundamental reproduction rates for susceptible and resistant strains of respiratory diseases are:

$$R_0^s = \frac{\beta_1 \kappa_1}{(\mu + \gamma_1 + d_1)\alpha_1} \quad \text{and} \quad R_0^r = \frac{\beta_2 \kappa_2}{(\mu + \gamma_2 + d_2)\alpha_2}.$$

This implies that $R_0 = \max\{R_0^s; R_0^r\}$ where R_0^s and R_0^r are the sensitive and the resistant strain, respectively.

3.6.7 Other Equilibrium Points(E_1, E_2)

Strain 1 Outcompetes Strain 2 E_1

This implies that in the absence of a strong infection ($i_2 = 0$), there is no recovery from a strong infection ($r_2 = 0$), and there is also no environment with a strong infection ($p_2 = 0$). Setting the right-hand side of the model (3.20) equations to zero and substitute ($i_2 = 0, r_2 = 0, p_2 = 0$) we have the following steady state

$$E_1 = \left\{ \begin{array}{l} s = \frac{1}{R_0^s} \\ i_1 = \frac{\mu(\mu + \sigma_1)(\mu + \gamma_1 + d_1)(1 - R_0^s)}{((\mu + \gamma_1 + d_1)(d_1(\mu + \sigma_1) + \gamma_1\delta_1)R_0^s - \frac{\beta_1\kappa_1}{\alpha_1}(\mu + \sigma_1))} \\ i_2 = 0 \\ p_1 = \frac{\mu(\mu + \sigma_1)(\mu + \gamma_1 + d_1)(1 - R_0^s)}{((\mu + \gamma_1 + d_1)(d_1(\mu + \sigma_1) + \gamma_1\delta_1)R_0^s - \frac{\beta_1\kappa_1}{\alpha_1}(\mu + \sigma_1))} \\ p_2 = 0 \\ r_1 = \frac{\mu\gamma_1(\mu + \gamma_1 + d_1)(1 - R_0^s)}{((\mu + \gamma_1 + d_1)(d_1(\mu + \sigma_1) + \gamma_1\delta_1)R_0^s - \frac{\beta_1\kappa_1}{\alpha_1}(\mu + \sigma_1))} \\ r_2 = 0 \end{array} \right\}$$

Strain 2 Outcompetes Strain 1 (E_1)

This implies that in the absence of a strong infection ($i_1 = 0$), there is no recovery from a strong infection ($r_1 = 0$), and there is also no environment with a strong infection ($p_1 = 0$). Setting the right-hand side of the model (3.20) equations to zero and substitute ($i_1 = 0, r_1 = 0, p_1 = 0$) we have the following steady state:

$$E_1 = \left\{ \begin{array}{l} s = \frac{1}{R_0^r} \\ i_1 = 0 \\ i_2 = \frac{\mu(\mu + \sigma_2)(\mu + \gamma_2 + d_2)(1 - R_0^r)}{((\mu + \gamma_2 + d_2)(d_2(\mu + \sigma_2) + \gamma_2\delta_2)R_0^r - \frac{\beta_2\kappa_2}{\alpha_2}(\mu + \sigma_2))} \\ p_1 = 0 \\ p_2 = \frac{\mu(\mu + \sigma_2)(\mu + \gamma_2 + d_2)(1 - R_0^s)}{((\mu + \gamma_2 + d_2)(d_2(\mu + \sigma_2) + \gamma_2\delta_2)R_0^r - \frac{\beta_2\kappa_2}{\alpha_2}(\mu + \sigma_2))} \\ r_1 = 0 \\ r_2 = \frac{\mu\gamma_2(\mu + \gamma_2 + d_2)(1 - R_0^r)}{((\mu + \gamma_2 + d_2)(d_2(\mu + \sigma_2) + \gamma_2\delta_2)R_0^r - \frac{\beta_2\kappa_2}{\alpha_2}(\mu + \sigma_2))} \\ r_1 = 0 \end{array} \right\}$$

3.6.8 Local Stability of Disease Free

We establish E_0 , which represents the point when there are no strong or weak infections, implying no weak or strong recovery or environmental influence. At this point, the system has a constant solution $E_0 = (1, 0, 0, 0, 0, 0, 0)$.

Proposition 1. *The disease-free equilibrium point is locally asymptotically stable if $R_0 < 1$ and unstable if $R_0 > 1$.*

Proof. To prove this theorem, first, we obtain the Jacobian matrix of system (3.20) at the disease-free equilibrium E_0 as follows:

$$J(E_0) = \begin{pmatrix} -\mu & d_1 & -\theta_1 & d_2 & -\theta_2 & \delta_1 & \delta_2 \\ 0 & -m_1 & \theta_1 & 0 & 0 & 0 & 0 \\ 0 & \kappa_1 & -\kappa_1 & 0 & 0 & 0 & 0 \\ 0 & 0 & 0 & -m_2 & \theta_2 & 0 & 0 \\ 0 & 0 & 0 & \kappa_2 & -\kappa_2 & 0 & 0 \\ 0 & \gamma_1 & 0 & 0 & 0 & -m_3 & 0 \\ 0 & 0 & 0 & \gamma_2 & 0 & 0 & -m_4 \end{pmatrix}. \quad (3.57)$$

where $m_1 = (\mu + \gamma_1 + d_1)$, $m_2 = (\mu + \gamma_2 + d_2)$, $\theta_1 = \frac{\beta_1 \kappa_1}{\alpha_1}$, $\theta_2 = \frac{\beta_2 \kappa_2}{\alpha_2}$, $m_3 = (\mu + \sigma_1)$ and $m_4 = (\mu + \sigma_2)$

From the Jacobian (3.57) above the eigenvalues are

$$\lambda = -\mu, \lambda = -m_3, \lambda = -m_4, \lambda = -m_2,$$

and the roots are of the characteristic equation

$$a_1 \lambda^4 + a_2 \lambda^3 + a_3 \lambda^2 + a_4 \lambda + a_5 = 0, \quad (3.58)$$

with

$$a_1 = 1$$

$$a_2 = m_1 + m_2 + \kappa_1 + \kappa_2,$$

$$a_3 = m_1 m_2 + m_1 \kappa_1 (1 - R_0^s) + m_2 \kappa_1 + m_1 \kappa_2 + m_2 \kappa_2 (1 - R_0^r) + \kappa_1 \kappa_2,$$

$$a_4 = m_1 m_2 \kappa_2 (1 - R_0^r) \kappa_1 \kappa_1 \kappa_2 (1 - R_0^s) + m_2 \kappa_1 \kappa_2 (1 - R_0^s) + m_1 m_2 \kappa_2 (1 - R_0^s),$$

$$a_5 = m_1 m_2 \kappa_1 \kappa_2 (1 - R_0^r) + \theta_1 \theta_2 (1 - \frac{1}{R_0^r}).$$

Now we observe that

$$\lambda = -\mu < 0,$$

$$\lambda = -m_3 < 0,$$

$$\lambda = -m_4 < 0,$$

$$\lambda = -m_2 < 0,$$

We applied Routh-Hurwitz criteria. By the principle of Routh-Hurwitz criteria, (3.58) has strictly negative real roots if and only if $a_1 > 0$, $a_3 > 0$, $a_4 > 0$, and $a_1 a_2 a_3 > a_3^2 + a_1 a_4$.

Obviously, we see that a_2 is positive because it is a sum of positive variables, but for a_3 to be positive, $m_1 m_2 + m_1 \kappa_1 (1 - R_0^s) + m_2 \kappa_1 + m_1 \kappa_2 + m_2 \kappa_2 (1 - R_0^r) + \kappa_1 \kappa_2, R_0^s$ and R_0^r must be less 1. Also, for a_4 to be positive, $m_1 m_2 \kappa_2 (1 - R_0^r) \kappa_1 \kappa_1 \kappa_2 (1 - R_0^s) + m_2 \kappa_1 \kappa_2 (1 - R_0^s) + m_1 m_2 \kappa_2 (1 - R_0^s), R_0^s$ and R_0^r must be less 1. Lastly, for a_5 to be positive, $m_1 m_2 \kappa_1 \kappa_2 (1 - R_0^r) + \theta_1 \theta_2 (1 - \frac{1}{R_0^r}), R_0^s < 1$ leads to $R_0 < 1$. Therefore, the disease-free equilibrium (DFE) will be locally asymptotically stable if and only if $R_0 < 1$.

3.6.9 Local Stability of Strain 1 Outcompetes Strain 2 (E_1)

Proposition 2. *The equilibrium point E_1 is locally asymptotically stable if $R_0 < 1$ and unstable if $R_0 > 1$.*

Proof. To prove this theorem, first, we obtain the Jacobian matrix of system (3.20) at equilib-

rium E_1 as follows:

$$\begin{bmatrix}
 -\mu - \frac{m_3 m_1 \mu (1 - R_0^s)}{(d_1 m_3 - m_1 m_3 + \gamma_1 \delta_1)} & d_1 & -m_1 & d_2 & -\frac{m_1 \theta_2}{\theta_1} & \delta_1 & \delta_2 \\
 \frac{m_3 m_1 \mu (1 - R_0^s)}{(d_1 m_3 - m_1 m_3 + \gamma_1 \delta_1)} & -m_1 & m_1 & 0 & -\frac{m_3 m_1 \mu \phi (1 - R_0^s)}{(d_1 m_3 - m_1 m_3 + \gamma_1 \delta_1)} & 0 & 0 \\
 0 & \kappa_1 & -\kappa_1 & 0 & 0 & 0 & 0 \\
 0 & 0 & 0 & -m_2 & \frac{m_3 m_1 \mu \phi (1 - R_0^s)}{(d_1 m_3 - m_1 m_3 + \gamma_1 \delta_1)} + \frac{m_1 \theta_2}{\theta_1} + \frac{\epsilon \mu \gamma_1 m_1 (1 - R_0^s)}{(d_1 m_3 - m_1 m_3 + \gamma_1 \delta_1)} & 0 & 0 \\
 0 & 0 & 0 & \kappa_2 & -\kappa_2 & 0 & 0 \\
 0 & \gamma_1 & 0 & 0 & -\frac{\epsilon \mu \gamma_1 m_1 (1 - R_0^s)}{(d_1 m_3 - m_1 m_3 + \gamma_1 \delta_1)} & -m_3 & 0 \\
 0 & 0 & 0 & \gamma_2 & 0 & 0 & -m_4
 \end{bmatrix}. \quad (3.59)$$

now we simplify the above matrix to

$$J(E_2) = \begin{bmatrix}
 -\Phi_1 & d_1 & -m_1 & d_2 & -\Phi_2 & \delta_1 & \delta_2 \\
 \Phi_3 & -m_1 & m_1 & 0 & -\Phi_4 & 0 & 0 \\
 0 & \kappa_1 & -\kappa_1 & 0 & 0 & 0 & 0 \\
 0 & 0 & 0 & -m_2 & \Phi_5 & 0 & 0 \\
 0 & 0 & 0 & \kappa_2 & -\kappa_2 & 0 & 0 \\
 0 & \gamma_1 & 0 & 0 & \Phi_6 & -m_3 & 0 \\
 0 & 0 & 0 & \gamma_2 & 0 & 0 & -m_4
 \end{bmatrix}. \quad (3.60)$$

Where

$$\begin{aligned}
 \Phi_1 &= \mu + \frac{m_3 m_1 \mu (1 - R_0^s)}{(d_1 m_3 - m_1 m_3 + \gamma_1 \delta_1)}, \\
 \Phi_2 &= \frac{m_1 \theta_2}{\theta_1}, \\
 \Phi_3 &= \frac{m_3 m_1 \mu (1 - R_0^s)}{(d_1 m_3 - m_1 m_3 + \gamma_1 \delta_1)}, \\
 \Phi_4 &= \frac{m_3 m_1 \mu \phi (1 - R_0^s)}{(d_1 m_3 - m_1 m_3 + \gamma_1 \delta_1)}, \\
 \Phi_5 &= \frac{m_3 m_1 \mu \phi (1 - R_0^s)}{(d_1 m_3 - m_1 m_3 + \gamma_1 \delta_1) \theta_1} + \frac{m_1 \theta_2}{\theta_1} + \frac{\epsilon \mu \gamma_1 m_1 (1 - R_0^s)}{(d_1 m_3 - m_1 m_3 + \gamma_1 \delta_1)}, \\
 \Phi_6 &= \frac{\epsilon \mu \gamma_1 m_1 (1 - R_0^s)}{(d_1 m_3 - m_1 m_3 + \gamma_1 \delta_1)}
 \end{aligned}$$

with eigenvalues satisfying the following characteristic equation:

$$|\lambda I - J(E_1)| = 0. \quad (3.61)$$

Where I represents the identity matrix. To simplify, let $\lambda I - J(E_1)$ be denoted as $(b_{ij})_{7 \times 7}$. Here, if $i \neq j$, $b_{ij} = -a_{ij}$, and if $i = j$, $b_{ii} = \lambda - a_{ii}$. It's noteworthy that $-\kappa_2 = \lambda$. When expanding Equation (3.60) along the last column, we have:

$$|\lambda E - J(E_1)| = b_{77} \begin{vmatrix} b_{11} & b_{12} & b_{13} & b_{14} & b_{15} & b_{16} \\ b_{21} & b_{22} & 0 & 0 & b_{25} & 0 \\ 0 & b_{32} & b_{33} & 0 & 0 & 0 \\ 0 & 0 & 0 & b_{44} & b_{45} & 0 \\ 0 & 0 & b_{53} & b_{54} & b_{55} & 0 \\ 0 & b_{62} & 0 & 0 & b_{65} & b_{66} \end{vmatrix} \quad (3.62)$$

Expanding along the first column results in

$$|\lambda I - J(E_1)| = b_{77} b_{44} \begin{vmatrix} b_{11} & b_{25} \\ b_{51} & b_{55} \end{vmatrix} \begin{vmatrix} b_{22} & b_{26} \\ b_{62} & b_{66} \end{vmatrix} \quad (3.63)$$

$$= (-\lambda - \Phi_1)(-\lambda - m_3)(-\lambda - m_1)(-\lambda - \kappa_1) |(\lambda I - D_1)| |(\lambda I - D_2)| \quad (3.64)$$

where

$$D_1 = \begin{bmatrix} -\Phi_1 & -\Phi_2 \\ 0 & -\kappa_2 \end{bmatrix}, \quad D_2 = \begin{bmatrix} -m_1 & 0 \\ \phi_1 & -m_3 \end{bmatrix}$$

It's evident that certain solutions to the given equation include $\lambda_1 = -m_1$, $\lambda_2 = -m_3$, $\lambda_3 = \kappa_2$, and $\lambda_4 = \kappa_1$. Now by Routh-Hurwitz criteria, the stability assessment of the matrix $J(E_2)$ relies on matrices D_1 and D_2 . It's notable that $\text{Tr}(D_1) < 0$, $\text{Det}(D_1) > 0$, and all eigenvalues of D_1 exhibit negative real components.

When $R_0 < 1$, $\text{Tr}(D_2) < 0$, $\text{Det}(D_2) > 0$, and all eigenvalues of D_2 have negative real components. Consequently, all eigenvalues of $J(E_1)$ have negative real components. Conversely, when $R_0 > 1$, $\text{Det}(D_2) < 0$, indicating the presence of at least one positive eigenvalue of $J(E_1)$. Thus, E_1 is locally asymptotically stable for $R_0 < 1$ and unstable for $R_0 > 1$. This concludes the stability proof for E_1 .

3.6.10 Local Stability of Strain 2 Outcompetes Strain 1 (E_2)

Proposition 2. *The equilibrium point E_2 is locally asymptotically stable if $R_0 < 1$ and unstable if $R_0 > 1$.*

Proof. To prove this theorem, first, we obtain the Jacobian matrix of system (3.20) at equilibrium E_1 as follows:

$$\begin{bmatrix}
 -\mu - \frac{m_4 m_2 \mu (1 - R_0^r)}{(d_2 m_2 - m_2 m_4 + \gamma_2 \delta_2)} & d_1 & -\frac{m_2 \theta_1}{\theta_2} & d_2 & -m_2 & \delta_1 & \delta_2 \\
 0 & -m_1 - \frac{m_4 m_2 \mu \phi (1 - R_0^r)}{(d_2 m_2 - m_2 m_4 + \gamma_2 \delta_2)} & \frac{m_2 \theta_1}{\theta_2} & 0 & 0 & 0 & 0 \\
 0 & \kappa_1 & -\kappa_1 & 0 & 0 & 0 & 0 \\
 \frac{m_4 m_2 \mu (1 - R_0^r)}{(d_2 m_2 - m_2 m_4 + \gamma_2 \delta_2)} & \frac{m_4 m_2 \mu \phi (1 - R_0^r)}{(d_2 m_2 - m_2 m_4 + \gamma_2 \delta_2)} & 0 & -m_2 & m_2 & \frac{m_4 m_2 \mu \epsilon (1 - R_0^r)}{(d_2 m_2 - m_2 m_4 + \gamma_2 \delta_2)} & 0 \\
 0 & 0 & 0 & \kappa_2 & -\kappa_2 & 0 & 0 \\
 0 & \gamma_1 & 0 & 0 & 0 & -m_3 - \frac{m_4 m_2 \mu \epsilon (1 - R_0^r)}{(d_2 m_2 - m_2 m_4 + \gamma_2 \delta_2)} & 0 \\
 0 & 0 & 0 & \gamma_2 & 0 & 0 & -m_4
 \end{bmatrix} \quad (3.65)$$

now we simplify the above matrix to

$$J(E_2) = \begin{bmatrix}
 -\Gamma_1 & d_1 & -\frac{m_2 \theta_1}{\theta_2} & d_2 & -m_2 & \delta_1 & \delta_2 \\
 0 & -\Gamma_2 & \frac{m_2 \theta_1}{\theta_2} & 0 & 0 & 0 & 0 \\
 0 & \kappa_1 & -\kappa_1 & 0 & 0 & 0 & 0 \\
 \Gamma_3 & \Gamma_4 & 0 & -m_2 & m_2 & \Gamma_5 & 0 \\
 0 & 0 & 0 & \kappa_2 & -\kappa_2 & 0 & 0 \\
 0 & \gamma_1 & 0 & 0 & 0 & -\Gamma_6 & 0 \\
 0 & 0 & 0 & \gamma_2 & 0 & 0 & -m_4
 \end{bmatrix}. \quad (3.66)$$

Where

$$\begin{aligned}
 \Gamma_1 &= \mu + \frac{m_4 m_2 \mu (1 - R_0^r)}{(d_2 m_2 - m_2 m_4)}, \\
 \Gamma_2 &= m_1 + \frac{m_4 m_2 \mu \phi (1 - R_0^r)}{(d_2 m_2 - m_2 m_4 + \gamma_2 \delta_2)}, \\
 \Gamma_3 &= \frac{m_4 m_2 \mu (1 - R_0^r)}{(d_2 m_2 - m_2 m_4 + \gamma_2 \delta_2)}, \\
 \Gamma_4 &= \frac{m_4 m_2 \mu \phi (1 - R_0^r)}{(d_2 m_2 - m_2 m_4 + \gamma_2 \delta_2)}, \\
 \Gamma_5 &= \frac{m_4 m_2 \mu \epsilon (1 - R_0^r)}{(d_2 m_2 - m_2 m_4 + \gamma_2 \delta_2)}, \\
 \Gamma_6 &= m_3 + \frac{m_4 m_2 \mu \epsilon (1 - R_0^r)}{(d_2 m_2 - m_2 m_4 + \gamma_2 \delta_2)}.
 \end{aligned}$$

with eigenvalues satisfying the following characteristic equation:

$$|\lambda I - J(E_2)| = 0. \quad (3.67)$$

Where I represents the identity matrix. To simplify, let $\lambda I - J(E_2)$ be denoted as $(b_{ij})_{7 \times 7}$. Here, if $i \neq j$, $b_{ij} = -a_{ij}$, and if $i = j$, $b_{ii} = \lambda - a_{ii}$. It's noteworthy that $\Gamma_2 = \lambda$. When expanding Equation (3.60) along the last column, we have:

$$|\lambda E - J(E_2)| = c_{77} \begin{vmatrix} c_{11} & c_{12} & c_{13} & c_{14} & c_{15} & c_{16} \\ 0 & c_{22} & c_{22} & 0 & 0 & 0 \\ 0 & c_{32} & c_{33} & 0 & 0 & 0 \\ c_{41} & c_{42} & 0 & c_{44} & c_{45} & c_{46} \\ 0 & 0 & 0 & c_{54} & c_{55} & 0 \\ 0 & b_{62} & 0 & 0 & 0 & c_{66} \end{vmatrix}. \quad (3.68)$$

Expanding along the first column results in

$$\begin{aligned}
 |\lambda I - J(E_2)| &= c_{77} c_{44} \begin{vmatrix} c_{11} & c_{25} \\ c_{51} & c_{55} \end{vmatrix} \begin{vmatrix} c_{22} & c_{26} \\ c_{62} & c_{66} \end{vmatrix}, \\
 &= (-\lambda - \Gamma_1)(-\lambda - m_4)(-\lambda - \kappa_1)(-\lambda - \kappa_2) |(\lambda I - H_1)| |(\lambda I - H_2)|
 \end{aligned} \quad (3.69)$$

where

$$H_1 = \begin{bmatrix} -\Gamma_1 & -\delta_1 \\ 0 & -\Gamma_2 \end{bmatrix} \quad H_2 = \begin{bmatrix} -\Gamma_2 & \delta \\ 0 & -m_4 \end{bmatrix}$$

It's evident that certain solutions to the given equation include $\lambda_1 = -m_4$, $\lambda_2 = -\Gamma_1$, $\lambda_3 = \kappa_2$, and $\lambda_4 = \kappa_1$. Now by Routh-Hurwitz criteria, the stability assessment of the matrix $J(E_2)$ relies on matrices H_1 and H_2 . It's notable that $\text{Tr}(H_1) < 0$, $\text{Det}(H_1) > 0$, and all eigenvalues of D_1 exhibit negative real components.

When $R_0 < 1$, $\text{Tr}(H_2) < 0$, $\text{Det}(H_2) > 0$, and all eigenvalues of H_2 have negative real components. Consequently, all eigenvalues of $J(E_1)$ have negative real components. Conversely, when $R_0 > 1$, $\text{Det}(H_2) < 0$, indicating the presence of at least one positive eigenvalue of $J(E_2)$. Thus, E_1 is locally asymptotically stable for $R_0 < 1$ and unstable for $R_0 > 1$. This concludes the stability proof for E_2 .

3.6.11 Global Stability Analysis for (E_0)

The diseases free equilibrium point (E_0) for the system (3.20) is globally asymptotically stable provided $R_0 < 1$ and unstable if $R_0 > 1$

Proof: Following [14], we write the system (3.20) in the form:

$$\begin{aligned} X'(t) &= F(X, Y), \\ Y'(t) &= G(X, Y), \quad G(X, 0) = 0. \end{aligned} \tag{3.70}$$

where $X = (s, r_1, r_2)$ and $Y = (i_1, i_2, p_1, p_2)$. Here the components of $X \in \mathbb{R}_+^3$ denote the number of uninfected individuals, and the components of $Y \in \mathbb{R}_+^4$ denote the number of infected individuals. The disease-free equilibrium is now denoted by E_0 . We have to prove two conditions,

- (K1) For $X(t) = F(X, 0)$, X is globally asymptotically stable;
- (K2) $G(X, Y) = UY - G(X, Y)$, $\hat{G}(X, Y)$, $\hat{G}(X, Y) \geq 0$ for $(X, Y) \in \Phi$ are satisfied, where Φ_1 is a positively invariant attracting domain.

Theorem 6. *The fixed point $U_0 = (x^*, 0)$ is a globally asymptotically stable equilibrium of (3.70) provided that $R_0 < 1$ and assumptions (K1) and (K2) are satisfied.*

Proof

$$F(X, Y) = \begin{bmatrix} \mu(1-s) - \frac{\beta_1 \kappa_1 p_1 s}{\alpha_1} - \frac{\beta_2 \kappa_2 p_2 s}{\alpha_2} + d_1 i_1 + d_2 i_2 + \delta_1 r_1 + \delta_2 r_2 \\ \gamma_1 i_1 - \mu r_1 - (1-\varepsilon) \frac{\beta_2 \kappa_2 p_2 r_1}{\alpha_2} - \delta_1 r_1 \\ \gamma_2 i_2 - \mu r_2 - \delta_2 r_2 \end{bmatrix} \quad (3.64)$$

Now we substitute the diseases free equilibrium point (E_0) in $F(X, Y)$ we have,

$$F(X, 0) = \begin{bmatrix} \mu(1-s) \\ 0 \\ 0 \end{bmatrix} \cdot \geq 0 \quad (3.65)$$

Since $\mu(1-s) \geq 0$, that is $s \leq 1$. Thus $F(X, 0)$ is globally asymptotically stable. \square

Now we find U

$$\hat{G}(X, Y) = \begin{bmatrix} \frac{\beta_1 \kappa_1 p_1 s}{\alpha_1} - (\mu + \gamma_1 + d_1) i_1 - \frac{\phi \beta_2 \kappa_2 p_2 i_1}{\alpha_2} \\ \kappa_1 i_1 - \kappa_1 p_1 \\ \frac{\beta_2 \kappa_2 p_2 s}{\alpha_2} - (\mu + \gamma_2 + d_2) i_2 + \frac{\phi \beta_2 \kappa_2 p_2 i_1}{\alpha_2} + (1-\varepsilon) \frac{\beta_2 \kappa_2 p_2 r_1}{\alpha_2} \\ \kappa_2 i_2 - \kappa_2 p_2 \end{bmatrix} \cdot \quad (3.66)$$

Finding the Jacobian of u and substitute the disease free equilibrium point we have,

$$U = \begin{bmatrix} -(\mu + \gamma_1 + d_1) & \frac{\beta_1 \kappa_1}{\alpha_1} & 0 & 0 \\ \kappa_1 & -\kappa_1 & 0 & 0 \\ 0 & 0 & -(\mu + \gamma_2 + d_2) & \frac{\beta_2 \kappa_2}{\alpha_2} \\ 0 & 0 & -\kappa_2 & -\kappa_2 \end{bmatrix} \cdot \quad (3.67)$$

Now we find UY as follows

$$UY = \begin{bmatrix} -(\mu + \gamma_1 + d_1) & \frac{\beta_1 \kappa_1}{\alpha_1} & 0 & 0 \\ \kappa_1 & -\kappa_1 & 0 & 0 \\ 0 & 0 & -(\mu + \gamma_2 + d_2) & \frac{\beta_2 \kappa_2}{\alpha_2} \\ 0 & 0 & -\kappa_2 & -\kappa_2 \end{bmatrix} \begin{bmatrix} i_1 \\ p_1 \\ i_2 \\ p_2 \end{bmatrix}. \quad (3.68)$$

This simplifies to ,

$$UY = \begin{bmatrix} -(\mu + \gamma_1 + d_1)i_1 + \frac{\beta_1 \kappa_1 p_1}{\alpha_1} \\ \kappa_1 i_1 - \kappa_1 p_1 \\ -(\mu + \gamma_2 + d_2)i_2 + \frac{\beta_2 \kappa_2 p_2}{\alpha_2} \\ \kappa_2 i_2 - \kappa_2 p_2 \end{bmatrix}. \quad (3.69)$$

Now we use UY and $\hat{G}(X, Y)$ to find $G(X, Y)$

$$G(X, Y) = UY - \hat{G}(X, Y)$$

$$G(X, Y) = \begin{bmatrix} -(\mu + \gamma_1 + d_1)i_1 + \frac{\beta_1 \kappa_1 p_1}{\alpha_1} \\ \kappa_1 i_1 - \kappa_1 p_1 \\ -(\mu + \gamma_2 + d_2)i_2 + \frac{\beta_2 \kappa_2 p_2}{\alpha_2} \\ \kappa_2 i_2 - \kappa_2 p_2 \end{bmatrix} - \begin{bmatrix} \frac{\beta_1 \kappa_1 p_1 s}{\alpha_1} - (\mu + \gamma_1 + d_1)i_1 - \frac{\phi \beta_2 \kappa_2 p_2 i_1}{\alpha_2} \\ \kappa_1 i_1 - \kappa_1 p_1 \\ \frac{\beta_2 \kappa_2 p_2 s}{\alpha_2} - (\mu + \gamma_2 + d_2)i_2 + \frac{\phi \beta_2 \kappa_2 p_2 i_1}{\alpha_2} + (1 - \varepsilon) \frac{\beta_2 \kappa_2 p_2 r_1}{\alpha_2} \\ \kappa_2 i_2 - \kappa_2 p_2 \end{bmatrix}. \quad (3.70)$$

$$G(X, Y) = \begin{bmatrix} \frac{\beta_1 \kappa_1 p_1}{\alpha_1} - \frac{\beta_1 \kappa_1 p_1 s}{\alpha_1} + \frac{\phi \beta_2 \kappa_2 p_2 i_1}{\alpha_2} \\ 0 \\ \frac{\beta_2 \kappa_2 p_2}{\alpha_2} - \frac{\beta_2 \kappa_2 p_2 s}{\alpha_2} - \frac{\phi \beta_2 \kappa_2 p_2 i_1}{\alpha_2} - (1 - \varepsilon) \frac{\beta_2 \kappa_2 p_2 r_1}{\alpha_2} \\ 0 \end{bmatrix}. \quad (3.71)$$

Factoring out the common terms we have,

$$G(X, Y) = \begin{bmatrix} \frac{\beta_1 \kappa_1 p_1}{\alpha_1} (1 - s) + \frac{\phi \beta_2 \kappa_2 p_2 i_1}{\alpha_2} & 0 \\ \frac{\beta_2 \kappa_2 p_2}{\alpha_2} (1 - (s + \phi i_1 + (1 - \varepsilon))) & 0 \end{bmatrix} \geq 0. \quad (3.72)$$

If $\phi > 1$, then $(s + \phi i_1 + (1 - \varepsilon)) > 1$, and if $\phi < 1$, then $(s + \phi i_1 + (1 - \varepsilon)) < 1$, implying that $G(X, Y)$ is conditionally globally asymptotically stable.

3.6.12 Analysis of Bifurcation

Theorem

1. If $R_0 < 1$, system (3.20) exhibits a forward bifurcation when $R_0 = 1$.
2. If $R_0 > 1$, system (3.20) exhibits a backward bifurcation when $R_0 = 1$.

Proof: We make use of the centre manifold approach as described[13] in and introduce $x_1 = s, x_2 = i_1, x_3 = i_2, x_4 = x_1, x_5 = p_2, x_6 = r_1$, and $x_7 = r_2$. The system of equations in (3.20) becomes,

$$\left. \begin{aligned} \frac{dx_1}{dt} &= \mu(1 - x_1) - \frac{\beta_1 \kappa_1 x_4 x_1}{\alpha_1} - \frac{\beta_2 \kappa_2 x_5 x_1}{\alpha_2} + d_1 x_2 + d_2 x_3 + \delta_1 x_6 + \delta_2 x_7 \\ \frac{dx_2}{dt} &= \frac{\beta_1 \kappa_1 x_4 x_1}{\alpha_1} - (\mu + \gamma_1 + d_1) x_2 - \frac{\phi \beta_2 \kappa_2 x_5 x_2}{\alpha_2} \\ \frac{dx_3}{dt} &= \frac{\beta_2 \kappa_2 x_5 x_1}{\alpha_2} - (\mu + \gamma_2 + d_2) x_3 + \frac{\phi \beta_2 \kappa_2 x_5 x_2}{\alpha_2} + (1 - \varepsilon) \frac{\beta_2 \kappa_2 x_5 x_6}{\alpha_2} \\ \frac{dx_4}{dt} &= \kappa_1 x_2 - \kappa_1 x_4 \\ \frac{dx_5}{dt} &= \kappa_2 x_3 - \kappa_2 x_5 \\ \frac{dx_6}{dt} &= \gamma_1 x_2 - \mu x_6 - (1 - \varepsilon) \frac{\beta_2 \kappa_2 x_5 x_6}{\alpha_2} - \delta_1 x_6 \\ \frac{dx_7}{dt} &= \gamma_2 x_3 - \mu x_7 - \delta_2 x_7 \end{aligned} \right\}. \quad (3.71)$$

The Jacobian of the above system of equation (3.71) at disease free is given by;

$$J(E_0) = \begin{bmatrix} -\mu & d_1 & -\frac{\beta_1 \kappa_1}{\alpha_1} & d_2 & -\frac{\beta_2 \kappa_2}{\alpha_2} & \delta_1 & \delta_2 \\ 0 & -(\mu + \gamma_1 + d_1) & \frac{\beta_1 \kappa_1}{\alpha_1} & 0 & 0 & 0 & 0 \\ 0 & \kappa_1 & -\kappa_1 & 0 & 0 & 0 & 0 \\ 0 & 0 & 0 & -(\mu + \gamma_2 + d_2) & \frac{\beta_2 \kappa_2}{\alpha_2} & 0 & 0 \\ 0 & 0 & 0 & \kappa_2 & -\kappa_2 & 0 & 0 \\ 0 & \gamma_1 & 0 & 0 & 0 & -(\mu + \sigma_1) & 0 \\ 0 & 0 & 0 & \gamma_2 & 0 & 0 & -(\mu + \sigma_2) \end{bmatrix}. \quad (3.72)$$

Castillo Chavez and Song describe the following method to examine the direction of the bifurcation at $R_0 = 1$:

$$A = D_{wf}(0, 0) = \left(\frac{\partial f_i}{\partial w_1}(0, 0) \right) \quad (3.73)$$

is the linearization matrix of a general system of ordinary differential equations, the linearization matrix is computed around the equilibrium point 0, considering a bifurcation parameter evaluated at 0. The matrix A has a simple eigenvalue of zero, while all other eigenvalues have negative real parts. A possesses both a right eigenvector, denoted as R , and a left eigenvector, denoted as L , corresponding to the zero eigenvalue.

An eigenvector associated with the eigenvalue 0 for matrix A is denoted as

$$\mathbf{W} = (w_1, w_2, w_3, w_4, w_5, w_6, w_7)^T.$$

Now

$$\begin{bmatrix} -\mu & d_1 & -\frac{\beta_1 \kappa_1}{\alpha_1} & d_2 & -\frac{\beta_2 \kappa_2}{\alpha_2} & \delta_1 & \delta_2 \\ 0 & -(\mu + \gamma_1 + d_1) & \frac{\beta_1 \kappa_1}{\alpha_1} & 0 & 0 & 0 & 0 \\ 0 & \kappa_1 & -\kappa_1 & 0 & 0 & 0 & 0 \\ 0 & 0 & 0 & -(\mu + \gamma_2 + d_2) & \frac{\beta_2 \kappa_2}{\alpha_2} & 0 & 0 \\ 0 & 0 & 0 & \kappa_2 & -\kappa_2 & 0 & 0 \\ 0 & \gamma_1 & 0 & 0 & 0 & -(\mu + \sigma_1) & 0 \\ 0 & 0 & 0 & \gamma_2 & 0 & 0 & -(\mu + \sigma_2) \end{bmatrix} \begin{bmatrix} w_1 \\ w_2 \\ w_3 \\ w_4 \\ w_5 \\ w_6 \\ w_7 \end{bmatrix} = \begin{bmatrix} 0 \\ 0 \\ 0 \\ 0 \\ 0 \\ 0 \\ 0 \end{bmatrix}. \quad (3.74)$$

Now multiplying the row by column and let $w_i > 0$, so we also let $w_2 = 1$ and $w_4 = 1$, simplify

we have:

$$\begin{aligned}
 w_1 &= -\frac{1}{\mu} \left(\frac{\beta_2 \kappa_2}{\alpha_2} \frac{1}{R_0^s} + (d_1 + \mu + \gamma_2) + \frac{\delta_1 \gamma_1}{(\mu + \gamma_1 + d_1)} + \frac{\delta_2 \gamma_2}{(\mu + \gamma_2 + d_2)} \right), \\
 w_2 &= 1, \\
 w_3 &= \frac{1}{R_0^s}, \quad w_4 = 1, \quad w_5 = \frac{1}{R_0^r}, \\
 w_6 &= \frac{\gamma_1}{(\mu + \sigma_1)}, \quad w_7 = \frac{\gamma_2}{(\mu + \sigma_2)}.
 \end{aligned}$$

The left eigenvector \mathbf{L} corresponding to the zero eigenvalue meets the condition $\mathbf{LJ} = 0$ is given by $\mathbf{V} = (v_1, v_2, v_3, v_4, v_5, v_6, v_7)$. Such that

$$\begin{bmatrix}
 -\mu & 0 & 0 & 0 & 0 & 0 & 0 \\
 d_1 & -(\mu + \gamma_1 + d_1) & \kappa_1 & 0 & 0 & \gamma_1 & 0 \\
 -\frac{\beta_1 \kappa_1}{\alpha_1} & \frac{\beta_1 \kappa_1}{\alpha_1} & -\kappa_1 & 0 & 0 & 0 & 0 \\
 d_2 & 0 & 0 & -(\mu + \gamma_2 + d_2) & \kappa_2 & 0 & \gamma_2 \\
 -\frac{\beta_2 \kappa_2}{\alpha_2} & 0 & 0 & \frac{\beta_2 \kappa_2}{\alpha_2} & -\kappa_2 & 0 & 0 \\
 \delta_1 & 0 & 0 & 0 & 0 & -(\mu + \sigma_1) & 0 \\
 \delta_2 & 0 & 0 & 0 & 0 & 0 & -(\mu + \sigma_2)
 \end{bmatrix}
 \begin{bmatrix}
 v_1 \\
 v_2 \\
 v_3 \\
 v_4 \\
 v_5 \\
 v_6 \\
 v_7
 \end{bmatrix}
 =
 \begin{bmatrix}
 0 \\
 0 \\
 0 \\
 0 \\
 0 \\
 0 \\
 0
 \end{bmatrix}. \quad (3.75)$$

Now multiplying the row by column and let $v_3 = 1$ and $v_5 = 1$, we simplify to obtain:

$$v_1 = 0, \quad v_2 = \frac{\gamma_2 \kappa_2}{\beta_2 \kappa_1}, \quad v_3 = 1, \quad v_4 = \frac{\gamma_2}{\beta_2}, \quad v_5 = 1, \quad v_6 = 0, \quad v_7 = 0$$

Let f_k be the k th component of f and

$$a = \sum_{k,i,j=1} v_k w_i w_j \frac{\partial^2 f_k}{\partial x_i \partial x_j}(0, 0); \quad (3.76)$$

$$b = \sum_{k,i=1} v_k w_i \frac{\partial^2 f_k}{\partial x_i \partial \phi}(0, 0); \quad (3.77)$$

If $a > 0$ and $b > 0$, the bifurcation at $\phi = 0$ is backward. The presence of a backward bifurcation implies the existence of multiple endemic equilibria. Specifically, an endemic equilibrium arises when $R_0 < 1$, and significant effort is needed to reduce R_0 to a sufficiently low level to eliminate the disease from the population (recall that the DFE has been shown to be locally asymptotically stable only). β_2 is the natural choice for the bifurcation parameter and we let $\beta_1 = \Theta \beta_2$

Now considering (3.76) and taking the second derivative of the system of equations in (3.76) using $\frac{\partial^2 f_k}{\partial x_i \partial x_j}(0, 0)$ and substituting $\beta_1 = \Theta\beta_2$ we get;

$$\begin{aligned} \frac{\partial^2 f_1}{\partial x_1 \partial x_4} &= -\frac{\Theta\beta_2\kappa_1}{\alpha_1}, & \frac{\partial^2 f_1}{\partial x_1 \partial x_5} &= -\frac{\beta_2\kappa_2}{\alpha_2}, \\ \frac{\partial^2 f_2}{\partial x_1 \partial x_5} &= -\phi\frac{\beta_2\kappa_2}{\alpha_2}, & \frac{\partial^2 f_6}{\partial x_6 \partial x_5} &= -(1-\epsilon)\frac{\beta_2\kappa_2}{\alpha_2}, \end{aligned}$$

Also by considering (3.77) and taking the second derivative of the system of equations in (3.20) using $\frac{\partial^2 f_k}{\partial x_i \partial \beta_2}(0, 0)$ we get:

$$\begin{aligned} \frac{\partial^2 f_1}{\partial x_1 \partial \beta_2} &= -\frac{\Theta\kappa_1}{\alpha_1}, & \frac{\partial^2 f_1}{\partial x_5 \partial \beta_2} &= \frac{\kappa_2}{\alpha_2}, \\ \frac{\partial^2 f_2}{\partial x_4 \partial \beta_2} &= \frac{\Theta\kappa_1}{\alpha_1}, & \frac{\partial^2 f_2}{\partial x_4 \partial \beta_2} &= \frac{\kappa_2}{\alpha_2}, \end{aligned}$$

Now all the non zero derivatives are as follows,

$$\begin{aligned} \frac{\partial^2 f_4}{\partial x_1 \partial x_5} &= \frac{\partial^2 f_4}{\partial x_5 \partial x_1} = \frac{\beta_2\kappa_2}{\alpha_2}, & \frac{\partial^2 f_4}{\partial x_5 \partial x_6} &= \frac{\partial^2 f_4}{\partial x_6 \partial x_5} = (1-\epsilon)\frac{\phi\beta_2\kappa_2}{\alpha_2}, \\ \frac{\partial^2 f_4}{\partial x_2 \partial x_5} &= \frac{\partial^2 f_4}{\partial x_2 \partial x_5} = \frac{\phi\beta_2\kappa_2}{\alpha_2}, & \frac{\partial^2 f_1}{\partial x_1 \partial x_5} &= -\frac{\beta_2\kappa_2}{\alpha_2}, \\ \frac{\partial^2 f_1}{\partial x_1 \partial x_4} &= -\frac{\Theta\beta_2\kappa_1}{\alpha_1}, & \frac{\partial^2 f_6}{\partial x_6 \partial x_5} &= -(1-\epsilon)\frac{\beta_2\kappa_2}{\alpha_2}, \\ \frac{\partial^2 f_2}{\partial x_1 \partial x_5} &= -\phi\frac{\beta_2\kappa_2}{\alpha_2}, & & \end{aligned}$$

Using the derivative above we calculate b using the formula:

$$b = \sum_{k,i=1} v_k w_i \frac{\partial^2 f_k}{\partial x_i \partial \beta_2}(0, 0); \quad (3.78)$$

$$= \left(\frac{\gamma_2\kappa_2}{\beta_2}\right) (1) \left(\frac{\Theta\kappa_1}{\alpha_1}\right) + \left(\frac{1}{R_0^r}\right) \left(\frac{\gamma_2}{\beta_2}\right) \left(\frac{\kappa_2}{\alpha_2}\right) > 0, \quad (3.79)$$

Using the non zero derivative we also calculate a using the following formula:

$$a = \sum_{k,i,j=1} v_k w_i w_j \frac{\partial^2 f_k}{\partial x_i \partial x_j}(0, 0); \quad (3.80)$$

$$\begin{aligned} &= -2 \left(\frac{\gamma_2 \kappa_2}{\beta_2 \kappa_1} \right) \left(\frac{1}{\mu} \right) \left(\left(\frac{\beta_2 \kappa_2}{\alpha_2} \frac{1}{R_0^s} + (d_1 + \mu + \gamma_2) + \frac{\delta_1 \gamma_1}{(\mu + \gamma_1 + d_1)} \right) \frac{\Theta \beta_2 \kappa_1}{\alpha_1} \right) \\ &\quad - 2 \left(\frac{\gamma_2 \kappa_2}{\beta_2 \kappa_1} \right) \left(\frac{1}{R_0^r} \right) \Theta \beta_2 \kappa_2 \\ &\quad - 2 \left(\frac{\gamma_2}{\beta_2} \right) \left(\frac{1}{\mu} \right) \left(\left(\frac{\beta_2 \kappa_2}{\alpha_2} \frac{1}{R_0^s} + (d_1 + \mu + \gamma_2) + \frac{\delta_1 \gamma_1}{(\mu + \gamma_1 + d_1)} \right) \frac{\beta_2 \kappa_2}{\alpha_2} \right) \\ &\quad + 2 \left(\frac{\gamma_2}{\beta_2} \right) \left(\frac{1}{R_0^r} \right) \frac{\phi \beta_2 \kappa_2}{\alpha_2}. \end{aligned} \quad (3.81)$$

So $a > 0$ if $\phi > 0$ and $a < 0$ if $\phi < 0$.

Thus, if $a > 0$ and $b > 0$, we will have a backward bifurcation and if $a < 0$ and $b > 0$, we will have a forward bifurcation.

3.6.13 Sensitivity Analysis of R_0

The sensitivity analysis is employed to assess the importance of individual parameters in the disease transmission model. Understanding the relative significance of different factors linked to the transmission of respiratory diseases is essential for effectively mitigating human mortality and morbidity resulting from their spread. This research utilizes numerical sensitivity indices to pinpoint parameters that notably influence the basic reproduction number, R_0 , and therefore warrant attention in intervention planning. The sensitivity analysis methodology in this thesis aligns with the approach initially introduced by. [24].

Definition The normalized forward sensitivity index of a function u that depends differentiably on a parameter p is defined as

$$\Gamma_u^p = \frac{\partial u}{\partial p} \cdot \frac{p}{u}.$$

Considering that R_0 has an explicit formula, we calculate the sensitivity of R_0 as

$$\Gamma_{R_0}^p = \frac{\partial R_0}{\partial p} \times \frac{p}{R_0}.$$

Sensitivity of R_0^s

For example, the sensitivity index of R_0^s with respect to γ_1 is:

$$\Gamma_{R_0^s}^{\gamma_1} = \frac{\partial R_0^s}{\partial \gamma_1} \times \frac{\gamma_1}{R} = \left| \frac{-\gamma_1}{(\mu + d_1 + \gamma_1)} \right| < 0.$$

The sensitivity index of R_0^r with respect to μ is:

$$\Gamma_{R_0^s}^\mu = \frac{\partial R_0^s}{\partial \mu} \times \frac{\mu}{R} = \left| \frac{-\mu}{(\mu + d_1 + \gamma_1)} \right| < 0.$$

The sensitivity index of R_0^s with respect to d_1 is:

$$\Gamma_{R_0^s}^{d_1} = \frac{\partial R_0^s}{\partial d_1} \times \frac{d_1}{R_0^s} = \left| \frac{-d_1}{(\mu + d_1 + \gamma_1)} \right| < 0.$$

The sensitivity index of R_0^s with respect to α_1 is:

$$\Gamma_{R_0^s}^{\alpha_1} = \frac{\partial R_0^s}{\partial \alpha_1} \times \frac{\alpha_1}{R_0^s} = -1 < 0.$$

The sensitivity index of R_0^s with respect to β_1 is:

$$\Gamma_{R_0^s}^{\beta_1} = \frac{\partial R_0^s}{\partial \beta_1} \times \frac{\beta_1}{R_0^s} = 1 > 0.$$

The sensitivity index of R_0^s with respect to κ_1 is:

$$\Gamma_{R_0^s}^{\kappa_1} = \frac{\partial R_0^s}{\partial \kappa_1} \times \frac{\kappa_1}{R_0^s} = 1 > 0.$$

Sensitivity of R_0^r

The sensitivity index of R_0^r with respect to γ_2 is:

$$\Gamma_{R_0^r}^\gamma = \frac{\partial R_0^r}{\partial \gamma_2} \times \frac{\gamma_2}{R} = \left| \frac{-\gamma_2}{(\mu + d_2 + \gamma_2)} \right| < 0.$$

The sensitivity index of R_0^r with respect to μ is:

$$\Gamma_{R_0^r}^\mu = \frac{\partial R_0^r}{\partial \mu} \times \frac{\mu}{R} = \left| \frac{-\mu}{(\mu + d_2 + \gamma_2)} \right| < 0.$$

The sensitivity index of R_0^r with respect to d_2 is:

$$\Gamma_{R_0^r}^{d_2} = \frac{\partial R_0^r}{\partial d_2} \times \frac{d_2}{R_0^r} = \left| \frac{-d_2}{(\mu + d_2 + \gamma_2)} \right| < 0.$$

The sensitivity index of R_0^r with respect to α_2 is:

$$\Gamma_{R_0^r}^{\alpha_2} = \frac{\partial R_0^r}{\partial \alpha_2} \times \frac{\alpha_2}{R_0^r} = -1 < 0.$$

The sensitivity index of R_0^r with respect to β_2 is:

$$\Gamma_{R_0^r}^{\beta_2} = \frac{\partial R_0^r}{\partial \beta_2} \times \frac{\beta_2}{R_0^r} = 1 > 0.$$

The sensitivity index of R_0^r with respect to α_2 is:

$$\Gamma_{R_0^r}^{\kappa_2} = \frac{\partial R_0^r}{\partial \kappa_2} \times \frac{\kappa_2}{R_0^r} = 1 > 0.$$

It's deduced that R_0^s and R_0^r are highly responsive to changes in β_1 , β_2 , κ_1 , and κ_2 . An increase in these parameters results in a proportional increase in R_0^s and R_0^r , while a decrease leads to an equivalent decrease, indicating a direct correlation. On the other hand, γ_1 , γ_2 , μ , δ_1 , and δ_2 demonstrate an inverse relationship with R_0^s and R_0^r . Elevating any of these factors triggers a decrease in R_0^s and R_0^r , although the reduction is relatively smaller in proportion. These findings highlight the importance of understanding the sensitivity of R_0^s and R_0^r to variations in parameters like β_1 , β_2 , κ_1 , and κ_2 , as well as γ_1 , γ_2 , μ , δ_1 , and δ_2 , in formulating effective strategies for controlling disease transmission.

3.7 Chapter Overview

In Chapter 3, we explored infectious disease modeling, starting with creating detailed math models based on real-life factors. We looked at different ways to study these models, like understanding how diseases spread and if they'll keep spreading. We talked about numbers that show how easily diseases spread and how we can stop them. By studying reproduction numbers, stability, bifurcation, and sensitivity, we gained valuable insights into disease behavior and control.

4 Numerical Simulations

In this chapter, we harness the power of numerical simulation to explore the complex dynamics of respiratory disease transmission, utilizing Python and R as our primary computational tools. Acknowledged for their versatility in algorithm development, data visualization, analysis, and numeric computation, Python and R provide an ideal environment for tackling computationally intensive tasks with precision and efficiency. To solve our models, we utilize the `odeint` function from `scipy.integrate` in Python and leverage the visualization capabilities of `ggplot2` in R. Our approach involves systematically varying both variables and parameters to investigate a range of conditions and scenarios relevant to respiratory disease transmission. In order to capture the complexity of real-world dynamics, we incorporate a diverse range of parameter values sourced from various reputable sources these are shown in Table 4.1. These values, essential to our numerical simulations, are carefully selected to ensure accuracy and relevance to the problem at hand. The results of our simulations, illustrating the nuanced dynamics of disease spread, are presented in the table below. Subsequently, through qualitative analysis, we interpret these findings and clarify their implications in the context of real-world scenarios, thereby contributing to a deeper understanding of respiratory disease dynamics and informing evidence-based strategies for disease control and prevention.

Table 4.1: Parameter Definitions, Values, and Sources

Symbol	Definition	Value	Source
μ	Natural death rate	$4 \times 10^{-5}/\text{day}$	[39]
β_1	Transmission rate of weak infection i_1	$2.24 \times 10^{-5}/\text{day}$	[39]
β_2	Transmission rate of strong infection i_2	$4.48 \times 10^{-5}/\text{day}$	[39]
κ_1	Weak infection into environment p_1	$4.1 \times 10^5/\text{day}$	[39]
κ_2	Strong infection into environment p_2	$8.2 \times 10^5/\text{day}$	[39]
α_1	Weak infection from the Environment p_1	37.44/day	[39]
α_2	Strong infection from the Environment p_2	74.88/day	[39]
d_1	Death rate from weak infection i_1	$3.5 \times 10^{-5}/\text{day}$	[39]
d_2	Death rate from strong infection i_2	$7 \times 10^{-5}/\text{day}$	[39]
δ_1	Immunity from the recovered group r_1 that suffered weak infection	$5.5 \times 10^{-4}/\text{day}$	[39]
δ_2	Immunity from the recovered group r_2 that suffered strong infection	$11 \times 10^{-4}/\text{day}$	[39]
γ_1	Recovery rate from weak infection i_1	0.2/day	[39]
γ_2	Recovery rate from strong infection i_2	0.4/day	[39]
ϕ	Cross-immunity parameter	1-3	Estimated
ϵ	Reduction factor for cross-immunity	0-0.9	Estimated

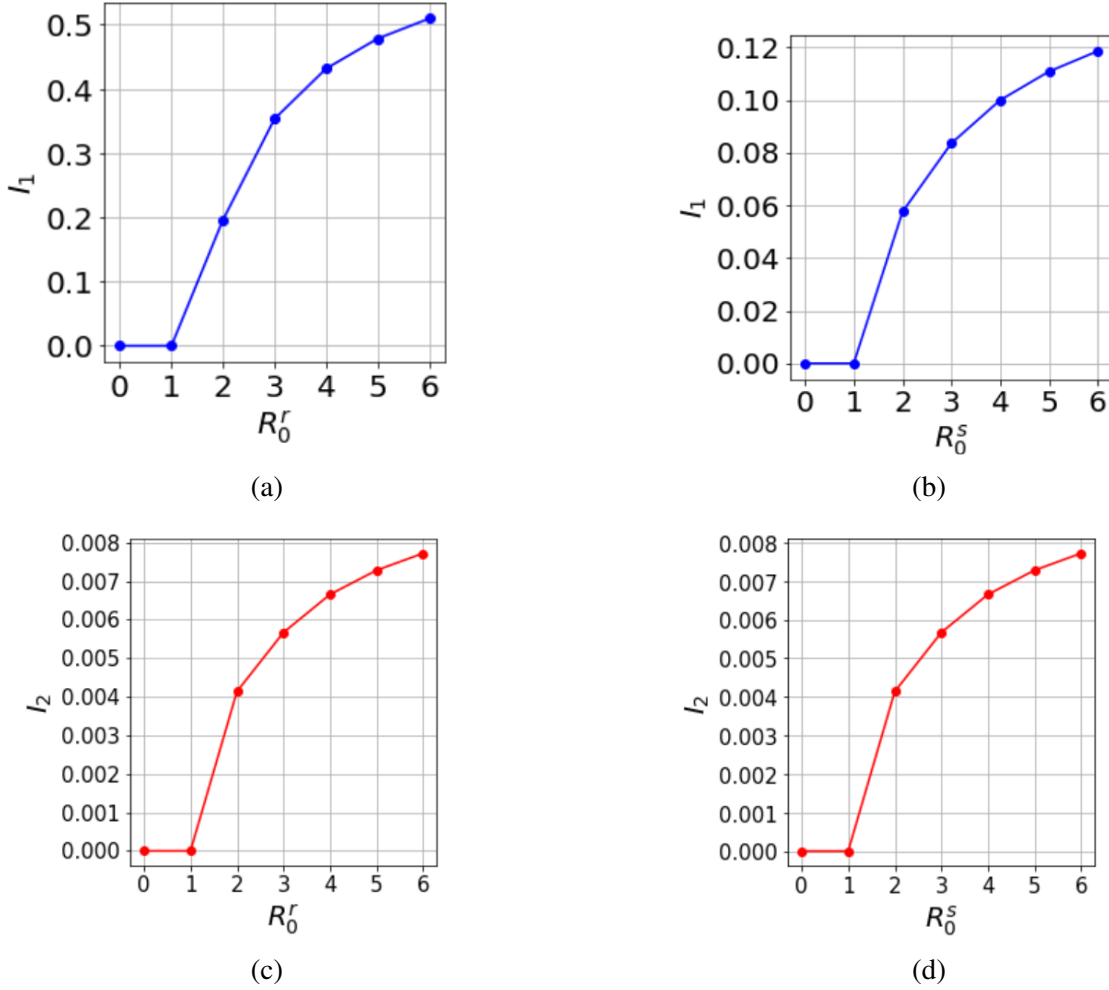


Figure 4.1: Graphical presentation of the bifurcation for the model 3.3 for all values of $\phi > 1$

From the illustration in Figure 4.1 above, we observe the bifurcation analysis for the basic reproduction number $R_0 = (R_0^s, R_0^r)$. The graphical representation clearly indicates a forward bifurcation for the weakly infected compartment in 4.1a and 4.1b, as shown by $R_0^s > 1$ and $R_0^r > 1$. In this scenario, the disease-free equilibrium becomes unstable, and a stable endemic equilibrium appears as R_0 crosses the critical threshold of 1.

Similarly, the illustration for the strongly infected compartment in 4.1c and 4.1d, where $R_0 = (R_0^s, R_0^r)$, demonstrates a forward bifurcation when $R_0^s > 1$ and $R_0^r > 1$. This implies that beyond this threshold, the system transitions from a disease-free state to an endemic state, signifying persistent disease presence within the population. Thus, the illustrations confirm that a forward bifurcation occurs for $R_0 > 1$. This critical insight is derived from observing the stability changes in equilibrium states as R_0 increases.

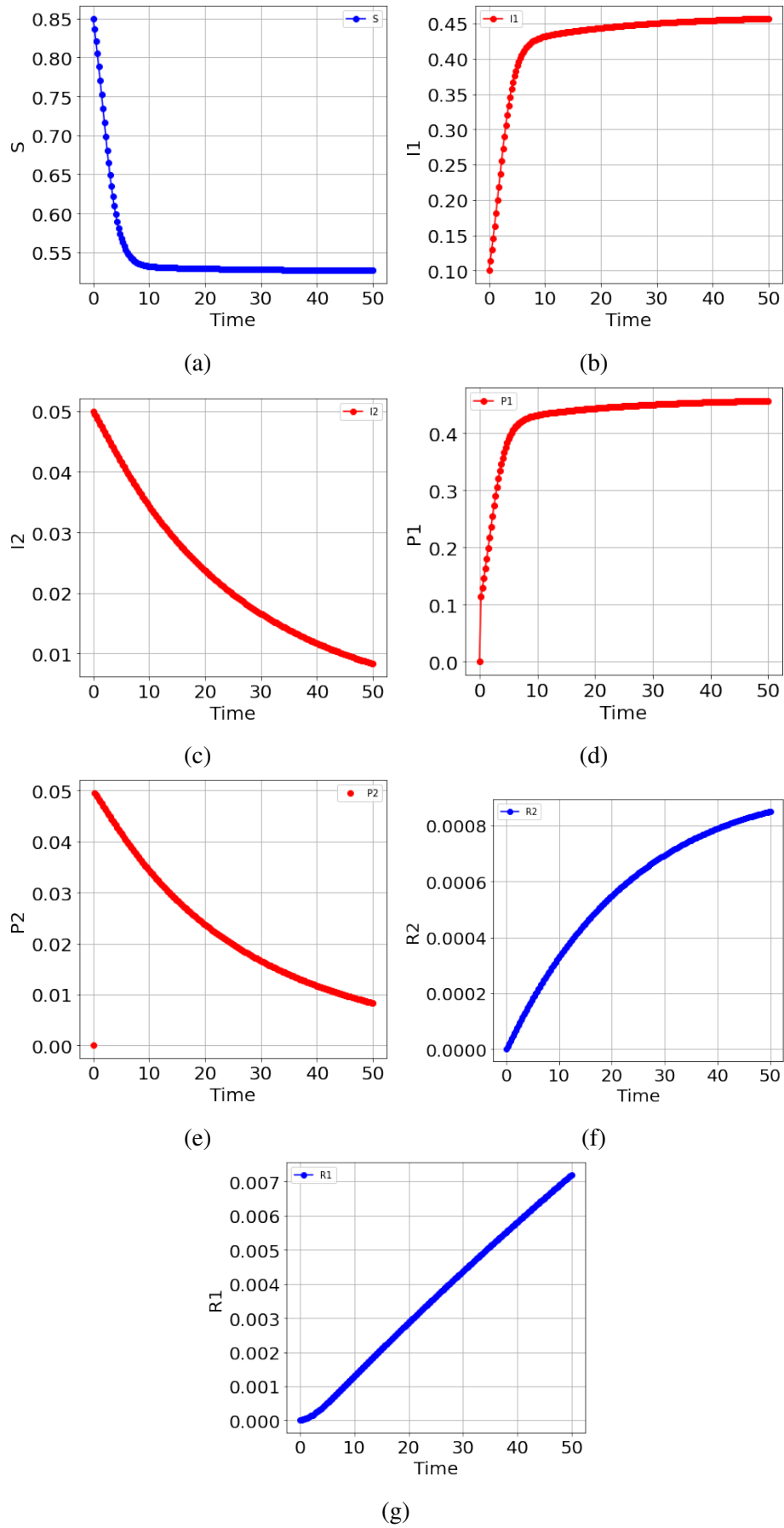


Figure 4.2: The population dynamics with initial conditions $S(0) = 0.85$, $I1_0 = 0.1$, and $I2_0 = 0.05$. When the basic reproduction numbers (R_0^s)=1.916 and (R_0^r)=0.918

Based on the initial conditions with $S(0) = 0.85$, $I1(0) = 0.1$, and $I2(0) = 0.05$, as depicted in Figure 4.2, the susceptible population decreases from an initial value of 0.85 to stabilize at 0.55 within a period of 10 days as shown in 4.2a, indicating a significant reduction in the number of individuals at risk of infection. The weakly infected compartment experiences a sharp linear increase from 0.10 to 0.45 within the first 10 days in figure 4.2b, demonstrating a rapid spread of the weaker form of the infection, after which it stabilizes, suggesting the infection reaches a steady state. The concentration of the pathogen responsible for weak infection also rises from 0.1 to 0.44 within the same 10-day period as shown in 4.2c, stabilizing thereafter, which aligns with the trend observed in the weakly infected population, reflecting the pathogen's prevalence in the environment.

In contrast, the population affected by strong infection shows a decrease from an initial value of 0.05 to extinction as shown in 4.3c, indicating that the stronger form of the infection is eventually eradicated. Correspondingly, the concentration of the pathogen responsible for strong infection decreases from 0.05 to below detectable levels over a span of 50 days as shown in 4.3e, supporting the decline and eventual elimination of the strong infection from the environment. The recovery trends also reveal interesting dynamics. Individuals recovering from weak infection exhibit a sharp linear increase during the first 50 days as shown in 4.3g, indicating a best recovery process. Specifically, the recovery rate for this group stabilizes after this initial period, suggesting that most individuals have either recovered or the infection rate has decreased significantly. Lastly, those recovering from strong infection show a concave increase from 0 to 0.0008 over the 50-day period, highlighting a slower but steady recovery from the more severe form of the infection. This gradual increase suggests that while recovery from strong infection is slower, it is consistent and leads to eventual improvement in health outcomes for the affected individuals.

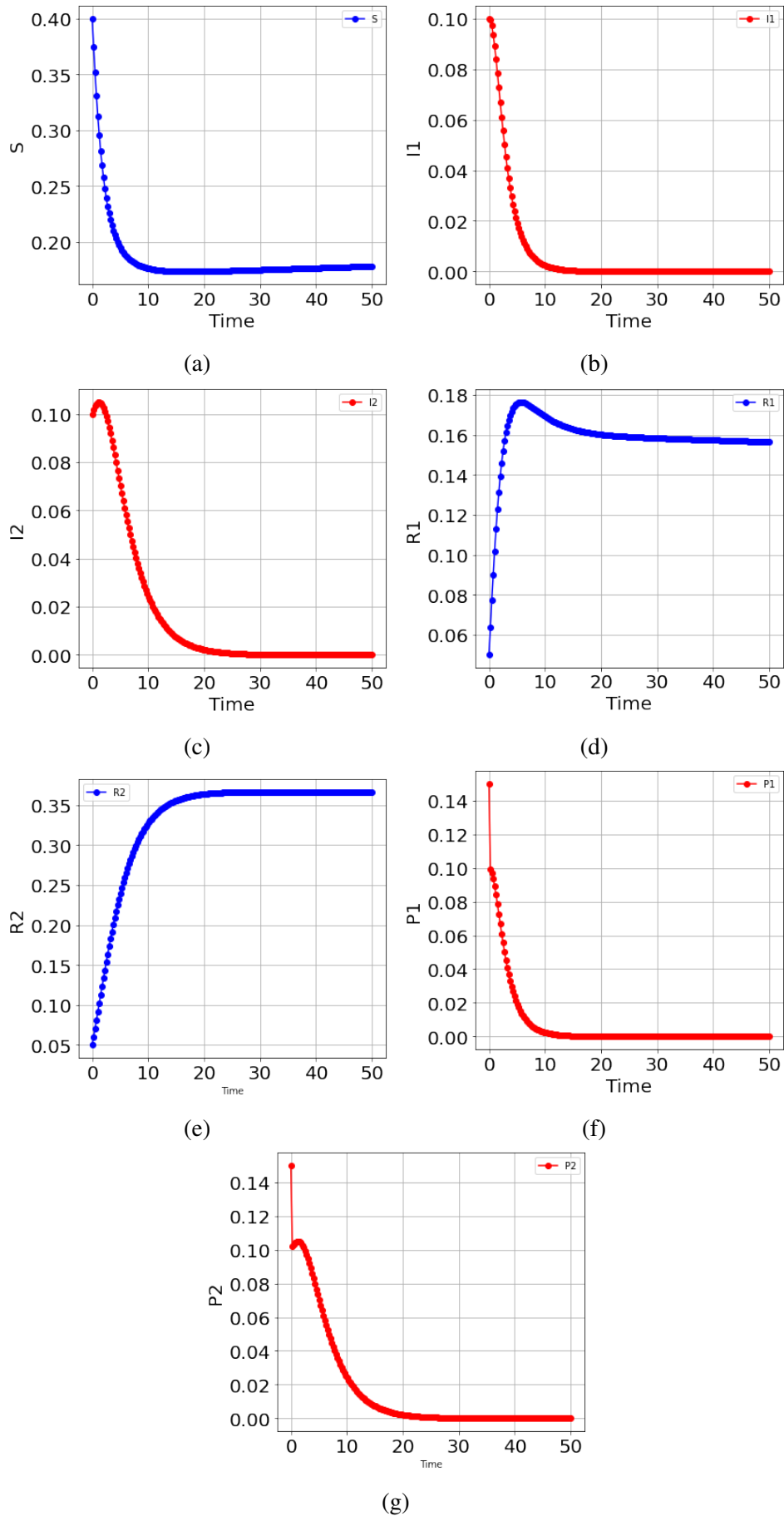


Figure 4.3: The population variations with initial conditions $(S, I1, I2, R1, P1, P2, R1, R2) = (0.4, 0.1, 0.1, 0.15, 0.15, 0.05, 0.05)$. When $R_0 = (0.674, 0.751)$, comprising $R_0^s = 0.674$ and $R_0^r = 0.751$

We observe that $R_0 < 1$. Consequently, the susceptible, weakly infected, and strongly infected compartments all approach zero Figure 4.3a, 4.3b and 4.3c, indicating that the populations will die out. Additionally, both weak and strong infections will also diminish as shown in 4.3f and 4.3g respectively. Notably, individuals recovering from weak infections exhibit a linear increase to 0.18 within 10 days, followed by a decrease to 0.16 within 20 days, and then stabilization. Similarly, individuals recovering from strong infections experience a linear increase to 0.35 within 20 days before stabilizing. This scenario underscores the importance of maintaining effective infection control measures to prevent outbreaks and ensure population health.

All the above compartments are easily shown all in one in Figure 4.4 below;

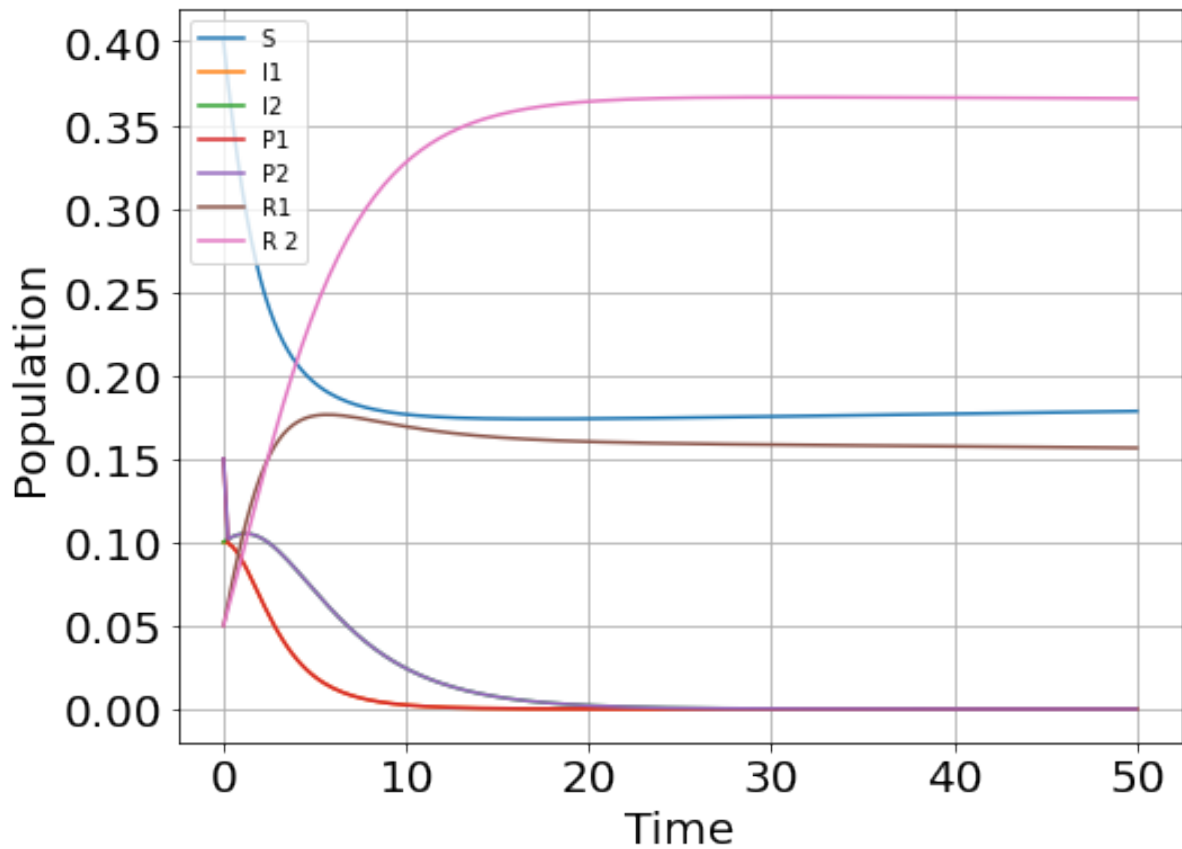


Figure 4.4: The combined population variations with initial conditions $(S, I1, I2, R1, P1, P2, R1, R2) = (0.4, 0.1, 0.1, 0.15, 0.15, 0.05, 0.05)$. When $R_0 = (0.674, 0.751)$, comprising $R_0^s = 0.674$ and $R_0^r = 0.751$,

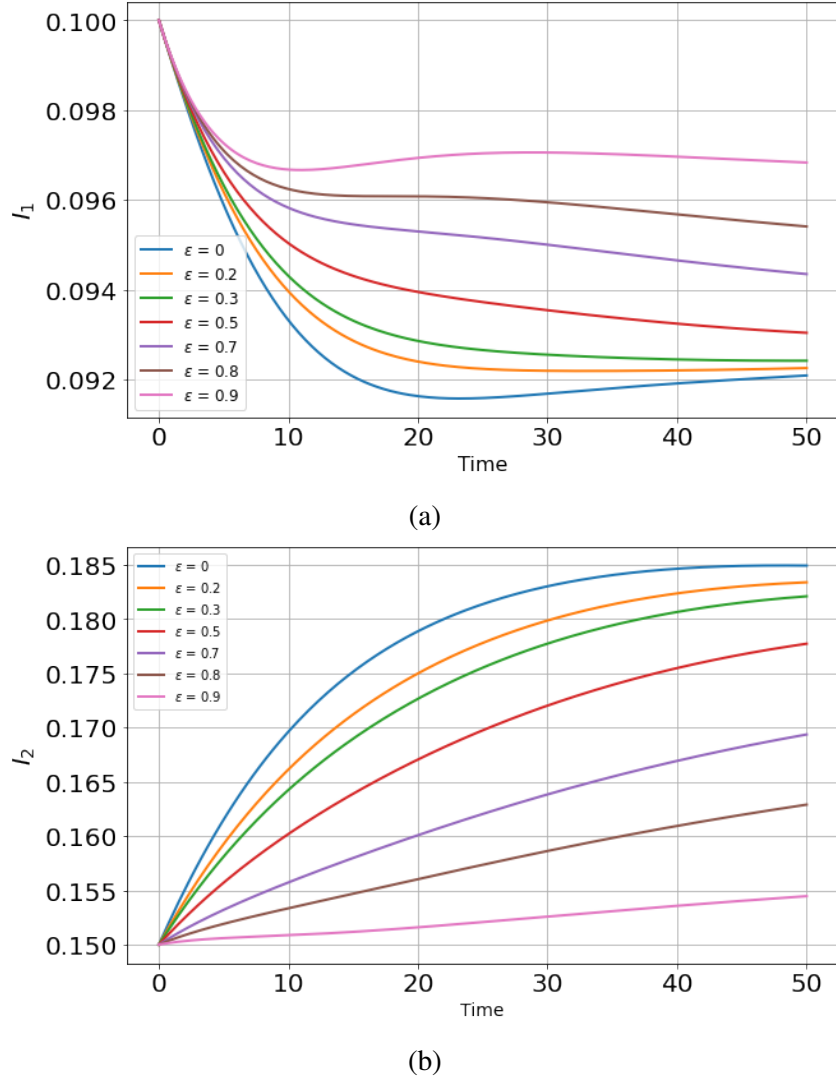


Figure 4.5: Effects of Reduction in Immunity On the Weakly Infected and Strongly Infected Group with $R_0^s = 2.432$ and $R_0^r = 1.854$

The graph in Figure 4.5a illustrates the effect of varying immunity loss (ϵ) on the dynamics of a respiratory disease characterized by weak infections (I_1). When $\epsilon = 0$, indicating that there is no immunity loss, the weakly infected population decreases from 10% to less than 9% within a period of 20 days. This suggests that in the absence of immunity loss, the disease's prevalence among the weakly infected individuals declines over time. As the immunity loss (ϵ) increases, the behavior of the weakly infected population changes notably. With an increase in the immunity reduction factor, the weakly infected population starts to rise gradually. This indicates that higher rates of immunity loss lead to a greater proportion of the population becoming weakly infected, as their immunity wanes and they become susceptible to infection once again.

In contrast, the strongly infected population in Figure 4.5b exhibits a different trend in response to changes in the immunity reduction factor. When $\epsilon = 0$, the strongly infected population is relatively high, suggesting that without immunity loss, a significant portion of the population

remains strongly infected. However, as ϵ increases, the strongly infected population decreases gradually. This decrease continues with rising values of ϵ , and at higher levels of immunity loss. This trend implies that increased immunity loss reduces the proportion of strongly infected individuals, potentially because these individuals either recover and gain some immunity.

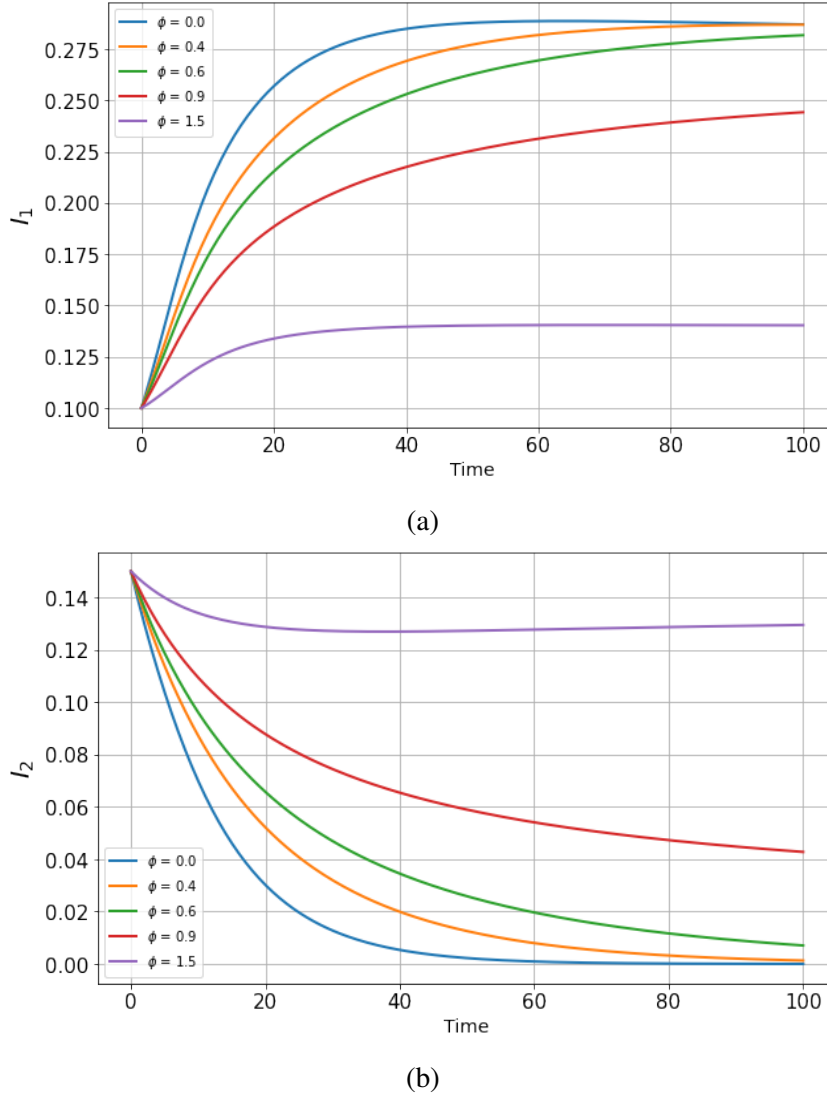
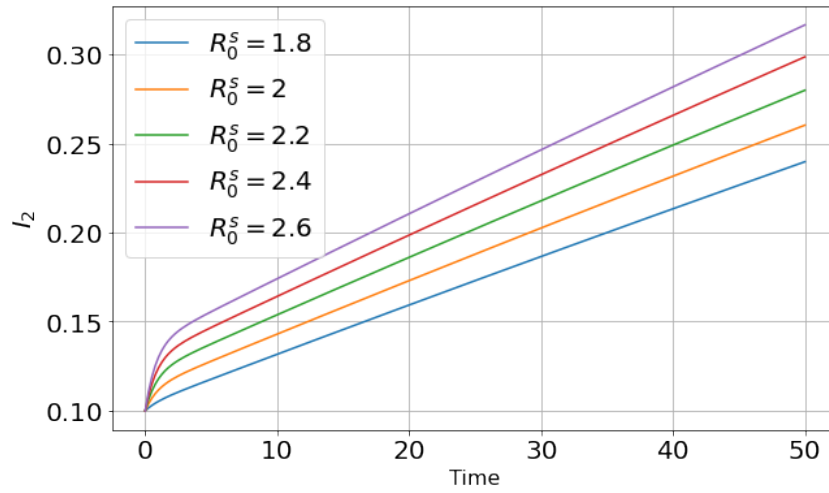


Figure 4.6: Effects of Cross Immunity On the Weakly Infected and Strongly Infected Class with $R_0^s = 2.432$ and $R_0^r = 1.854$

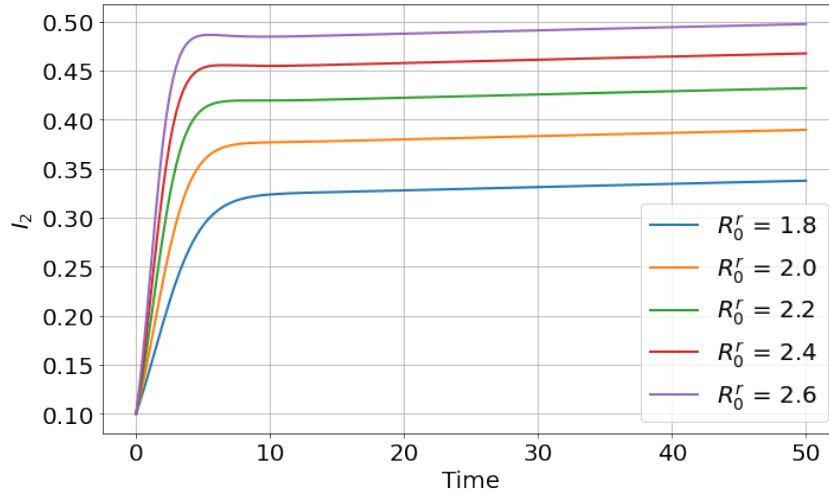
The effects of varying the cross-immunity factor, ϕ , on the weakly infected and strongly infected compartments are illustrated in Figures 4.6a and 4.6b, respectively. When the cross-immunity factor ϕ is zero, the weakly infected compartment increases from 10% to 28% within 20 days before stabilizing. This indicates that in the absence of cross-immunity, a significant portion of the population transitions to the weakly infected state, likely due to the absence of any protective immunity between different strains or types of the pathogen. As the cross-immunity factor increases, the weakly infected population starts to decrease gradually. This suggests that higher levels of cross-immunity reduce the susceptibility of individuals to weak

infections, leading to a lower prevalence of weakly infected individuals as ϕ rises.

Conversely, the behavior of the strongly infected compartment is different. When the cross-immunity factor ϕ is zero, the strongly infected population decreases from 14% to extinction within a period of 60 days. This decline indicates that without cross-immunity, the strongly infected population cannot sustain itself, possibly due to recovery or transition to other compartments. However, as the cross-immunity factor increases, the strongly infected population starts to increase gradually. This trend implies that higher cross-immunity provides a protective effect against weak infections, allowing more individuals to progress to the strongly infected state when they do become infected.



(a)



(b)

Figure 4.7: Effects of $R_0^s > 1$ and $R_0^r > 1$ on the Strongly Infected Class

The visual representations provided by the graphs in Figure 4.7 offer valuable insights into the intricate dynamics of population infection rates concerning R_0^s and R_0^r , representing the sensitive and resistant strains, respectively. As these fundamental reproductive numbers increase,

their impact on the population with strong infections becomes increasingly pronounced. Figure 4.7a vividly portrays a consistent and linear escalation in the proportion of the population exhibiting strong infections with each incremental rise in R_0^s . This steady upward trend signifies a direct correlation between the spread of the sensitive strain and the growth of the infected population. For instance, when R_0^s achieves a value of 2.6, there is a substantial surge in the population proportion, soaring from 10% to 35% within a mere 50-day timeframe.

Conversely, Figure 4.7b unveils a distinct pattern in the population response to changes in R_0^r . Initially, there is a sharp increase in the population proportion with strong infections, followed by a stabilization phase as R_0^r continues to rise. For example, when R_0^r reaches 2.6, the population proportion rises notably, expanding from 10% and stabilizes at 48% within the same 50-day period.

4.1 Chapter Overview

In this chapter, we conduct comprehensive numerical simulations to visualize trends and dynamics within various population compartments, focusing on the effects of cross-immunity, reductions in immunity, and bifurcation directions. We explore the role of cross-immunity, where partial protection against one strain affects susceptibility to another, providing insights into the interplay between different pathogen strains and their collective impact on population health. Additionally, we examine scenarios involving reductions in immunity, such as waning immunity over time or due to external factors, to assess the long-term effectiveness of vaccination programs and natural immunity, and to identify critical thresholds for maintaining population immunity. Furthermore, we investigate bifurcation directions to understand how small parameter changes can lead to significant shifts in disease dynamics, including stability analysis and potential tipping points that could result in sudden outbreaks or changes in disease prevalence. Detailed graphs and discussions are presented throughout the chapter to elucidate these complex dynamics, offering a comprehensive understanding of the mechanisms driving infectious disease transmission and control.

5 Discussion and Conclusion

5.1 Introduction

This chapter explores a detailed examination of respiratory diseases, uncovering their spread, impact, and methods to control them. By conducting thorough research and analysis, this chapter consolidates significant findings that illuminate the complex nature of respiratory infections, providing valuable insights into their transmission and consequences. From understanding how infections spread to assessing the effectiveness of interventions, the study presents a comprehensive overview of respiratory disease dynamics. It ends with a brief overview of key findings, underscoring their relevance for healthcare professionals, policymakers, and the broader community. Additionally, the chapter proposes practical strategies to enhance disease management and identifies promising areas for future research, with the goal of advancing our understanding and response to respiratory infections.

5.2 Key Findings

The analysis of the effect of varying immunity loss (ϵ) on the dynamics of a respiratory disease, specifically concerning weak infections (I_1) and strong infections (I_2), reveals several important insights:

Impact on Weakly Infected Population

- **No Immunity Loss ($\epsilon = 0$):** The weakly infected population decreases from 10% to less than 9% within 20 days. This decline indicates that in the absence of immunity loss, the prevalence of the disease among weakly infected individuals diminishes over time. The maintenance of immunity effectively prevents reinfection, leading to a gradual reduction in the number of weakly infected individuals.
- **Increasing Immunity Loss:** As the immunity loss factor (ϵ) increases, the weakly infected population begins to rise gradually. This suggests that higher rates of immunity loss result in a greater proportion of the population becoming weakly infected. As immunity wanes,

individuals lose their protection against the disease, becoming susceptible to reinfection, which increases the weakly infected population over time.

Impact on Strongly Infected Population

- **No Immunity Loss** ($\epsilon = 0$): The strongly infected population remains relatively high, implying that a significant portion of the population stays strongly infected in the absence of immunity loss. Without the loss of immunity, individuals who become strongly infected do not experience a natural decline in infection severity or frequency, leading to a sustained high level of strong infections.
- **Increasing Immunity Loss**: With rising immunity loss, the strongly infected population decreases gradually. This trend continues as ϵ increases, indicating that higher immunity loss reduces the proportion of strongly infected individuals. This decrease could be due to individuals recovering and gaining partial immunity, which protects them from severe reinfection, or transitioning from a strong infection state to a weak infection state as their overall susceptibility changes.

Key Conclusions and Recommendations

The dynamics of respiratory diseases are significantly influenced by the rate of immunity loss. Key generalized insights include:

- **Immunity Maintenance**: Sustaining immunity in the population is crucial for reducing the prevalence of both weak and strong infections. In the absence of immunity loss, disease prevalence declines naturally over time, indicating the importance of maintaining a robust immune response to prevent reinfection and manage disease spread effectively.
- **Impacts of Immunity Waning**: Increased immunity loss leads to a higher incidence of weak infections, as individuals become more susceptible to reinfection. Conversely, it reduces the prevalence of strong infections, possibly due to recovery and partial immunity gain or a shift to milder infection states. These patterns highlight the dual impact of immunity loss on disease dynamics, where waning immunity increases vulnerability to infection but may also lead to less severe disease outcomes.
- **Strategic Importance**: Understanding and managing immunity dynamics is vital for disease control. Strategies such as vaccination to sustain immunity levels can significantly mitigate the overall disease burden by lowering both weak and strong infection rates. These approaches can help maintain a healthier population by preventing the spread of infections and reducing the severity of disease manifestations.

The analysis of the effect of the cross-immunity parameter (ϕ) on the dynamics of a respiratory

disease, specifically concerning weak infections (I_1) and strong infections (I_2), reveals several important insights:

Impact on Weakly Infected Population

- **No Cross-Immunity ($\phi = 0$):** In the absence of cross-immunity, the weakly infected population initially increases from 10% and stabilizes at 28%. This upward trend suggests that without any cross-protection, weak infections can proliferate and establish a significant presence within the population over time. The lack of cross-immunity allows the disease to spread more freely, resulting in a higher and sustained prevalence of weak infections.
- **Increasing Cross-Immunity:** With each increment in the cross-immunity parameter ϕ , the weakly infected population gradually decreases. Higher levels of cross-immunity lead to a more controlled spread of weak infections, as individuals with some level of immunity are less likely to become reinfected. Consequently, the weakly infected population diminishes over time, indicating the effectiveness of cross-immunity in limiting the spread of the disease.

Impact on Strongly Infected Population

- **No Cross-Immunity ($\phi = 0$):** When cross-immunity is absent ($\phi = 0$), the strongly infected population experiences a rapid decline, eventually dwindling to zero. This swift decrease suggests that strong infections are not sustained in the absence of cross-protection, as individuals are susceptible to severe disease outcomes without any immune defense.
- **Increasing Cross-Immunity:** As the cross-immunity parameter ϕ increases, the rate of decline in the strongly infected population slows down progressively. Higher levels of cross-immunity provide a protective effect, reducing the severity and incidence of strong infections. While strong infections persist with increasing ϕ , they decline at a slower pace, highlighting the role of cross-immunity in mitigating the impact of severe disease outcomes.

Key Conclusions and Recommendations

The dynamics of respiratory diseases are significantly influenced by the cross-immunity parameter (ϕ), which dictates the level of protection conferred by previous exposures to related pathogens. Key generalized insights from this analysis include:

- **Cross-Immunity and Weak Infections:** Higher levels of cross-immunity result in a gradual reduction in the weakly infected population, indicating a dampening effect on disease

spread. Cross-immunity plays a crucial role in limiting the prevalence of weak infections, thereby preventing unchecked transmission within the population.

- **Cross-Immunity and Strong Infections:** Enhanced cross-immunity slows down the decline of strongly infected cases, indicating a protective effect against severe disease outcomes. While strong infections persist with increasing ϕ , they decline at a slower pace, highlighting the role of cross-immunity in mitigating the severity and duration of disease episodes.
- **Strategic Importance of Cross-Immunity:** Understanding and leveraging cross-immunity are essential for effective disease control strategies. Interventions aimed at enhancing cross-immunity, such as vaccination campaigns or controlled exposure to related pathogens, can significantly reduce the overall disease burden by limiting both weak and strong infection rates. By bolstering immunity levels within the population, cross-immunity contributes to better public health outcomes and a reduced impact of respiratory diseases.

The bifurcation analysis conducted on the weakly and strongly infected populations provided critical insights into the influence of reproduction numbers R_0^s and R_0^r :

Weakly Infected Population

- **Forward Bifurcation:** A forward bifurcation occurs when both R_0^s and R_0^r exceed 1. This denotes a qualitative change in the system's behavior, signaling the transition from stable to unstable equilibrium points. As R_0^s and R_0^r surpass critical thresholds, the population dynamics undergo a significant shift, potentially leading to sustained epidemic outbreaks. This finding highlights the vulnerability of populations to epidemic spread when both susceptible and recovered individuals contribute to disease transmission, necessitating proactive control measures to contain outbreaks effectively.

Strongly Infected Population

- **Forward Bifurcation:** Similarly, a forward bifurcation is observed in the strongly infected population when both R_0^s and R_0^r are greater than 1. This indicates a notable change in the system's dynamics, where previously stable equilibria become unstable. The occurrence of a forward bifurcation in the strongly infected population signifies the potential for rapid epidemic spread, as individuals with strong infections play a significant role in disease transmission. Consequently, this underscores the critical importance of early intervention strategies to prevent epidemic escalation and mitigate the impact of infectious diseases.

Key Conclusions and Recommendations

The presence of $R_0 > 1$ serves as a critical indicator of a forward bifurcation, highlighting the heightened risk of epidemic outbreaks. Key conclusions derived from this analysis include:

- **Identification of Critical Thresholds:** The analysis identifies critical thresholds of R_0^s and R_0^r beyond which the system undergoes a qualitative change, indicating the potential for sustained epidemic outbreaks. Understanding these thresholds is crucial for predicting and preemptively addressing epidemic risks.
- **Urgent Need for Proactive Control Measures:** The occurrence of forward bifurcations underscores the urgent need for proactive control measures to mitigate disease transmission and safeguard public health. Implementing interventions to reduce R_0 below the critical thresholds is essential to prevent epidemic spread and control disease outbreaks effectively.
- **Importance of Monitoring Reproduction Numbers:** Regular monitoring of reproduction numbers, particularly R_0^s and R_0^r , is essential for early detection of epidemic risks and timely implementation of control measures. By closely monitoring these indicators, public health authorities can intervene promptly to prevent epidemic escalation and protect communities from the adverse effects of infectious diseases.

Different values of the basic reproduction number (R_0) significantly influence the infected populations in an epidemic. The basic reproduction number R_0 represents the average number of secondary infections produced by a single infected individual in a completely susceptible population. Here's how varying R_0 values affect the infected populations:

When $R_0 < 1$:

- The disease will eventually die out because each infected person, on average, transmits the disease to fewer than one other person. With fewer new infections occurring, the disease cannot sustain itself within the population.
- The number of infected individuals, both weakly and strongly infected, gradually decreases over time. As the transmission rate is low, the number of new infections decreases, leading to a decline in the overall number of infected individuals.

When $R_0 = 1$:

- The disease remains endemic, indicating that it persists within the population without significant growth or decline. Each infected individual, on average, transmits the disease to exactly one other person. This means that the disease is sustained at a steady state.
- The number of infected individuals remains relatively constant over time. While new infections occur, they are balanced by the recovery or removal of infected individuals.

from the population.

When $R_0 > 1$:

- The disease spreads through the population because each infected person, on average, transmits the disease to more than one other person. This leads to exponential growth in the number of infected individuals.
- Both weakly and strongly infected populations increase rapidly. The higher transmission rate results in a larger number of new infections, contributing to the rapid spread of the disease within the population.
- The increase in infected individuals can lead to an outbreak or epidemic, where the disease becomes widespread within a community or region.

As the basic reproduction number R_0 increases further, represented as $R_0 = (R_0^s, R_0^r)$, the impact on the infected populations varies:

Higher values of R_0 :

- The growth rate of the infected populations (both weakly and strongly infected) accelerates. With each infected person transmitting the disease to more individuals, the rate of new infections increases rapidly over time.
- More individuals become infected at a faster rate, resulting in a larger epidemic with a higher peak of infections.
- The healthcare system may become overwhelmed as the number of infected individuals requiring medical care surpasses the capacity of healthcare facilities to provide adequate treatment and support.

In summary, with higher values of $R_0 > 1$, both the weakly and strongly infected populations tend to increase rapidly, leading to larger and more severe outbreaks or epidemics. Conversely, when $R_0 < 1$, the disease is likely to die out gradually, resulting in a decline in the number of infected individuals over time.

5.3 Summary

The aim of this project was to model the dynamics of respiratory diseases to better understand their spread and the behavior of populations as the disease increases or decreases. The table below shows the summarised key findings of this dissertation project.

Research Question	Answer
How does reduction in immunity affect population susceptibility to respiratory diseases over time?	Reduced immunity can significantly impact the susceptibility of the population to respiratory diseases over time. As immunity decreases, the number of individuals vulnerable to respiratory illnesses rises steadily. This decline in immunity not only increases the likelihood of weak infections but also reduces the proportion of the population that is strongly immune. Consequently, the overall ability of the population to effectively combat respiratory diseases diminishes over time due to this decrease in immunity.
How does cross-immunity influence disease dynamics?	Cross-immunity profoundly shapes disease dynamics by impacting both the transmission and severity of diseases within a population. An increase in cross-immunity typically diminishes the number of individuals susceptible to weak infections, thereby curbing the spread of diseases. However, it's worth noting that a surge in cross-immunity can paradoxically lead to a rise in the population of individuals experiencing strong infections.
What are the bifurcation directions in disease models?	The system exhibits a forward bifurcation for all $R_0 > 1$. This implies that both the reproductive numbers R_0^s and R_0^r undergo forward bifurcation in both the weakly infected and strongly infected populations. This suggests that as the basic reproduction number surpasses unity, the system undergoes significant qualitative changes in its dynamics, impacting both levels of infection within the population.
How does different values of basic reproduction number (R_0) influence the infected populations?	As the basic reproduction number (R_0) increases, represented as $R_0 = (R_0^s, R_0^r)$, the impact on infected populations intensifies. With $R_0 > 1$, both weakly and strongly infected populations grow. Higher R_0^s values increase the weakly infected population, showing a linear trend. Similarly, higher R_0^r values cause a sharp rise in the strongly infected population, which then stabilizes. Conversely, when $R_0 < 1$, the infection dies out in both populations, highlighting the critical threshold of $R_0 = 1$ for disease control and eradication.

5.4 Future Works

While this study provides valuable insights into the dynamics of respiratory diseases, it also reveals several areas that warrant further investigation to enhance our understanding and control of these diseases. Future work should focus on the following:

- **Exploration of Stochastic Models:** Future research should incorporate stochastic elements into the model to better understand the effects of random events and variations in disease spread. Stochastic models can capture the inherent randomness in disease transmission and progression, providing a more realistic depiction of how outbreaks may evolve under different conditions and interventions. This approach can help identify potential outcomes and risks that deterministic models may overlook, thereby improving our ability to predict and manage disease outbreaks.
- **Assessment of Seasonal Effects:** Investigating the impact of seasonal variations on disease transmission and recovery rates can provide a more comprehensive understanding of disease dynamics. By examining how factors such as temperature, humidity, and seasonal human behavior influence the spread and progression of respiratory diseases, we can develop more accurate models and predictions. This understanding can inform public health strategies that account for seasonal trends, thereby enhancing our ability to mitigate and control outbreaks throughout the year.
- **Longitudinal Data Analysis:** Collecting and analyzing longitudinal data from real-world outbreaks can validate and refine the model, significantly improving its predictive power and reliability. By examining data over extended periods, researchers can observe the actual progression and impact of the disease, allowing for adjustments and enhancements to the model's parameters and assumptions. This approach ensures that the model accurately reflects real-world conditions, making it a more dependable tool for predicting future outbreaks and assessing the effectiveness of intervention strategies.
- **Spatial Modeling:** Extend the model to incorporate spatial dynamics by considering population movement and interactions between different geographical regions. This can provide insights into how diseases spread across regions and the effectiveness of localized interventions.
- **Age-Structured Model:** Develop an age-structured model to capture the differential susceptibility and transmission dynamics of respiratory diseases among different age groups. This can be particularly relevant for diseases that disproportionately affect certain age demographics, such as influenza and COVID-19.

Bibliography

- [1] Thamina Acter, Nizam Uddin, Jagotamoy Das, Afroza Akhter, Tasrina Rabia Choudhury, and Sunghwan Kim. Evolution of severe acute respiratory syndrome coronavirus 2 (sars-cov-2) as coronavirus disease 2019 (covid-19) pandemic: A global health emergency. *Science of the Total Environment*, 730:138996, 2020.
- [2] Michael O Adeniyi, Segun I Oke, Matthew I Ekum, Temitope Benson, and Matthew O Adewole. Assessing the impact of public compliance on the use of non-pharmaceutical intervention with cost-effectiveness analysis on the transmission dynamics of covid-19: Insight from mathematical modeling. *Modeling, control and drug development for COVID-19 outbreak prevention*, pages 579–618, 2022.
- [3] Daniel Ankamu. *Mathematical model for H1N1 human to human transmission In Brong Ahafo Region*. PhD thesis, 2015.
- [4] Rym Ayadi. Covid-19 in the mediterranean and africa, 2020.
- [5] Rachel E Baker, Ayesha S Mahmud, Ian F Miller, Malavika Rajeev, Fidisoa Rasambainarivo, Benjamin L Rice, Saki Takahashi, Andrew J Tatem, Caroline E Wagner, Lin-Fa Wang, et al. Infectious disease in an era of global change. *Nature Reviews Microbiology*, 20(4):193–205, 2022.
- [6] Praveen Belagal, Hemanth Naick Banavath, and Buddolla Viswanath. Swine-origin influenza a (h1n1) virus: current status, threats, and challenges. In *Pandemic Outbreaks in the 21st Century*, pages 57–86. Elsevier, 2021.
- [7] CP Bhunu, S Mushayabasa, G Magombedze, and LI Roeger. Tuberculosis transmission model with case detection and treatment. *Journal of applied mathematics & informatics*, 29(3_4):529–546, 2011.
- [8] M Bocchino, A Sanduzzi°, and F Bariffi. Mycobacterium tuberculosis and hiv. *Monaldi Arch Chest Dis*, 55(5):381–388, 2000.
- [9] Fred Brauer, Carlos Castillo-Chavez, and Zhilan Feng. Endemic disease models. In *Mathematical models in epidemiology*, pages 63–116. Springer, 2019.

- [10] Marc Brisson, Élodie Bénard, Mélanie Drolet, Johannes A Bogaards, Iacopo Baussano, Simopekka Vänskä, Mark Jit, Marie-Claude Boily, Megan A Smith, Johannes Berkhof, et al. Population-level impact, herd immunity, and elimination after human papillomavirus vaccination: a systematic review and meta-analysis of predictions from transmission-dynamic models. *The Lancet Public Health*, 1(1):e8–e17, 2016.
- [11] Barbara M Byrne. *Structural equation modeling with EQS: Basic concepts, applications, and programming*. Routledge, 2013.
- [12] Wen Cao, Haoran Dai, Jingwen Zhu, Yuzhen Tian, and Feilin Peng. Analysis and evaluation of non-pharmaceutical interventions on prevention and control of covid-19: a case study of wuhan city. *ISPRS International Journal of Geo-Information*, 10(7):480, 2021.
- [13] Jack Carr. *Applications of centre manifold theory*, volume 35. Springer Science & Business Media, 2012.
- [14] C Castillo, Z Feng, and W Huang. On the computation of r_0 and its role on global stability. *Mathematical approaches for emerging and reemerging infectious diseases: an introduction (Minneapolis, MN, 1999)*, pages 229–250, 2002.
- [15] Betty Chinhara. Lived experiences of zimbabwean labour migrants in the informal economy in urban cape town during the covid-19 pandemic. 2023.
- [16] Nyuk Sian Chong, Jean Michel Tchuente, and Robert J Smith. A mathematical model of avian influenza with half-saturated incidence. *Theory in biosciences*, 133:23–38, 2014.
- [17] SMEK Chowdhury, Mohammad Forkan, Shams Forruque Ahmed, Praveen Agarwal, ABM Shawkat Ali, and SM Muyeen. Modeling the sars-cov-2 parallel transmission dynamics: asymptomatic and symptomatic pathways. *Computers in Biology and Medicine*, 143:105264, 2022.
- [18] Gerardo Chowell, Zhilan Feng, and Baojun Song. From the guest editors: Special issue dedicated to carlos castillo-chavez on his 60th birthday. 2013.
- [19] Brian J Coburn, Bradley G Wagner, and Sally Blower. Modeling influenza epidemics and pandemics: insights into the future of swine flu (h1n1). *BMC medicine*, 7:1–8, 2009.
- [20] M Colombo, P Vakaoti, R Richards, M Schaaf, M Taumoepeau, L Moata’ane, et al. Pacific voices xviii: Abstracts for the pacific postgraduate symposium 2021. 2021.
- [21] Severino Jefferson Ribeiro da Silva, Jessica Catarine Frutuoso do Nascimento, Renata Pessoa Germano Mendes, Klarissa Miranda Guarines, Caroline Targino Alves da Silva, Poliana Gomes da Silva, Jurandy Júnior Ferraz de Magalhães, Justin RJ Vigar, Abelardo Silva-Júnior, Alain Kohl, et al. Two years into the covid-19 pandemic: lessons learned. *ACS infectious diseases*, 8(9):1758–1814, 2022.

- [22] Zhilan Feng, Wenzhang Huang, and Carlos Castillo-Chavez. On the role of variable latent periods in mathematical models for tuberculosis. *Journal of dynamics and differential equations*, 13:425–452, 2001.
- [23] Gabriel Obed Fosu, Emmanuel Akweitley, and Albert Adu-Sackey. Next-generation matrices and basic reproductive numbers for all phases of the coronavirus disease. *Gabriel Obed Fosu, Emmanuel Akweitley, and Albert Adu-Sackey. Next-generation matrices and basic reproductive numbers for all phases of the coronavirus disease. Open Journal of Mathematical Sciences*, 4(1):261–272, 2020.
- [24] Tapiwa Ganyani, Cécile Kremer, Dongxuan Chen, Andrea Torneri, Christel Faes, Jacco Wallinga, and Niel Hens. Estimating the generation interval for coronavirus disease (covid-19) based on symptom onset data, march 2020. *Eurosurveillance*, 25(17):2000257, 2020.
- [25] Abadi Abay Gebremeskel, Hailay Weldegiorgis Berhe, Adugna Temesgen Abay, et al. A mathematical modelling and analysis of covid-19 transmission dynamics with optimal control strategy. *Computational and Mathematical Methods in Medicine*, 2022, 2022.
- [26] David E Gordon, Joseph Hiatt, Mehdi Bouhaddou, Veronica V Rezelj, Svenja Ulferts, Hannes Braberg, Alexander S Jureka, Kirsten Obernier, Jeffrey Z Guo, Jyoti Batra, et al. Comparative host-coronavirus protein interaction networks reveal pan-viral disease mechanisms. *Science*, 370(6521):eabe9403, 2020.
- [27] Zoher Gueroui and Albert Libchaber. Single-molecule measurements of gold-quenched quantum dots. *Physical Review Letters*, 93(16):166108, 2004.
- [28] AA Haghdoust, MOHAMMAD MAHDI GOUYA, and Mohammad Reza Baneshi. Modelling of h1n1 flu in iran. 2009.
- [29] Oke Isaiah Idisi, Akindele Akano Onifade, and Lateef Kareem. Modeling the impact of genetically modified humans on the transmission dynamics of covid-19: Case study of nigeria. 2024.
- [30] Zhong-wei Jia, Xiao-wen Li, FENG Dan, and Wu-chun Cao. Transmission models of tuberculosis in heterogeneous population. *Chinese medical journal*, 120(15):1360–1365, 2007.
- [31] Laura D Kramer and Norma P Tavakoli. Viruses of terrestrial mammals. *Studies in Viral Ecology*, pages 541–583, 2021.
- [32] Martin Alexander Lauxmann, Natalia Estefanía Santucci, and Ana María Autrán-Gómez. The sars-cov-2 coronavirus and the covid-19 outbreak. *International braz j urol*, 46:6–18, 2020.

- [33] Martin Matakanure. *The impact of the Covid-19 pandemic on immigrant entrepreneurs' informal livelihoods and businesses in Mamelodi Township*. PhD thesis, University of Johannesburg (South Africa), 2021.
- [34] C Connell McCluskey and P van den Driessche. Global analysis of two tuberculosis models. *Journal of Dynamics and Differential Equations*, 16:139–166, 2004.
- [35] Marcia Fagan McInerney. *Complete Freund's adjuvant suppresses anti-islet autoimmunity and diabetes in nonobese diabetic (NOD) mice*. University of Michigan, 1989.
- [36] Stella Mugisha. *Mathematical analysis of tuberculosis models with differential infectivity, general contact rates, migration and staged progression*. PhD thesis, North-West University, 2013.
- [37] Ashesh Nandy, Tapati Sarkar, Subhash C Basak, Papiya Nandy, and Sukhen Das. Characteristics of influenza ha-na interdependence determined through a graphical technique. *Current computer-aided drug design*, 10(4):285–302, 2014.
- [38] Esteban Ortiz-Prado, Katherine Simbaña-Rivera, Lenin Gómez-Barreno, Mario Rubio-Neira, Linda P Guaman, Nikolaos C Kyriakidis, Claire Muslin, Ana María Gómez Jaramillo, Carlos Barba-Ostria, Doménica Cevallos-Robalino, et al. Clinical, molecular, and epidemiological characterization of the sars-cov-2 virus and the coronavirus disease 2019 (covid-19), a comprehensive literature review. *Diagnostic microbiology and infectious disease*, 98(1):115094, 2020.
- [39] Marguerite Robinson, Nikolaos I Stilianakis, and Yannis Drossinos. Spatial dynamics of airborne infectious diseases. *Journal of theoretical biology*, 297:116–126, 2012.
- [40] Wenhan Shao, Xinxin Li, Mohsan Ullah Goraya, Song Wang, and Ji-Long Chen. Evolution of influenza a virus by mutation and re-assortment. *International journal of molecular sciences*, 18(8):1650, 2017.
- [41] Cruz Vargas-De-León and Alberto d'Onofrio. Global stability of infectious disease models with contact rate as a function of prevalence index. *Mathematical Biosciences & Engineering*, 14(4):1019–1033, 2017.
- [42] Yongshi Yang, Fujun Peng, Runsheng Wang, Kai Guan, Taijiao Jiang, Guogang Xu, Jinlyu Sun, and Christopher Chang. The deadly coronaviruses: The 2003 sars pandemic and the 2020 novel coronavirus epidemic in china. *Journal of autoimmunity*, 109:102434, 2020.

A Python Codes

```

import warnings
# Filter out DeprecationWarnings
warnings.filterwarnings("ignore", category=DeprecationWarning)
import numpy as np
from scipy.integrate import odeint
import matplotlib.pyplot as plt

def deriv(y, t, params):
    mu, beta1, beta2, kappa1, kappa2, alpha1, alpha2, d1, d2, delta1,
    delta2, gamma1, gamma2, phi, epsilon = params
    S, I1, I2, P1, P2, R1, R2 = y

    dSdt = mu*(1-S) - (beta1*kappa1*P1*S)/alpha1 -
    (beta2*kappa2*P2*S)/alpha2 + d1*I1 + d2*I2 + delta1*R1 + delta2*R2
    dI1dt = (beta1*kappa1*P1*S)/alpha1 - (mu+gamma1+d1)*I1 -
    (phi*beta2*kappa2*P2*I1)/alpha2
    dI2dt = (beta2*kappa2*P2*S)/alpha2 - (mu+gamma2+d2)*I2 +
    (phi*beta2*kappa2*P2*I1)/alpha2 + (1-
    epsilon)*(beta2*kappa2*P2*R1)/alpha2
    dP1dt = kappa1*I1 - kappa1*P1
    dP2dt = kappa2*I2 - kappa2*P2
    dR1dt = gamma1*I1 - mu*R1 - (1-
    epsilon)*(beta2*kappa2*P2*R1)/alpha2 - delta1*R1
    dR2dt = gamma2*I2 - mu*R2 - delta2*R2

    return dSdt, dI1dt, dI2dt, dP1dt, dP2dt, dR1dt, dR2dt

# Initial conditions
S0 = 0.4
I10 = 0.1
I20 = 0.15
P10 = 0.15
P20 = 0.1
R10 = 0.05
R20 = 0.05
y0 = [S0, I10, I20, P10, P20, R10, R20]

# Parameters
mu = 0.00004
beta1 = 0.000224
beta2 = 0.0000448
kappa1 = 410000
kappa2 = 614000
alpha1 = 37.44
alpha2 = 74.88
d1 = 0.88
d2 = 0.22
delta1 = 0.00055
delta2 = 0.00011
gamma1 = 0.0004

```

```

gamma2 = 0.0008
phi = 2
epsilon = 0.4

import numpy as np
import matplotlib.pyplot as plt

# Define different values of epsilon
epsilon_values = [0,0.2,0.3,0.5,0.7,0.8,0.9]

# Initialize a list to store the solutions for each epsilon value
solutions = []

# Iterate over each epsilon value
for epsilon in epsilon_values:
    # Pack parameters for odeint with the current epsilon value
    params = [mu, beta1, beta2, kappa1, kappa2, alpha1, alpha2, d1,
              d2, delta1, delta2, gamma1, gamma2, phi, epsilon]

    # Run the simulation
    solution = odeint(deriv, y0, t, args=(params,))

    # Append the solution to the list of solutions
    solutions.append(solution)

# Plot I1 population against time for each epsilon value
plt.figure(figsize=(10, 6))
for i, epsilon in enumerate(epsilon_values):
    plt.plot(t, solutions[i][:, 1], label=f'$\epsilon$ = {epsilon}',
             linewidth=2)

plt.xlabel('Time', fontsize=16)
plt.ylabel('$I_1$', fontsize=20)
# plt.title('Effect of Reduction in Immunity on $I_1$ over Time',
#           fontsize=16)
plt.xticks(fontsize=20) # Increase font size for x-axis ticks
plt.yticks(fontsize=20) # Increase font size for y-axis ticks
plt.legend(fontsize=12)
plt.grid(True)
plt.show()

import numpy as np
import matplotlib.pyplot as plt

# Define specific values of epsilon
epsilon_values = [0,0.2,0.3,0.5,0.7,0.8,0.9]

# Initialize a list to store the solutions for each epsilon value
solutions = []

```



```

# Iterate over each epsilon value
for epsilon in epsilon_values:
    # Pack parameters for odeint with the current epsilon value
    params = [mu, beta1, beta2, kappa1, kappa2, alpha1, alpha2, d1,
              d2, delta1, delta2, gamma1, gamma2, phi, epsilon]

    # Run the simulation
    solution = odeint(deriv, y0, t, args=(params,))

    # Append the solution to the list of solutions
    solutions.append(solution)

# Plot I2 population against time for each epsilon value
plt.figure(figsize=(10, 6))
for i, epsilon in enumerate(epsilon_values):
    plt.plot(t, solutions[i][:, 2], label=f'$\epsilon$ = {epsilon}',
             linewidth=2)

plt.xlabel('Time', fontsize=14)
plt.ylabel('$I_2$', fontsize=20)
# plt.title('Effect of Reduction in Immunity on $I_2$ over Time',
#           fontsize=16)
plt.xticks(fontsize=20) # Increase font size for x-axis ticks
plt.yticks(fontsize=20) # Increase font size for y-axis ticks
plt.legend(fontsize=10)
plt.grid(True)
plt.show()

import numpy as np
import matplotlib.pyplot as plt
# Time points to compute solutions at
t = np.linspace(0, 100, 200)

# Define specific values of phi
phi_values = [0.0, 0.4, 0.6, 0.9, 1.5]

# Initialize a list to store the solutions for each phi value
solutions = []

# Iterate over each phi value
for phi in phi_values:
    # Pack parameters for odeint with the current phi value
    params = [mu, beta1, beta2, kappa1, kappa2, alpha1, alpha2, d1,
              d2, delta1, delta2, gamma1, gamma2, phi, epsilon]

    # Run the simulation
    solution = odeint(deriv, y0, t, args=(params,))

    # Append the solution to the list of solutions

```

```

        solutions.append(solution)

# Plot I1 population against time for each phi value
plt.figure(figsize=(10, 6))
for i, phi in enumerate(phi_values):
    plt.plot(t, solutions[i][:, 1], label=f'$\phi$ = {phi}',
             linewidth=2)

plt.xlabel('Time', fontsize=14)
plt.ylabel('$I_1$', fontsize=20)
#plt.title('Effect of Cross-Immunity Factor on $I_1$ over Time',
#          fontsize=16)
plt.xticks(fontsize=15) # Increase font size for x-axis ticks
plt.yticks(fontsize=15) # Increase font size for y-axis ticks
plt.legend(fontsize=10)
plt.grid(True)
plt.show()

import numpy as np
import matplotlib.pyplot as plt
# Time points to compute solutions at
t = np.linspace(0, 100, 200)

# Define specific values of phi
phi_values = [0.0, 0.4, 0.6, 0.9, 1.5]

# Initialize a list to store the solutions for each phi value
solutions = []

# Iterate over each phi value
for phi in phi_values:
    # Pack parameters for odeint with the current phi value
    params = [mu, beta1, beta2, kappa1, kappa2, alpha1, alpha2, d1,
              d2, delta1, delta2, gamma1, gamma2, phi, epsilon]

    # Run the simulation
    solution = odeint(deriv, y0, t, args=(params,))

    # Append the solution to the list of solutions
    solutions.append(solution)

# Plot I2 population against time for each phi value
plt.figure(figsize=(10, 6))
for i, phi in enumerate(phi_values):
    plt.plot(t, solutions[i][:, 2], label=f'$\phi$ = {phi}',
             linewidth=2)

plt.xlabel('Time', fontsize=14)
plt.ylabel('$I_2$', fontsize=20)
#plt.title('Effect of Cross-Immunity Factor on $I_2$ over Time',

```

```

fontsize=16)
plt.xticks(fontsize=15) # Increase font size for x-axis ticks
plt.yticks(fontsize=15) # Increase font size for y-axis ticks
plt.legend(fontsize=10)
plt.grid(True)
plt.show()

import numpy as np
from scipy.integrate import odeint
import matplotlib.pyplot as plt

# Define the model parameters and initial conditions
mu = 0.00004
beta2 = 0.000118
kappa2 = 614000
alpha2 = 74.88
d2 = 0.14
delta2 = 0.00011
gamma2 = 0.4
phi = 0.9
epsilon = 0.2
S0 = 0.4
I10 = 0.1
I20 = 0.1
P10 = 0.15
P20 = 0.15
R10 = 0.05
R20 = 0.05
y0 = [S0, I10, I20, P10, P20, R10, R20]

# Time points to compute solutions at
t = np.linspace(0, 50, 200)

# Define the differential equation system
def deriv(y, t, params):
    mu, beta2, kappa2, alpha2, d2, delta2, gamma2, R0s = params
    S, I1, I2, P1, P2, R1, R2 = y

    beta1 = R0s * ((mu + gamma1 + d1) * alpha1) / kappa1

    dSdt = mu*(1-S) - (beta1*kappa1*P1*S)/alpha1 -
(beta2*kappa2*P2*S)/alpha2 + d1*I1 + d2*I2 + delta1*R1 + delta2*R2
    dI1dt = (beta1*kappa1*P1*S)/alpha1 - (mu+gamma1+d1)*I1 -
(phi*beta2*kappa2*P2*I1)/alpha2

    return dSdt, dI1dt, 0, 0, 0, 0, 0

# Define R0s values
R0s_values = [0.5, 0.9, 1.5, 1.8, 2]

```

```

# Plot weakly infected (I1) against time for different R0s values
plt.figure(figsize=(10, 6))

for R0s in R0s_values:
    # Pack parameters for odeint
    params = [mu, beta2, kappa2, alpha2, d2, delta2, gamma2, R0s]

    # Run the simulation
    solution = odeint(deriv, y0, t, args=(params,))

    # Extracting weakly infected population (I1)
    I1 = solution[:, 1]

    # Plotting
    plt.plot(t, I1, label=f'$R_0^s={R0s}$')

plt.xlabel('Time', fontsize=16)
plt.ylabel('$I_1$', fontsize=20)
# plt.title('Effect of $R_0^s$ on Weakly$I_1$'), fontsize=16)
plt.xticks(fontsize=20) # Increase font size for x-axis ticks
plt.yticks(fontsize=20) # Increase font size for y-axis ticks
plt.legend(fontsize=12)
plt.grid(True)
plt.show()

import numpy as np
from scipy.integrate import odeint
import matplotlib.pyplot as plt

# Define the model parameters and initial conditions
mu = 0.00004
beta2 = 0.000118
kappa2 = 614000
alpha2 = 74.88
d2 = 0.14
delta2 = 0.00011
gamma2 = 0.4
phi = 0.9
epsilon = 0.2
S0 = 0.4
I10 = 0.1
I20 = 0.1
P10 = 0.15
P20 = 0.15
R10 = 0.05
R20 = 0.05
y0 = [S0, I10, I20, P10, P20, R10, R20]

# Time points to compute solutions at
t = np.linspace(0, 50, 200)

```

```

# Define the differential equation system
def deriv(y, t, params):
    mu, beta2, kappa2, alpha2, d2, delta2, gamma2, R0s = params
    S, I1, I2, P1, P2, R1, R2 = y

    beta1 = R0s * ((mu + gamma1 + d1) * alpha1) / kappa1

    dSdt = mu*(1-S) - (beta1*kappa1*P1*S)/alpha1 -
(beta2*kappa2*P2*S)/alpha2 + d1*I1 + d2*I2 + delta1*R1 + delta2*R2
    dI1dt = (beta1*kappa1*P1*S)/alpha1 - (mu+gamma1+d1)*I1 -
(phi*beta2*kappa2*P2*I1)/alpha2

    return dSdt, dI1dt, 0, 0, 0, 0, 0

# Define R0s values
R0s_values = [0.5, 0.9, 1.5, 1.8, 2]

# Plot weakly infected (I1) against time for different R0s values
plt.figure(figsize=(10, 6))

for R0s in R0s_values:
    # Pack parameters for odeint
    params = [mu, beta2, kappa2, alpha2, d2, delta2, gamma2, R0s]

    # Run the simulation
    solution = odeint(deriv, y0, t, args=(params,))

    # Extracting weakly infected population (I1)
    I1 = solution[:, 1]

    # Plotting
    plt.plot(t, I1, label=f'$R_0^s={R0s}$')

plt.xlabel('Time', fontsize=16)
plt.ylabel('$I_1$', fontsize=20)
#plt.title('Effect of $R_0^s$ on Weakly Infected Population ($I_1$)
over Time', fontsize=16)
plt.xticks(fontsize=20) # Increase font size for x-axis ticks
plt.yticks(fontsize=20) # Increase font size for y-axis ticks
plt.legend(fontsize=12)
plt.grid(True)
plt.show()

import numpy as np
from scipy.integrate import odeint
import matplotlib.pyplot as plt

# Define the model parameters and initial conditions
mu = 0.00004

```

```

beta2 = 0.000118
kappa2 = 614000
alpha2 = 74.88
d2 = 0.14
delta2 = 0.00011
gamma2 = 0.4
phi = 0.9
epsilon = 0.2
S0 = 0.4
I10 = 0.1
I20 = 0.1
P10 = 0.15
P20 = 0.15
R10 = 0.05
R20 = 0.05
y0 = [S0, I10, I20, P10, P20, R10, R20]

# Time points to compute solutions at
t = np.linspace(0, 50, 200)

# Define the differential equation system
def deriv(y, t, params):
    mu, beta2, kappa2, alpha2, d2, delta2, gamma2, R0r = params
    S, I1, I2, P1, P2, R1, R2 = y

    beta1 = R0r * ((mu + gamma1 + d1) * alpha1) / kappa1

    dSdt = mu*(1-S) - (beta1*kappa1*P1*S)/alpha1 -
(beta2*kappa2*P2*S)/alpha2 + d1*I1 + d2*I2 + delta1*R1 + delta2*R2
    dI1dt = (beta1*kappa1*P1*S)/alpha1 - (mu+gamma1+d1)*I1 -
(phi*beta2*kappa2*P2*I1)/alpha2

    return dSdt, dI1dt, 0, 0, 0, 0, 0

# Define R0r values
R0r_values = [0.5, 0.9, 1.5, 1.8, 2]

# Plot weakly infected (I1) against time for different R0r values
plt.figure(figsize=(10, 6))

for R0r in R0r_values:
    # Pack parameters for odeint
    params = [mu, beta2, kappa2, alpha2, d2, delta2, gamma2, R0r]

    # Run the simulation
    solution = odeint(deriv, y0, t, args=(params,))

    # Extracting weakly infected population (I1)
    I1 = solution[:, 1]

```

```

# Plotting
plt.plot(t, I1, label=f'$R_0^r={R0r}$')

plt.xlabel('Time', fontsize=16)
plt.ylabel('$I_1$', fontsize=20)
plt.xticks(fontsize=20) # Increase font size for x-axis ticks
plt.yticks(fontsize=20) # Increase font size for y-axis ticks
plt.legend(fontsize=12)
plt.grid(True)
plt.show()

import numpy as np
from scipy.integrate import odeint
import matplotlib.pyplot as plt

# Define the model parameters and initial conditions
mu = 0.00004
beta2 = 0.000118
kappa2 = 614000
alpha2 = 74.88
d2 = 0.14
delta2 = 0.00011
gamma2 = 0.4
phi = 0.9
epsilon = 0.2
S0 = 0.4
I10 = 0.1
I20 = 0.1
P10 = 0.15
P20 = 0.15
R10 = 0.05
R20 = 0.05
y0 = [S0, I10, I20, P10, P20, R10, R20]

# Time points to compute solutions at
t = np.linspace(0, 50, 200)

# Define the differential equation system
def deriv(y, t, params):
    mu, beta2, kappa2, alpha2, d2, delta2, gamma2, R0r = params
    S, I1, I2, P1, P2, R1, R2 = y

    beta1 = R0r * ((mu + gamma1 + d1) * alpha1) / kappa1

    dSdt = mu*(1-S) - (beta1*kappa1*P1*S)/alpha1 -
(beta2*kappa2*P2*S)/alpha2 + d1*I1 + d2*I2 + delta1*R1 + delta2*R2
    dI2dt = (beta2*kappa2*P2*S)/alpha2 - (mu+gamma2+d2)*I2 -
(phi*beta1*kappa1*P1*I2)/alpha1

    return dSdt, 0, dI2dt, 0, 0, 0, 0

```

```

# Define R0r values
R0r_values = [0.5, 0.9, 1.5, 1.8, 2]

# Plot strongly infected (I2) against time for different R0r values
plt.figure(figsize=(10, 6))

for R0r in R0r_values:
    # Pack parameters for odeint
    params = [mu, beta2, kappa2, alpha2, d2, delta2, gamma2, R0r]

    # Run the simulation
    solution = odeint(deriv, y0, t, args=(params,))

    # Extracting strongly infected population (I2)
    I2 = solution[:, 2]

    # Plotting
    plt.plot(t, I2, label=f'$R_0^r={R0r}$')

plt.xlabel('Time', fontsize=20)
plt.ylabel('$I_2$', fontsize=20)
plt.xticks(fontsize=20) # Increase font size for x-axis ticks
plt.yticks(fontsize=20) # Increase font size for y-axis ticks
plt.legend(fontsize=12)
plt.grid(True)
plt.show()

import numpy as np
from scipy.integrate import odeint
import matplotlib.pyplot as plt

# Define the model parameters and initial conditions
mu = 0.00004
beta2 = 0.000118
kappa2 = 614000
alpha2 = 74.88
d2 = 0.14
delta2 = 0.00011
gamma2 = 0.4
phi = 0.9
epsilon = 0.2
S0 = 0.4
I10 = 0.1
I20 = 0.1
P10 = 0.15
P20 = 0.15
R10 = 0.05
R20 = 0.05
y0 = [S0, I10, I20, P10, P20, R10, R20]

```



```

# Time points to compute solutions at
t = np.linspace(0, 50, 200)

# Define the differential equation system
def deriv(y, t, params):
    mu, beta2, kappa2, alpha2, d2, delta2, gamma2, R0r = params
    S, I1, I2, P1, P2, R1, R2 = y

    beta2 = R0r * ((mu + gamma2 + d2) * alpha2) / kappa2

    dSdt = mu*(1-S) - (beta1*kappa1*P1*S)/alpha1 -
    (beta2*kappa2*P2*S)/alpha2 + d1*I1 + d2*I2 + delta1*R1 + delta2*R2
    dI2dt = (beta2*kappa2*P2*S)/alpha2 - (mu+gamma2+d2)*I2 +
    (phi*beta2*kappa2*P2*I1)/alpha2 + (1-
    epsilon)*(beta2*kappa2*P2*R1)/alpha2

    return dSdt, 0, dI2dt, 0, 0, 0, 0

# Define R0r values
R0r_values = [0.5, 0.9, 1.5, 1.8, 2]

# Plot strongly infected (I2) against R0r
plt.figure(figsize=(10, 6))

for R0r in R0r_values:
    # Pack parameters for odeint
    params = [mu, beta2, kappa2, alpha2, d2, delta2, gamma2, R0r]

    # Run the simulation
    solution = odeint(deriv, y0, t, args=(params,))

    # Extracting strongly infected population (I2)
    I2 = solution[:, 2]

    # Plotting
    plt.plot(t, I2, label=f'$R_0^r={R0r}$')

plt.xlabel('Time', fontsize=16)
plt.ylabel('$I_2$', fontsize=20)
#plt.title('Effect of $R_0^r$ on Strongly Infected Population
($I_2$)', fontsize=16)
plt.xticks(fontsize=15) # Increase font size for x-axis ticks
plt.yticks(fontsize=15) # Increase font size for y-axis ticks
plt.legend(fontsize=12)
plt.grid(True)
plt.show()

```